Retinoic Acid Deficiency During Gastrulation Induces Craniofacial Malformations in Mouse Resembling Fetal Alcohol Syndrome

By

Berardino Petrelli

A Thesis submitted to the Faculty of Graduate Studies of

The University of Manitoba

In fulfillment of the requirements of the degree of

MASTER OF SCIENCE

Department of Biochemistry and Medical Genetics

University of Manitoba

Winnipeg, Canada

Table of Contents:

Abstract (Lay Abstract):

Fetal Alcohol Spectrum Disorder is caused by maternal consumption of alcohol during pregnancy, and the clinical term given to children with birth defects, behavioral difficulties, and cognitive impairments. It can be associated with other co-morbidities which include heart defects, malocclusions, hearing loss, and immune deficiencies. Vitamin A Deficiency (retinoic acid deficiency) is caused by maternal deficiency of Vitamin A (retinol) (and consequently its active metabolite retinoic acid), and is the clinical term given to babies/children who present with (night) blindness, craniofacial malformations, brain aberrations and many of the FASD co-morbidities like heart defects, malocclusions, and immune deficiencies to name a few. The linking of these two streams of research lies in the family of enzymes both pathways share to convert their respective metabolites: ethanol to acetic acid and Vitamin A (retinol) to retinoic acid. The Vitamin A hypothesis suggests that during a binge exposure of alcohol the family of enzymes required to convert retinol to retinoic acid instead converts ethanol to acetic acid, causing the craniofacial malformations, brain aberrations, and co-morbidities present in both disorders. This paper will present a genetically modified mouse that biochemically mimics retinoic acid deficiency producing the craniofacial malformations and brain aberrations comparable to those found in PAE mouse models and clinical FASD outcomes.

List of Figures:

List of Tables:

Chapter 1: Introduction

This thesis is in partial fulfillment of the Master's degree program in the Department of Biochemistry and Medical Genetics at the University of Manitoba. The title of my thesis is: "**Retinoic Acid Deficiency During Gastrulation Induces Craniofacial Malformations in Mouse Resembling Fetal Alcohol Syndrome.**"

Fetal Alcohol Spectrum Disorder (FASD) is the most common cause of neurodevelopmental impairments in the western world, with a prevalence of 1-2% in Canada (Cook *et al.*, 2016; Popova *et al.*, 2016). FASD is currently understood as an umbrella of related disorders, caused by maternal consumption of alcohol (Prenatal Alcohol Exposure – PAE) during pregnancy. Comprising approximately 10% of all FASD cases, FASD with sentinel facial features is the most clinically severe form of FASD exhibiting the strongest manifestations of the disorder which include: craniofacial sentinel features and malformations, brain aberrations, and behavioral deficits as well as other co-morbidities (Chudley *et al.*, 2005). The less clinically severe form, FASD without Sentinel facial features do not have the visual clinical manifestations of the disorder and is neurodevelopmental and behavioral in nature, thus 90% of FASD cases are almost invisible and under diagnosed (Chudley *et al.*, 2005; Rasmussen *et al.*, 2008). There are many risk factors for FASD that include: PAE, maternal age, nutritional deficiencies, lower education and employment, and genetic factors (Jones KL, 2011). Unfortunately, the mechanism

by which alcohol causes FASD currently remains unknown and there is currently no known cure for the disorder. In this thesis I explore new insights into the molecular etiology of FASD and the role of alcohol-associated perturbation of the Vitamin A / retinoic acid pathway in early gastrulation.

The Vitamin A Hypothesis is one of the several theories of Fetal Alcohol Spectrum Disorder (FASD) etiology. The Vitamin A theory postulates that alcohol exposure results in retinoic acid deficiency, and when this occurs at an early critical time-point during development, it causes the malformations associated with the spectrum disorder (Yelin et al. 2005; Yelin et al. 2007; Kot-Leibovich and Fainsod 2009). Deficiency at early gastrulation is considered a particularly sensitive window as this is during a developmental process when the two germ layers (endoderm and ectoderm) become three germ layers (endoderm, mesoderm, and ectoderm). During gastrulation, endodermal cells directs ectodermal lineage cells to fold inwards to produce the neural fold (containing neural crest cell lineage) and paraxial mesoderm (containing mesoderm cell lineage) to develop in between the endodermal and ectodermal lineages a cellular process called epithelial to mesenchymal transition (Carlson BM 2014). This process is driven by retinoic acid (RA) and perturbations in neural crest cell induction at this developmental stage can explain the craniofacial and brain malformations seen later in FASD (Carlson BM 2014).

During an alcohol exposure the alcohol dehydrogenase and aldehyde dehydrogenase enzymes actively work to remove the teratogens from the cell. Acetaldehyde is a known teratogen to the cell and has been previously shown to be involved in ROS production, DNA damage, and cell death (Zakhari and Hoek, 2015). Ethanol is first oxidized to acetaldehyde and then to acetic acid by alcohol dehydrogenase (ADH, ADH1A1) and aldehyde dehydrogenase (ALDH, ALDH1A2) enzymes, respectively. During an acute ethanol exposure alcohol and aldehyde dehydrogenase

enzymes become overwhelmed, and as a result ADH1A and ALDH1A family member enzymes aide the cell remove the teratogens. Unfortunately, Vitamin A pathway enzymes retinol dehydrogenase (RDH, ADH4) and retinaldehyde dehydrogenase (RLDH, ALDH1A1-3) are alcohol pathway family member enzymes (Yelin *et al.*, 2005; Kot-Leibovich and Fainsod, 2009; Sharon *et al.*, 2011; Shabtai *et al.*, 2016). In this manner, ethanol competitively inhibits RLDH enzymes to actively convert the ethanol pathway substrates, and consequently, causing retinoic acid deficiency.

Retinoic acid deficiency has been known to cause developmental malformations in newborn babies for over a century although it has never been cemented as a cause of FASD. Vitamin A Deficiency / Hypovitaminosis A is a clinical term given to newborns that present with the disorder and clinical features including: blindness, impaired immune function, and birth defects to name a few (Humphrey, West and Sommer, 1992; Huerta *et al.*, 2002; Goez, Scott and Hasal, 2011). Retinoic acid deficiency has also been studied extensively in animal models, specifically in rodents models where retinol, retinoic acid, and B-carotene deficiency outcomes have been studied producing results similar to those seen in clinical assessments (White *et al.*, 1998; Clagett-Dame and Knutson, 2011). Over the past few decades researchers have begun studying knockout (KO) models for enzymes in the RA pathway, specifically *Rdh10, Raldh1, 2, 3*, as well as direct transcriptional targets including retinoic acid response elements (RAREs): *Rarα, β, γ* and *Rxrα, β, γ* subtypes (Rhinn et al. 2011; Niederreither et al. 2003, Niederreither et al. 2002). It should be noted that approximately 3% of the entire genome is under control of retinol/retinoic acid by RARE-dependent transcriptional activity (Balmer and Blomhoff, 2002; Paschaki *et al.*, 2013).

RA pathway knockout mouse models have shown a variety of developmental malformations including: arrested development due to impaired organogenesis (*Rdh10* KO and *Raldh2* KO), nasal and optic abnormalities including altered neuronal differentiation in forebrain (*Raldh3* KO), growth deficiency, vertebral abnormalities, male sterility (*Rarα* KO), growth deficiency, vertebral abnormalities, ocular abnormalities, and locomotor defects (*Rarβ* KO), growth deficiency, vertebral abnormalities, and male sterility (*Rarγ* KO) (Luo *et al.*, 1995; Niederreither *et al.*, 2002; Clagett-Dame and Knutson, 2011; Rhinn *et al.*, 2011). Interestingly, when two or more Rar-subtypes are knocked out in mice, a more extreme aberrant developmental phenotype is observed including craniofacial malformations, heart flow tract defects, and lung, thymus, and thyroid hypoplasia (Kam *et al.*, 2012; Rhinn and Dolle, 2012). This indicates that there is overlap among Rar- and Rxr- subtype transcriptional targets and that multiple Rar- or Rxr- subtype KOs produce a phenotype similar to *Raldh2* KOs (Szanto *et al.*, 2004).. *Rxrα* KO embryos have heart outflow tract defects, myocardial hypoplasia, and ocular defects, *Rxrβ* KO mice have abnormal sertoli cells and male sterility, *Rxrγ* KO mice have behavioral and depression-like defects (Szanto *et al.*, 2004; Rhinn and Dolle, 2012). When *Rdh/Raldh* and *Rar* KO phenotypes are taken into consideration it becomes compelling to consider that the Vitamin A hypothesis may be a legitimate cause of FASD.

PAE mouse models recapitulate clinical FASD outcomes including craniofacial malformations (sentinel facial features), brain aberrations, and behavioral deficits. The variation in gestational timing, dosage, and delivery of PAE directs the type of FASD outcomes in mouse models. Early gestation acute intraperitoneal PAE causes severe craniofacial malformations, whereby late gestation chronic liquid diet PAE causes brain aberrations (Godin et al. 2010; Allan, Goggin, and Caldwell 2014). Using these robust PAE model paradigms one can observe reproducible PAE

phenotypes including: craniofacial malformations, ocular defects including microphthalmia, medial facial cleft, midfacial hypoplasia, cleft palate, micrognathia, reduced snout width, reduced head circumference, smaller brain volume, growth deficiency, general behavioral and depression-like defects, increased anxiety, impaired fine motor coordination, and aberrant cortical neuron development (Scott E. Parnell et al. 2009; Lipinski et al. 2012; Caldwell et al. 2008). Many of these PAE phenotypes are found in Rdh/Raldh , Rar, and Rxr KO mouse models previously described, and moreover, these phenotypes are derived from cell lineages/tissues that form during early development. It is specifically the mesodermal and neural crest cell lineages from which these developmental aberrations form and it is retinoic acid during late gastrulation and early neurulation that directs cell lineage proliferation and migration patterns in the developing embryo. This is the reasoning for the Vitamin A Hypothesis and why it is believed retinoic acid deficiency is one of the causes of FASD.

A research group in Israel led by our colleague and collaborator Abraham Fainsod has shown that ethanol exposure at developmental stage 11 (early gastrulation) in *Xenopus* produces the most severe craniofacial malformations, microcephaly and axial defects compared to ethanol exposure at any other developmental stage. Moreover, Fainsod et al. found that when a retinoic acid synthesis inhibitor (DEAB) is provided to *Xenopus* at developmental stage 11, the same severity of craniofacial malformations, microcephaly, and axial defects are achieved (Yelin et al. 2005; Yelin et al. 2007). Furthermore, ethanol exposure and retinoic acid inhibitor deficits can be rescued and restored to normal development by Vitamin A (retinol) supplementation during development (Kot-Leibovich and Fainsod 2009; Yelin et al. 2007). The deficits seen in *Xenopus* are comparable to those observed in PAE mouse models and in humans with FASD. Fainsod's research has shown the molecular etiology between the ethanol and retinol (retinoic acid)

pathways. More importantly, Fainsod is able to rescue the FASD-like outcomes in *Xenopus* using Vitamin A supplementation, proving the FASD - Vitamin A hypothesis in a vertebrate model. In order to establish RA deficiency as an etiology of clinical FASD, a mammalian model system, a mouse model (closest to a human) must demonstrate the reduction or prevention of FASD outcomes (craniofacial and neurodevelopmental malformations) using Vitamin A supplementation.

To this end, we engineered a genetic mouse model designed to biochemically mimic the reduced RA levels (due to acute ethanol exposure), at the right time, early gastrulation, and in the right place, the node (Spemann Mangold organizer). To biochemically mimic the alcohol-induced RA deficiency *in vivo,* we genetically engineered a mouse expressing Cyp26A1-eGFP from the endogenous *Goosecoid* (*Gsc*) promoter. The *Gsc* promoter dictates spatial-temporal expression to the node at the start of gastrulation. Cyp26A1 degrades endogenous RA in these cells, mimicking the reduced RA levels induced by acute alcohol exposure and dysregulating the induction of neural crest cells. An exogenous Green Fluorescent Protein (eGFP) cDNA was placed downstream of the Cyp26A1 cDNA as a visual reporter for the activation of the Cyp26A1 expression cassette. Hence, the mouse model is named Gsc:Cyp26A1. My thesis will characterize the craniofacial and neurodevelopmental malformations observed in the Gsc:Cyp26A1 mouse model and establish retinoic acid deficiency at gastrulation as a likely or potential major etiological factor in the clinical presentation of FASD.

Chapter 2: Effects of Prenatal Alcohol Exposure: Insights into FASD using PAE Rodent Models

Foreword

The goal of this review paper to is to describe the past few decades of robust and reproducible PAE mouse models. Moreover, the dosage, duration, and gestational timing of these PAE paradigms will be taken into consideration and mouse models will be assessed for the full spectrum of FASD-like outcomes. Prenatal Alcohol Exposure (PAE) is a medical condition in pregnant women who consume alcohol during pregnancy, even without knowledge of pregnancy during early first trimester. PAE is known to cause birth defects and neurodevelopmental abnormalities, and is one of the requirements for diagnosis of Fetal Alcohol Spectrum Disorder (FASD). Therefore a diagnosis of FASD requires PAE, but PAE does not assure an FASD outcome. Mouse models of PAE are not considered models of FASD for the same reason that PAE does not assure the full, or partial, spectrum of outcomes: craniofacial malformations, brain aberrations, and behavioral deficits as seen in clinical FASD outcomes. The aim of this review is to identify robust and reproducible PAE mouse models that do result in FASD-like phenotypes, and in this regard, better reflect a clinically relevant FASD mouse model.

This chapter is published as a review paper in a special FASD issue of Biochemistry and Cell Biology (NRC Research Press) and is considered the literature review portion of my Master's Thesis.

Authors: Petrelli B[1], Weinberg J[2] and Hicks GG[1]

[1] Department of Biochemistry & Medical Genetics; Regenerative Medicine Program, Faculty of Medicine, University of Manitoba, Winnipeg, Canada.
[2]Department of Psychiatry, University of British Columbia, UBC Institute of Mental Health, Vancouver, Canada.

Author Contribution: I am the lead author. My contributions to this work are: I conceptualized the review paper, the PAE mouse model perspective (references) and wrote the manuscript (co-wrote Section 1 and fully wrote Section 2). Dr. Joanne Weinberg is a colleague and is internationally recognized for her expertise in rodent models of PAE, behavioral outcomes and the underlying genetics and epigenetics of PAE. She co-wrote Section 1 and provided an expert perspective of the field, and relevance of mouse phenotypes to FASD in humans. Dr. Geoff Hicks co-conceptualized the review paper, collaboratively developed the data visualization with me presented in Table 1, provided advice and review of the manuscript.

The revised manuscript is currently under review for the journal Biochemistry and Cell Biology.

Introduction

Clinical and experimental studies have clearly demonstrated that alcohol (ethanol) consumption during pregnancy produces a range of pervasive and long-lasting developmental, neurobehavioral and physiological impairments (Chudley *et al.*, 2005; Sokol, Delaney-Black, & Nordstrom, 2003). The umbrella term fetal alcohol spectrum disorder (FASD) is currently a non-diagnostic term used to describe the postnatal structural and functional defects produced by prenatal alcohol exposure (PAE), and encompasses four alcohol-related clinical diagnostic categories defined by the Institute of Medicine (Stratton *et al.*, 1996): fetal alcohol syndrome (FAS), partial fetal alcohol syndrome (pFAS), alcohol-related neurodevelopmental disorder (ARND), and alcohol-related birth defects (ARBD) (Koren, Nulman, Chudley, & Loock, 2003; Sokol *et al.*, 2003). A diagnosis of FAS, with or without confirmed maternal ethanol consumption during pregnancy, requires the presence of three principal features: characteristic craniofacial dysmorphology, prenatal and postnatal growth restriction, and central nervous system (CNS) neurodevelopmental deficits (K. L. Jones, Smith, Ulleland, & Streissguth, 1973). Individuals that lack some of the characteristic facial features, but present with some of the other diagnostic criteria, may be diagnosed with pFAS if there is confirmed maternal ethanol consumption (Stratton, Howe, & Battaglia, 1996). A diagnosis of ARBD requires confirmed maternal ethanol consumption and one or more congenital anomalies, including cardiac, skeletal, renal, ocular, and auditory, or malformations and dysplasias (Stratton *et al.*, 1996). ARND is the most difficult diagnosis to make, since children present with normal growth and structural development, but display a complex pattern of behavioral and/or cognitive abnormalities induced by confirmed maternal alcohol consumption (Hoyme *et al.*, 2005; Stratton *et al.*, 1996). In

addition to the formal diagnosis of an FASD, psychopathologies (e.g. anxiety, depression, other mood disorders, and substance use disorders), often referred to as "secondary disabilities," are expressed at disproportionally higher rates in individuals prenatally exposed to alcohol (Kodituwakku, 2007; O'Connor *et al.*, 2002; O'Connor & Paley, 2006; Roebuck, Mattson, & Riley, 1999), which increases the health risks of these individuals as well as the emotional and financial cost to the family and health care system (Stade *et al.*, 2009). Overall, the estimated incidence of FASD is thought to be approximately 1 in 100 live births, although recent epidemiological studies indicate prevalence rates as high as 2–5% (May *et al.*, 2009).

1. Risk Factors for Alcohol Teratogenicity and FASD

The potential impact of prenatal alcohol exposure varies considerably among exposed individuals, with some infants displaying serious alcohol-related effects and others showing no overt signs of an FASD (Khaole, Ramchandani, Viljoen, & Li, 2004). Therefore, it is important to understand the variables that may increase or decrease the probability that PAE will produce deleterious effects on fetal development. These factors include the gestational timing, duration, and dose of alcohol exposure (Astley, Magnuson, Omnell, & Clarren, 1999), amount consumed per drinking session (Khaole *et al.*, 2004), genetic and epigenetic factors (Kaminen-Ahola *et al.*, 2010; Mantha, Laufer, & Singh, 2014), maternal and fetal stress (Weinberg & Bezio, 1987; Weinberg, 1989), nutritional status (Keen *et al.*, 2010; Weinberg, 1985), and alcohol metabolism capacity of the mother, factors which are all known to be critically involved in alcohol teratogenicity (Ramchandani, Bosron, & Li, 2001; Riley, Infante, & Warren, 2011).

1.1 Dose, Duration, and Timing of Alcohol Exposure

Studies by Chernoff (1977), and Randall and Taylor (1979), verified a positive correlation between maternal blood alcohol concentration (BAC) and developmental malformations, a finding further validated by the seminal research of West and colleagues (Pierce and West, 1986b, West *et al.*, 1987, West *et al.*, 1989, Pierce and West, 1986a). The use of varying alcohol treatment regimens in animal models has been critical in elucidating alcohol's teratogenic effects. Regimens may involve acute maternal administration (i.e., 1-2 doses) during critical periods of fetal development (Godin *et al.*, 2010; Idrus & Napper, 2012; Sulik, Johnston, & Webb, 1981), trimester-equivalent fetal and/or neonatal alcohol exposure (Bake, Tingling, & Miranda, 2012; G. F. Hamilton, Boschen, Goodlett, Greenough, & Klintsova, 2012; Murawski, Jablonski, Brown, & Stanton, 2013; Wagner, Klintsova, Greenough, & Goodlett, 2013), intermittent binge-like exposure (Ramadoss, Wu, & Cudd, 2008; Sawant *et al.*, 2013), or chronic exposure throughout gestation (Green *et al.*, 2005; K. G. Hellemans, Verma, Yoon, Yu, & Weinberg, 2008; Iqbal *et al.*, 2005; Iqbal, Brien, Kapoor, Matthews, & Reynolds, 2006; Probyn *et al.*, 2013; Uban, Comeau, Ellis, Galea, & Weinberg, 2013).

Timing of alcohol exposure may be equally as important as BAC. In the early and mid-1980s, Webster *et al.* (1980), as well as Sulik and colleagues (Sulik and Johnston, 1983; Sulik and Schoenwolf, 1985), demonstrated that the timing of alcohol exposure was crucial to the development of craniofacial anomalies, a signature feature of FAS in humans. In addition, the timing of exposure can have major implications for brain development. The teratogenic effects of alcohol may be particularly detrimental to CNS development during critical periods of vulnerability, such as during the brain growth spurt, which occurs in the third trimester in the human and in the early postnatal period in the rat and mouse (Dobbing & Sands, 1979). Nevertheless, PAE can impair brain development throughout all stages of gestation, including

effects on neurogenesis, differentiation, and synaptogenesis (Cudd, 2005; Dobbing & Sands, 1979; Guerri, 1998; West, Chen, & Pantazis, 1994). Indeed, using a rat model of PAE, early postnatal alcohol exposure has highlighted the enduring effects of PAE on neurogenesis, a process that continues throughout life in select areas of the brain, most notably the dentate gyrus within the hippocampus (Klintsova *et al.*, 2007; Sliwowska *et al.*, 2010).

1.2 Genetics, Maternal Nutrition, Alcohol Metabolism

Various maternal factors act to increase the risk of alcohol teratogenicity in the developing fetus. Firstly, the presence of genetic polymorphisms of alcohol-metabolizing enzymes may significantly increase or decrease the risk of alcohol teratogenicity in the fetus. For example, maternal polymorphisms manifesting as increased alcohol dehydrogenase activity and enhanced alcohol metabolism have been associated with a decreased incidence of alcohol teratogenicity (Eriksson *et al.*, 2001); Jacobson *et al.*, 2006). Secondly, inadequate maternal nutrition may increase the risk of alcohol teratogenicity throughout fetal development. Deficiencies in various nutrients, including folic acid, iron, choline, and omega-3 fatty acids, are associated with alcohol-induced fetal growth restriction and neurobehavioral teratogenicity in postnatal offspring (Fuglestad *et al.*, 2013; Idrus, Happer, & Thomas, 2013; Patten, Brocardo, & Christie, 2013; Rufer *et al.*, 2012; Thomas, Idrus, Monk, & Dominguez, 2010; Wainwright *et al.*, 1990; L. L. Wang *et al.*, 2009). Thirdly, the ability and extent of the maternal-fetal unit to metabolize alcohol may greatly affect the risk of alcohol teratogenicity. The capacity for alcohol metabolism among pregnant women varies up to eightfold (from 0.0025 to 0.02 g/dl/h), which may help to explain the variation in phenotypic presentation of FASD following maternal consumption of similar doses of alcohol (Burd, Blair, & Dropps, 2012). The capacity for alcohol metabolism in pregnant

women varies with age, ethnicity, hormonal status, body composition and lean body mass, liver size, and food intake (Ramchandani *et al.*, 2001). Ultimately, the peak BAC achieved from maternal alcohol consumption is critical to the risk of alcohol teratogenicity and depends on the rate of drinking, gastric emptying, and phase I biotransformation, involving alcohol dehydrogenase and cytochrome P450 2E1, as well as whether the mother is in a fed or a fasted state (Ramchandani *et al.*, 2001). In general, however, mothers of children with FASD consumed more alcohol and achieved a higher BAC than mothers who consumed alcohol, but did not give birth to a child with FASD (Khaole *et al.*, 2004).

1.3 Mechanism of Alcohol's Teratogenic Effects

Direct toxic effects of alcohol on the embryo are well known. Alcohol readily crosses the placental and blood-brain barriers and can thus act directly on developing fetal cells. However, in mammals it is likely that interactions between direct and indirect (maternally-mediated) effects of alcohol are responsible for its adverse effects (Randall, Ekblad and Anton, 1990). Moreover, as alcohol is known to act on or modulate many different target molecules, multiple mechanisms, activated at different stages of development or at different dose thresholds of exposure, probably contribute to the diverse phenotypes seen in FASD (Goodlett, Horn and Zhou, 2005). In this review we will describe the major direct and indirect mechanisms underlying alcohol teratogenicity, and provide examples of some of these mechanisms. An indirect mechanism, endocrine imbalance, will be discussed at greater length, as this is the focus of research in our laboratory.

1.3.1 Direct Teratogenic Effects

Studies have provided abundant evidence that alcohol can have direct effects on fetal growth and development. Studies on non-mammalian species, where the organism develops outside the mother and there are no effects of the placenta or the maternal environment, have provided unique insights into the teratogenic effects of alcohol. For example, using *Caenorhabditis elegans (C. elegans),* a microscopic nematode worm, Davis et al (Davis, Li and Rankin, 2008) showed that chronic exposure to alcohol during larval development temporarily delayed physical growth, slowed development, delayed the onset of reproductive maturity, and decreased both reproductive fertility and longevity. Similarly, acute embryonic exposure of *C. elegans* eggs to high concentrations of alcohol at different stages of development resulted in a lower probability that exposed eggs would hatch into larval worms, at least at some stages. For worms that did hatch, many displayed distinct physical dysmorphologies. Studies in chicks have similarly revealed direct adverse effects of alcohol on the fetus. Pennington *et al.* (Pennington *et al.*, 1983) reported dose-response effects of alcohol on suppression of the rate of cell division in embryonic tissue, resulting in fewer cells/embryo for a given time in gestation. Interestingly, it was suggested that the suppression in cell division may be related to alcohol-induced changes in the metabolism of the prostaglandins, which are naturally produced hormone-like fatty acids known to be involved in a wide range of biological processes, including the regulation of blood pressure, metabolism and immune response (see further discussion on prostaglandins below). Cartwright and Smith (Cartwright and Smith, 1995) used a chick model to study mechanisms underlying the craniofacial abnormalities observed in FAS. A single alcohol exposure was shown to result in a range of craniofacial abnormalities, depending on dose and timing of exposure. This work

provided important evidence indicating that the timing of alcohol exposure relative to stage of development could account, in part, for the variations in craniofacial defects observed in FAS.

Importantly, direct effects of alcohol on mammalian embryos have also been observed. For example, Brown et al (Brown, Goulding and Fabro, 1979) showed that rat embryos grown in culture media containing alcohol displayed dose-dependent embryonic retardation of growth and differentiation, with specific reduction in both DNA and protein content. Consistent with these findings, data from *in vivo* studies have shown that both acute and chronic alcohol exposure *in utero* can inhibit protein synthesis and decrease RNA and DNA content in the fetal and neonatal brain (Rawat, 1975). Similarly, Gallo & Weinberg (Gallo and Weinberg, 1986) reported that prenatal and early postnatal alcohol exposure can reduce brain, heart and kidney weights in newborns due to direct effect on protein and/or DNA content. Alcohol-induced disruptions in the proliferation of stem cell populations are another example of the direct actions of alcohol on the fetus, leading to a reduction in the generation of both new neurons and new glial cells (Miller, 1992; Guerri *et al.*, 1993). Neuronal cell damage and/or cell death can also occur through both programmed cell death (Ikonomidou *et al.*, 2000) and inhibition or disruption of enzymes that play a role in metabolism in neural tissue (Goodlett, Horn and Zhou, 2005). Importantly, extensive changes in organ weight, although not detrimental in and of themselves, may be indicative of altered functioning that could potentially increase vulnerability to later diseases/disorders. Of particular interest to both researchers and clinicians, are the fairly large differences in the susceptibility of different brain regions to alcohol, depending on dose and timing of exposure. The hippocampus, amygdala and cerebellum show particular sensitivity to inhibition of protein synthesis by alcohol, resulting in decreased numbers of mature neurons. Furthermore, prenatal exposure to alcohol can result in a disorganized cortical architecture,

which ultimately influences the pattern of communication in and across regions involved in higher cognitive function. This suggests one possible mechanism by which prenatal alcohol exposure might produce cognitive deficits in children with FASD (Clarren, 1986). Similarly, alcohol-induced changes in function of the hippocampus and cerebellum are known to be involved in the behavioral alterations that occur in FASD (Michaelis, 1990; Guerri, 1998). Whether the latter changes are due to direct or indirect effects of alcohol remains to be determined.

1.3.2 Indirect Teratogenic Effects

Numerous secondary or indirect mechanisms mediating the adverse effects of alcohol on neurobiological and neurobehavioral outcomes have been demonstrated in animal models and *in vitro* studies. These include: nutritional deprivation or deficiencies (e.g., calories, protein, zinc, folate, vitamin A); abnormalities in calcium signaling; altered alcohol-prostaglandin interactions; placental dysmorphology/dysfunction; alcohol-induced circulatory changes in placenta and/or fetus; disrupted cell-cell interactions (cell adhesion); interference with growth factors or other cell signaling mechanisms that mediate cell proliferation, growth, differentiation, migration and maturation; oxidative stress and free radical damage; disruption of neuronal development in specific cell populations (e.g. serotonergic neurons); and disruption of endocrine balance (Randall, Ekblad and Anton, 1990; West, Chen and Pantazis, 1994; Guerri, 1998; Shibley, McIntyre and Pennington, 1999; Goodlett, Horn and Zhou, 2005). Here we will discuss several of these indirect mechanisms, and then present an in-depth discussion of one of these – disruption of endocrine balance.

Alcohol effects on prostaglandins

Seminal work by Carrie Randall's group (Randall, Anton and Becker, 1987; Randall *et al.*, 1989) has shown that prostaglandins may play a role in mediating the adverse effects of alcohol. Acute alcohol exposure stimulates prostaglandin synthesis, and prostaglandin degradation is impaired following chronic alcohol exposure. If abnormally high levels occur due to such disruption of the balance between synthesis and degradation, prostaglandins themselves may increase fetal mortality during development. Randall's work in a mouse model shows that inhibition of prostaglandin synthesis can attenuate some of the deficits induced by prenatal alcohol exposure. Thus, for example, treatment of pregnant mice with low dose aspirin, which inhibits prostaglandin synthesis, attenuated the effects of prenatal alcohol exposure on fetal mortality and reduced the incidence of birth defects by 50%. Clearly, prostaglandins do not mediate all of alcohol's effects on fetal growth and development. However, the data reveal one potential mechanism that could contribute to at least some of alcohol's adverse effects, and suggest one possible direction for the development of therapeutic interventions.

Alcohol-induced disruption of cell-cell interactions or cell adhesion

Cell adhesion molecules (CAMs) are proteins that aide in cell-cell binding and facilitate interaction between nerve cells and their surrounding environment, both of which are critical in normal development of the nervous system. One such CAM is the L1 cell adhesion molecule, a member of the immunoglobulin superfamily (Ramanathan *et al.*, 1996; Bearer, 2001a, 2001b; Wilkemeyer *et al.*, 2002; Gubitosi-Klug, Larimer and Bearer, 2007). When L1 binds to neurons, it activates cell signaling cascades that mediate functions such as cell-cell adhesion, outgrowth of nerve cell processes, and neuron migration. Children with mutations of the gene for L1 may

show mental retardation and a variety of brain lesions similar to those in children with FAS. Research has shown that alcohol can inhibit the functions of L1 and that antagonists that prevent alcohol inhibition may be neuroprotective. *In vivo* studies have tested the effects of two small peptides secreted by glial cells: SALLRSIPA (SAL), an active fragment of activity-dependent neurotrophic factor (ADNF); and NAPVSIPQ (NAP), an active fragment of activity-dependent neuroprotective protein. The data demonstrated that NAP and SAL are extremely potent and effective antagonists of alcohol inhibition of L1 adhesion. Ongoing work is examining the therapeutic potential of NAP and SAL in attenuating adverse effects of prenatal exposure to alcohol on the ability of nerve cells to interact appropriately with each other or with their environment.

Alcohol and oxidative stress

Data have shown that, in addition to its ability to antagonize alcohol inhibition of L1, NAP may also be a potential therapeutic treatment for the oxidative stress associated with alcohol exposure (Sari, 2009). Oxidative stress (interaction of high levels of free radicals or reactive oxygen species with molecules within the cell) is a known mechanism of alcohol-induced cellular injury, and has been shown to play a role in alcohol teratogenesis (LeBel and Bondy, 1991; Kotch, Chen and Sulik, 1995). Fetal tissues generally have lower activities and levels of oxidative defences than adult tissues, and thus the fetus is highly sensitive to oxidative stress, especially early in gestation. Oxidative stress in the fetus can cause a wide range of problems, from structural malformations to embryonic death, through effects of free radicals on cell membranes, cytoskeleton, mitochondria and membrane protein receptors (Henderson *et al.*, 1995). Interestingly, Spong et al (Spong *et al.*, 2001) found that treatment with NAP and SAL in

combination prevented fetal death and growth restriction in a mouse model of FAS. Protection from the toxic effects of alcohol appeared to result from blockade of induction of free radicals by alcohol. Further support for this possibility comes from the work of Sari and colleagues (Sari, 2009) who showed that prenatal alcohol-induced cell death is mediated in part through mitochondrial dysfunction. Administration of NAP together with alcohol to pregnant mice on embryonic day 7 reversed alcohol-induced changes in mitochondrial pathways and thus blocked the increased cell death resulting from alcohol-induced oxidative stress. Moreover, Wilkemeyer et al (Wilkemeyer *et al.*, 2002) suggest the possibility that loss of L1-mediated cell-cell adhesion may also be linked to oxidative injury through induction of programmed cell death triggered by loss of contact of nerve cells with each other or with their environment. The possibility that NAP could be utilized as a therapeutic agent against the oxidative stress associated with alcohol exposure is a very exciting translational outcome of this basic research on the mechanisms of alcohol's actions on the embryo.

Disruption of endocrine balance

Alcohol has long been known to alter endocrine function in the adult organism. Studies in both humans and animal models, involving acute administration of alcohol or chronic alcohol consumption, have demonstrated effects of alcohol on secretory activity of the adrenal, ovaries, testes and thyroid, as well as on secretion of numerous pituitary hormones, including growth hormone, prolactin, vasopressin, adrenocorticotropin and the gonadotropic hormones (reviewed in (Weinberg, Nelson and Taylor, 1986; Weinberg, 1993; Weinberg J, 1993)). Furthermore, it has been shown that alcohol can act directly on the endocrine glands themselves as well as (or in addition to) having an action on central aspects of hypothalamic-pituitary function. Interestingly,

much of what is known of alcohol-related effects on endocrine function comes from male subjects. It is only relatively recently that studies in clinical settings and with animal models of alcoholism have begun to include female subjects. Even fewer studies have examined the effects of alcohol exposure on endocrine function during pregnancy.

We know that alterations in both maternal and offspring endocrine function are among the physiological abnormalities produced by maternal alcohol intake. Whether alcohol-induced endocrine imbalances contribute to the etiology of FASD is unknown, but it is certainly a possibility (Anderson, 1981). The effects of alcohol on interactions between the pregnant female and fetus are complex (Rudeen and Taylor, 1992; Weinberg, 1993, 1994; Weinberg J, 1993), and both direct and indirect effects of alcohol on fetal development are known to occur. Alcohol readily crosses the placenta, and can therefore act directly on developing fetal cells and tissues, including those related to endocrine function. In addition, because the pregnant female and fetus constitute an interrelated functional unit, disruption of the normal hormonal interactions between the pregnant female and the fetus by alcohol can indirectly alter the development of fetal metabolic, physiological and endocrine functions. Alcohol intake can also affect the female's ability to maintain a successful pregnancy, resulting in miscarriage or, if the fetus is carried to term, possible congenital defects.

Using a rat model, research in our laboratory has focused on the effects of maternal alcohol consumption on the maternal and offspring hypothalamic-pituitary-adrenal (HPA) axis, an endocrine system involved in multiple metabolic functions and in the ability to respond appropriately to stressors. A particular focus has been on fetal programming. Fetal or early programming refers to the concept that early environmental or non-genetic factors, including pre- or perinatal exposure to stress, drugs or other toxic agents, can permanently organize or

imprint physiological and behavioral systems and increase vulnerability to illnesses or disorders later in life (Bakker, Bel and Heijnen, 2001; Welberg and Seckl, 2001; Matthews, 2002). The HPA axis is highly susceptible to programming during fetal and neonatal development (Welberg and Seckl, 2001; Matthews, 2002), and data suggest the possibility that ethanol-induced disruption of the reciprocal interconnections between the maternal and neonatal HPA axes may provide a common pathway for fetal programming by a number of different agents (Angelucci *et al.*, 1985). We have been examining the hypothesis that alcohol-induced fetal programming of HPA activity sensitizes neuroadaptive mechanisms that mediate HPA activity and regulation, resulting in hyper-reactivity to subsequent life stressors, and, in turn, increased vulnerability to illnesses including mental health disorders such as depression, anxiety and addiction.

2 Rodent Models of Prenatal Alcohol Exposure

Clinical studies over the past 40 years have demonstrated that FASD results from maternal alcohol consumption during pregnancy. Prenatal Alcohol Exposure is a clinical term that simply records in the patient history admission or evidence of alcohol consumption during the pregnancy. It is a prerequisite fact for the diagnosis of FASD in a child; however, it's clear that PAE alone does not result in FASD for most children. The term PAE in animal models is quite different – it refers specifically to an experimental condition where the variables of dosage, duration and gestational timing can be controlled. In this review we examine rodent PAE models and focus on those with demonstrated craniofacial, aberrant brain development, and behavioral phenotypes that may be considered FASD-like outcomes.

FASD is a complex disorder, expected to involve multiple pathways in the developing embryo and fetus. Consequently, the etiology of the disorder remains unknown. Rodent models of PAE

have significantly advanced our insight over the past 10 years regarding this conundrum. The body of research determining the dosage of alcohol (Randall and Taylor 1979; Pierce and West 1986; Bonthius, Goodlett, and West 1988), duration (whether acute or chronic) and the gestational timing of alcohol exposure (Anthony *et al.*, 2010; Godin *et al.*, 2010b; Lipinski *et al.*, 2012; Parnell *et al.*, 2013) is now beginning to have a depth of collective outcomes that supersede the high degree of variation often associated within individual PAE models. Moreover, well established PAE models with reproducible phenotypes now allow the examination of other risk factors, such as maternal genetics and offspring epigenetics (Kaminen-Ahola, Ahola, Maga, *et al.*, 2010), maternal nutrition (Keen *et al.*, 2010), maternal metabolism (Burd, Blair and Dropps, 2012), and maternal and offspring stress (Weinberg, 1989; Alberry and Singh, 2016). Each play an additive role in the etiology of FASD.

In this review will examine PAE mouse models firstly based on gestational alcohol exposure (mouse gestation equivalent): first trimester (GD0-10), second trimester (GD11-20), and third trimester (PN1-10), taking into context the alcohol dosage and duration used. Next, we will overlay robust FASD-like phenotypes, including craniofacial, physiological/brain, and behavioral phenotypes observed in PAE mouse models that reflect FASD clinical features in children. Analysis of these data should provide a valuable tool for any researcher wishing to choose the best-suited PAE model in their research or to investigate established PAE models for FASD comorbidities. It should also allow patterns to be recognized linking gestational timing, dosage and duration of PAE with FASD-like outcomes. The latter could be particularly insightful and lead to a better understanding of the molecular mechanisms underlying FASD.

First Trimester PAE

The first trimester equivalent in mice comprises gestational days 0-10. It starts at the moment of conception and includes the pre-implantation period, implantation period, gastrulation, and the beginning of neurulation. First trimester PAE mouse models tend to use either an acute delivery of alcohol during the gastrulation-neurulation developmental stages, or a chronic exposure to alcohol during conception-gastrulation stages. Maternal alcohol delivery during this trimester is most often performed by oral gavage, intraperitoneal (ip) injection, liquid diet, or volunteer *ab libitum* drinking. Both oral gavage and ip injection are considered high BAC alcohol exposure (>200mg/dl) and usually performed for acute exposure studies. Liquid diet and *ab libitum* drinking are considered low to moderate BAC alcohol exposure (80-150mg/dl) and are usually performed for chronic exposure studies (Patten, Fontaine and Christie, 2014). The use of *ab libitum* drinking for alcohol exposure studies is commonly only seen when working with C57Bl6 mouse strains as these mice prefer alcohol over water (Wahlsten *et al.*, 2007). This section will focus on chronic exposures spanning the first trimester and acute exposures during gastrulation and early neurulation. Chronic and acute exposures in the preimplantation and implantation periods are extensively reviewed in elsewhere in this special issue.

There are a limited number of publications documenting chronic first trimester prenatal alcohol exposure studies spanning GD0-10. Kaminen-Ahola *et al.* utilize a 10% v/v ethanol, *ab libitum* drinking model, from GD0.5 to 8.5 as a chronic low-moderate BAC first trimester alcohol exposure study (Kaminen-Ahola, Ahola, Flatscher-Bader, *et al.*, 2010; Kaminen-Ahola, Ahola, Maga, *et al.*, 2010). Chronic *ab libitum* alcohol consumption during the pre-implantation period to late gastrulation/early neurulation demonstrates midfacial dysmorphologies, specifically a wider inter-orbital distance (the distance between the eye sockets) and cranium width, while

having a shorter midface compared to WT controls (Kaminen-Ahola, Ahola, Maga, *et al.*, 2010). Moreover, these mice at PN30 demonstrate pre-maxillary deviation of the midface (curved snout) and loss of the interfrontal bone that is normally found between the maxillary and parietal bone regions of the cranium in WT controls (Kaminen-Ahola, Ahola, Maga, *et al.*, 2010). These PAE offspring also consistently exhibit a smaller weight and skull size, suggesting intrauterine growth restriction and microcephaly, compared to control mice (Kaminen-Ahola, Ahola, Flatscher-Bader, *et al.*, 2010; Kaminen-Ahola, Ahola, Maga, *et al.*, 2010). Interestingly, midfacial and pre-maxillary malformations of the skull are seen in FASD, specifically FAS patients in whom midfacial hypoplasia and premaxillary rotational effects are common (Suttie *et al.*, 2013). Intrauterine growth restriction, including small skull size (<3rd percentile), are common features of children with FAS (Astley, Bledsoe and Davies, 2016).

Acute first trimester prenatal alcohol exposure studies typically encompass the gastrulation and early neurulation developmental stages (GD7-9). Seminal research performed by Sulik and colleagues have shown that a single acute dose of alcohol on each of these 3 days can produce distinct and profound craniofacial malformations in some embryos that are reminiscent of sentinel clinical FAS features (Lipinski *et al.* 2012; Godin *et al.* 2010; Parnell *et al.* 2013; Parnell *et al.* 2009). Sulik *et al.* used 2.9 g/kg ethanol (2 doses, 4 h apart, i.p.) at gestational day 7.0 to model an acute high BAC PAE (Sulik and Johnston 1983; Godin *et al.* 2010). This single day binge model exposure produces frontonasal prominence malformations: deficient medial nasal processes (closely set nostrils), abnormally longer maxillary processes (long upper lip), abnormal/deficient pre-maxillary bone, eye malformations, including anophthalamia, microphthalmia, colobomas, and incidence of forebrain exencephally (Sulik and Johnston, 1983; Godin *et al.*, 2010b). Varying the timing of the PAE dosage plus or minus 4 h from GD7.0

results in a strikingly different phenotype; frontonasal prominence malformations in embryos assessed at GD14 were 59.6%, 44.4% or 27%, depending on whether the PAE occurred at GD7-4h, GD7.0 or GD7+4h, respectively. Conversely, observed embryo reabsorption rates were 9.5%, 18.2% or 45.9% in the same PAE groups (Sulik and Johnston, 1983). This study demonstrates that PAE at early gastrulation is a very sensitive window for craniofacial development and viability.

Impact of acute GD7 PAE on the frontonasal prominence abnormalities can be further characterized at GD17. The frontonasal prominence is an early embryonic structure that develops into the future forebrain and face, as directed firstly by retinoic acid and later on by SHH during early neurulation (Carlson B 2014). Abnormal frontonasal prominence structure during embryogenesis is indicative of future forebrain and facial aberrations (DeMyer W, Zeman W, 1964). GD17 embryos exhibited many craniofacial malformations, including closely set nostrils, a long upper lip, eye malformations as well as midfacial hypoplasia and clefting, cleft palate, and micrognathia (Godin *et al.*, 2010b; Hong and Krauss, 2012; Lipinski *et al.*, 2012). GD7 PAE embryos at GD17 can exhibit forebrain dysmorphologies reminiscent of holoprosencephaly (HPE): pituitary agenesis, third ventricle dilation, reduction/loss of olfactory bulbs, reduction in cerebral cortex size, and malformed lateral ventricles (Godin *et al.* 2010a, DeMyer W, Zeman W 1964; Sulik and Johnston 1983). MRI studies at PN45 adult mice, found that the anterior commissure was significantly reduced in GD7 PAE mice compared to control mice. Moreover, the myelin content of the 3 largest white matter tract bundles, anterior commissure, corpus callosum, and hippocampal commissure, were significantly reduced (Cao *et al.*, 2014). These studies demonstrates that acute PAE at early gastrulation is sufficient to induce developmental

changes to brain structure and grey matter and white matter tracts that continue well into adulthood.

Development of robust PAE models with reproducible phenotypes allows one to take advantage of transgenic mouse models as a way to elucidate the underlying developmental mechanisms of FASD at the genetic level. Sonic Hedgehog, *SHH*, is an important gene required for proper craniofacial formation and growth; heterozygous/knock-out transgenic mouse models of *Shh* and downstream *Shh* pathway genes (*Cdon*, *Ptch1*, *Gas1*, and *Gli2*) have shown incidence of HPE (Roessler E, 2010). Interestingly, an acute ethanol dose administered at late gastrulation-early neurulation to a pregnant $Shh^{+/-}$ (or a downstream pathway gene) female, increases the incidence and severity of HPE (Roessler E, 2010). PAE $Cdon^{-/-}$ transgenic offspring on 129S6 background show a significant increase in Alobar and Lobar HPE incidence compared to $Cdon^{-/-}$ and WT PAE controls (Hong and Krauss, 2012)(Table 1). Moreover, there is a significant incidence of FASD related pathologies in PAE $Cdon^{-/-}$ offspring; these features include: external midline defects, deficient philtrum, shortened and fused pre-maxillary bone, and underdeveloped maxillary region (Hong and Krauss, 2012). *In situ* hybridization experiments on PAE $Cdon^{-/-}$ GD10.25 embryos show reduced mRNA expression of *Gli1* and *Ptch1*, both downstream *Shh* pathway genes (Hong and Krauss, 2012). PAE $Shh^{+/-}$ and $Gli2^{+/-}$ (haploinsufficient) transgenic offspring show an increased incidence of FASD related facial dysmorphology: medial facial deficiency, reduced/loss internasal distance, and loss of lip notch/longer philtrum compared to haploinsufficent and WT PAE controls (Kietzman *et al.*, 2014) (Table 1). $Shh^{+/-}$ and $Gli2^{+/-}$ PAE embryos had a 3.2 and 6.6 fold increase, respectively, in facial dysmorphology score compared to WT littermates. Interestingly, $Shh^{+/-}$ and $Gli2^{+/-}$ PAE embryos had incidence of HPE in which the severity of HPE correlated to the severity of facial dysmorphology (Kietzman *et al.*, 2014).

Similar observations were found in *Rdh10*$^{-/-}$ and *Raldh2*$^{-/-}$ mice, linking aberrant retinoic acid signaling as a cause of midfacial defects (Niederreither *et al.*, 2002; Rhinn *et al.*, 2011). Taken together, the use of transgenic mice in PAE models allows for the interpretation of the role that certain developmental genes and their downstream pathways may play in the mechanism of FASD. Moreover, it allows researchers to now study the role of maternal/offspring genetics, as well as epigenetic signatures to discover biomarkers and potential risk factors of FASD.

Acute GD8 PAE studies (late gastrulation) show less severe frontonasal prominence abnormalities than those seen in GD7 PAE. GD8-8.5 PAE craniofacial malformations include: eye malformations (microphthalmia and colobomas), midfacial hypoplasia, reduced snout width, shorter upper lip length, and micrognathia/mandibular hypoplasia. (Lipinski *et al.* 2012; Parnell *et al.* 2009). Interestingly, an FASD craniofacial dysmorphology feature seen in GD7 PAE embryos, a longer philtrum/upper lip length was no longer seen in GD8 or 8.5 PAE embryos. Instead, a shorter upper lip length was seen in GD8.5 PAE embryos, a feature that is more reminiscent of Di George Syndrome, a rare genetic disorder that at one time some considered was associated with FASD (Sulik *et al.* 1986). GD8-8.5 PAE embryos also do not exhibit clefting or cleft palate malformations in older embryos, as seen in GD7 PAE embryos.

Using Magnetic Resonance Microscopy Imaging, Parnell *et al.* demonstrated that GD8 PAE embryos have a 8.2% reduction in crown-rump lengths and a 25% reduction in total body volume (including a 19.5% smaller brain volume) compared to non-PAE control (Parnell *et al.* 2009, Godin *et al.* 2010). Although microcephaly is not specifically stated in the paper, the latter finding is indicative of microcephaly. Brain volume region changes exhibited in GD8 and GD8.5 PAE were quite different to those of GD7. GD8 PAE embryos studied at GD17 show: a significant reduction in brain volume; forebrain dysmorphologies, not in the form of HPE, but

instead reduction in olfactory bulbs; and a reduction in hippocampus and cerebellum volumes, compared to non-PAE controls (Parnell *et al.* 2009). The pituitary, septal region, and ventricles all were significantly larger in GD8 PAE embryos compared to non-PAE controls, even though total brain volumes were reduced. GD8.5 PAE embryos studied at GD17 show a significant increase in volume of olfactory bulb, hippocampus, third ventricle, and pituitary regions compared to non-PAE controls (Lipinski *et al.*, 2012). These data suggest that late gastrulation PAE (GD8-8.5) does not produce as severe an FASD-like craniofacial phenotype compared to early gastrulation PAE (GD7) when using the same dosage concentration and acute duration in studies.

Acute GD9 and 10 PAE studies show negligible frontonasal prominence abnormalities compared to GD7 and GD8 PAE embryos. Early neurulation GD9-10 PAE mouse models show brain volume aberrations compared to non-PAE controls, but do not produce facial dysmorphologies (Parnell *et al.* 2013; O'Leary-Moore *et al.* 2010). In MRI studies Parnell *et al.* demonstrated that GD9-10 PAE embryos have no statistically significant reduction in crown-rump length nor total body volume compared to non-PAE stage-matched controls, unlike GD7-8 PAE embryos (Parnell *et al.* 2013; O'Leary-Moore *et al.* 2010). GD9-10 PAE embryos have a significant reduction in total brain volume ~13.6% compared to non-PAE stage-matched controls (Parnell *et al.* 2013; O'Leary-Moore *et al.* 2010). These results reinforce the theory that without facial dysmorphologies, there are no severe brain aberrations (DeMyer W, Zeman W, 1964; Sulik and Johnston, 1983). Even though there was significant change in total brain volume in GD9-10 studies only certain regions of the brain exhibited significant change in volume and/or morphology. GD9 PAE embryos studied at GD17 show a significant reduction in cerebellar volume ~14%, and lateral, third, and fourth ventricles show a significant increase in volume and

altered morphology compared to non-PAE controls (Parnell *et al.*, 2013). GD10 PAE embryos examined at GD17 exhibit a reduction in cerebral cortex volume, a significant increase in third ventricle volume and further showed altered morphology in lateral, third, and fourth ventricles compared to non-PAE controls (O'Leary-Moore *et al.* 2010).

These data suggest that early neurulation PAE (GD9-10) predominantly results in changes to brain volume and morphology, rather than loss of complete brain regions as seen in GD8 PAE. Cerebellar reduction and ventricular enlargement are both features seen in clinical FASD outcomes (Spadoni *et al.*, 2007). Furthermore, the ventricular enlargement in both GD9-10 PAE embryo studies indicates that brain region morphology is being affected, most likely further showing a loss of neurons and glia at the cellular level. Ventricular regions are devoid of cellular material and instead hold cerebral spinal fluid, enlargement of these regions indicates a loss of neural cell lineages, as the overall brain volumes remain the same in GD9-10 PAE models. In GD9 PAE embryos the cerebral cortex volume is reduced by ~5%; although not significant, this demonstrates that regions adjacent to ventricles, in this case the lateral ventricle was enlarged, affect the cortex (Parnell *et al.*, 2013). In GD10 PAE embryos the enlarged third ventricle likely affected the changes in morphology of the thalamus and hypothalamus regions found directly adjacent to the third ventricle. These brain volumetric and morphological changes demonstrate that early neurulation PAE modulates neural cell progenitor lineages by apoptosis and epigenetic mechanisms that change brain structure at later developmental stages and into adulthood.

Most recently, the popularity of DNA modification (methylation) experiments in PAE studies have increased dramatically in an attempt to elucidate the genetic pathways/mechanisms of FASD. PAE mouse model studies are being performed to study global methylation patterns and identify specific genes currently implicated with FASD brain aberrations (Hill *et al.* 2014;

Kaminen-Ahola, Ahola, Maga, *et al.* 2010). Many of these methylation studies have used robust acute and chronic dosage paradigms already covered in this review. Garro *et al.* have shown in their GD9-11 (early neurulation) gavage model that global DNA methylation and *Dnmt1* activity is down in the whole embryo, showing that there are more genes actively transcribing than there should be at GD11. Acute GD9 PAE (5.8g/kg, intragastric intubation) causes a decrease in *Igf2* DNA methylation in the entire embryo, causing an increase in *Igf2* expression in older GD17 embryos. Chronic *ad libitum* first trimester PAE studies (GD0.5-8.5, 10% v/v ethanol) show increased DNA methylation of *Vmn2r64* and *Olfr110* in PN28 male mice and decreased DNA methylation of *Vglut2* in PN87 male mice. Taken together, the use of DNA methylation provides PAE researchers new tools to help elucidate the mechanisms of FASD.

Second Trimester PAE

The second trimester in mice comprises gestational days 11-20. It starts during neurulation, includes organogenesis and ends at birth. Second trimester PAE mouse models tend to more often use a chronic alcohol exposure or an acute delivery of alcohol at specific second trimester gestational timepoint. Maternal alcohol exposure delivery during this trimester is most often performed by oral gavage, i.p., liquid diet and *ad libitum* drinking.

Second trimester PAE studies typically use robust first-to-second trimester chronic PAE models and acute PAE second trimester models to assess craniofacial malformations, brain aberrations, behavioral consequences, organ development, cerebral blood flow, and gene expression in developing embryos (Anthony *et al.*, 2010; Cui *et al.*, 2010; Akers *et al.*, 2011; El Shawa, Abbott and Huffman, 2013; Shen *et al.*, 2013). Anthony *et al.* utilize a 4.8% v/v ethanol, liquid diet model, from GD0 to 19 as a chronic low-moderate BAC first-to-second trimester alcohol

exposure study. This chronic liquid diet model of alcohol exposure from conception to birth produced midfacial dysmorphologies, specifically, a reduction in upper- and mid- facial depth measurements in both C57Bl6 sub-strains of mice (BJ6 and BN6). B6N mice also show a reduction in snout height and a narrowed bigonial line (width of mouth/lips) (Anthony *et al.*, 2010). In a follow-up study, researchers showed that a similar PAE paradigm (4.2% v/v ethanol, liquid diet model, from GD7 to 16) but using a shorter PAE duration compared to the original study produced a smaller skull volume and circumference compared to controls in PN7 and 21 mice (Shen *et al.*, 2013). PN7 mice exhibited a significant reduction in the parietal region of the skull, whereas PN21 mice exhibited a significant reduction in frontal, parietal, occipital, and mandibular regions of the skull. Shen *et al.* observed that the cranium (frontal, parietal, occipital regions of the skull that cover the brain) had been more sensitive to PAE compared to the face (nasal and mandible regions of the skull). Anthony *et al.*'s study however saw significant reductions in length, height, and width of the embryos facial (face) region using an earlier/longer PAE duration and slightly higher alcohol concentration. This suggests that earlier (and/or longer) chronic PAE exposure produces FASD-like midfacial malformations, and that cranium (skeletal) and brain aberrations will be seen if the facial malformations are present (DeMyer W, Zeman W, 1964). Increasing the dosage in this chronic PAE model results in increased severity of the phenotype. A 10% v/v ethanol liquid diet model demonstrates a reduction in olfactory bulb, hippocampus (specifically the granule cell layer of the dentate gyrus region), and fourth ventricle region volumes at P60 in PAE alcohol exposed offspring. These regions are also affected in individuals with FASD (Akers *et al.*, 2011). Moreover, PAE mice have impaired odor discrimination, not having the ability to discriminate enantiomers R- and S-carvone compared to controls. Interestingly, neural precursor cells in the subependymal zone of the olfactory bulbs

seemed to be the most affected by the alcohol exposure (Akers *et al.*, 2011). The study also found that the basal forebrain, posterior anterior commissure, thalamus, and amygdala are larger in size in PAE exposed mice (Akers *et al.*, 2011). Reduction in the olfactory bulbs and hippocampus volume is consistent with acute first trimester PAE mouse models and clinical FASD diagnosis. However, increases in basal forebrain, thalamus, and amygdala are not commonly seen in PAE mouse models or in clinical FASD cases (Lipinski *et al.* 2012; Parnell *et al.* 2009; Godin *et al.* 2010; Coulter *et al.* 1993).

Cui *et al.* use a 2g/kg and 4g/kg, gavage, GD5 to 19 chronic high BAC alcohol exposures to produce aberrant dendritic spines of pyramidal neurons in the visual cortex. Not only is there a decrease in overall number of dendritic spines in PN30 adult mice, but the remaining dendritic spines have an increased mean length and a further reduction of synaptic vesicles compared to non-PAE controls (Cui *et al.*, 2010). Moreover, these dendritic spine phenotypes were more severe in the 4g/kg cohort compared to the 2g/kg cohort and suggest that persistent alcohol abuse during the first and second trimester produce visual cortex aberrations, in addition to eye malformations that are common in first trimester PAE mouse models and found in individuals with FAS (Coulter *et al.*, 1993; Abdelrahman and Conn, 2009; Godin *et al.*, 2010a). Although this study did not investigate craniofacial malformations, brain aberrations or behavioral deficits, it is likely that the research groups have seen these dysmorphologies to some degree. Acute gavage first trimester studies (evaluated earlier in this review) use comparable PAE doses on only one day (during gastrulation) and those studies achieved a plethora of FASD–like dysmorphologies.

Behavioral deficits due to cellular brain aberrations are also seen in PAE mouse models, commonly found in chronic exposures spanning two or more trimesters. El Shawa *et al.* use a 25%

v/v ethanol, *ab libitum* drinking model, from GD0 to 19 as a chronic low-moderate BAC first-to-second trimester alcohol exposure study. Using CD1 mice, the study shows aberrant somatosensory and visual cortex neuron development, specifically, significantly longer frontal cortex neurons projecting to an ectopically caudal position in visual cortex regions (El Shawa, Abbott and Huffman, 2013). These PAE induced frontal cortex neurons aberrations have been previously demonstrated in other chronic liquid diet PAE mouse models and aberrant neuronal circuitry is common in FASD patients (Sowell *et al.* 2008; Rema and Ebner 1999; Zhou *et al.* 2005). Frontal cortex aberrations have been observed in PAE mouse brains, specifically, malformed cortical layers 1-4, causing overlapping intra-neocortical connections that appear disorganized. PN20 PAE offspring further show increased anxiety and impaired gross and fine motor coordination (El Shawa, Abbott and Huffman, 2013). Abnormalities in forebrain/frontal cortex structure, as seen in this study and in acute first trimester PAE studies, produce anxiety and motor coordination behavioral impairments similar to the impaired executive function seen in FASD patients (Norman *et al.*, 2009).

Impaired organ development is commonly seen in FASD patients (Assadi 2014; Gilberti *et al.* 2013; Hofer and Burd 2009), but poorly examined in rodent PAE models. Despite a paucity of research in FASD comorbidities, some first-to-second trimester PAE models do show underdeveloped lungs and kidneys, cardiac anomalies, and gastrointestinal abnormalities. An acute PAE study using 3.75g/kg, from GD11.5 to 13.5 observed that GD18 PAE embryos have reduced body weight and lung weight. Moreover, lung/body weight ratio in PAE embryos is significantly reduced compared to non-PAE embryos, and upon histological analysis the lungs of PAE embryos are developmentally immature (Wang *et al.*, 2007). Interestingly, the exclusive second trimester acute high BAC alcohol exposure study did not produce craniofacial

malformations as seen in early GD PAE exposures, as noted by researchers of the study. In another acute PAE study using 3.0 g/kg, by ip injection (1X day) at GD12.5-14.5, it was observed using ultrasound that PAE embryos had significantly reduced arterial blood acceleration and velocity from the umbilical cord to the cerebral arteries. Interestingly, this effect was not due to a change in heart rate; rather, each binge exposure suppressed blood flow velocity for a minimum of 24 h (Bake *et al.* 2013). The reduction in arterial blood flow to the embryos brain and to other organs like the lungs, heart, and kidneys compromises their development at a critical stage of development (organogenesis). Not only is a reduction in oxygen (causing hypoxia or hypoxic conditions) a worry, but reduction in blood flow velocity carries other concerns like nutritional deficiencies leading to further cellular stress and ROS production (Wellen and Thompson, 2010).

These studies demonstrate that first-to-second trimester PAE mouse model produce similar, but not as severe craniofacial malformations or brain aberrations compared to acute GD7, 8, 8.5, and 9 PAE models. First-to-second trimester PAE models produce craniofacial malformations that are more IGR-like than those categorized as sentinel FASD features (Anthony *et al.*, 2010; Shen *et al.*, 2013). Furthermore, the brain aberrations seen tend to reflect changes in specific brain regions of the body like olfactory bulb or hippocampus (Akers *et al.*, 2011; El Shawa, Abbott and Huffman, 2013). Chronic first-to-second trimester PAE models aberrations may better resemble pFAS, ARBD and ARND, which lack the severe craniofacial malformations normally observed in FAS cases (Chudley, 2005). An advantage of using first-to-second trimester PAE models is that it allows researchers to study behavioral outcomes and possibly link them to the structural deficits observed (Cui *et al.*, 2010; El Shawa, Abbott and Huffman, 2013). Furthermore, acute second trimester PAE models allow researchers to study the effects of

alcohol exposure during organogenesis and ethanol's effect on organ development in particular (Wang *et al.* 2007; Bake *et al.* 2013).

Third Trimester PAE

The third trimester in mice comprises a 10 day period from postnatal day 1-10. It starts after birth and involves the beginning of the weaning period, when lungs, brain and endocrine system (HPA Axis) finish developing. Third trimester PAE mouse models tend to more often use chronic alcohol exposure or an acute delivery of alcohol at specific third trimester gestational stages (time points). Maternal alcohol exposure delivery for this trimester is most often performed by oral gavage, i.p. injection, liquid diet and *ab libitum* drinking.

Most research groups choose to use robust first-to-third trimester chronic PAE models to assess brain aberrations, behavioral consequences, and gene expression in mice that encompass the whole spectrum of development (Caldwell *et al.* 2008; Kleiber, Wright, and Singh 2011; Kleiber *et al.* 2013). Unlike first and second trimester PAE studies, there is a plethora of recent third and first-to-third trimester PAE studies. The PAE studies chosen for this section are those with the most interesting findings and include evidence of FASD-like outcomes. Caldwell *et al.* utilize a 5.0% v/v ethanol, *ab libitum* drinking model, from GD0 to PN6 as a chronic low-moderate BAC first-to-third trimester alcohol exposure study. Chronic liquid diet model of alcohol exposure from conception to PN6 produced a depressive-like phenotype in PN60-90 female mice (Caldwell *et al.*, 2008). Mice demonstrated increased immobility in the Porsolt forced swim test and learned helplessness in the Coulbourn™ Habitest© shuttle box, both behavioral outcomes are consistent with depressive-like behavior in recent behavioral studies (Hales *et al.*, 2014; Landgraf *et al.*, 2015). The mice did not exhibit immobility during the open activity test which is

indicative of anxiety and commonly associated with depression in FASD patients (Williams and Smith, 2015). Interestingly, the contrary results observed by Caldwell *et al.* may reflect the use of only female mice in their study. Wieczorek *et al.* found in an acute GD7 PAE model that PAE affects anxiety-like behavior in a sexually dimorphic manner. PAE males showed increases in anxiety-like behavior, whereas females exhibited a decrease in anxiety-like behavior (Wieczorek *et al.* 2015). Furthermore, BDNF (brain-derived neurotrophic factor) mRNA transcript levels are reduced in the medial frontal cortex and hippocampus, while protein levels were reduced in the medial frontal cortex, suggesting a role in depressive-like behavior, as seen in post-mortem hippocampi of clinically depressed and suicidal cases (Martinowich, Manji and Lu, 2007; Caldwell *et al.*, 2008; Lee and Kim, 2010; Autry and Monteggia, 2012).

Depressive-like behavior in PAE mice and in clinical cases is found to be linked to impaired glucocorticoid signaling, specifically, reductions in glucocorticoid receptors. In follow-up studies using a 10.0% v/v ethanol, *ab libitum* drinking model from GD0 to PN6 as a chronic low-moderate BAC first-to-third trimester alcohol exposure study, Caldwell and associates observed learning deficits in hippocampal and frontal cortex dependent tasks. PAE PN40-50 male mice show a decrease in delay and trace fear freezing, including fewer correct arm entries in the radial arm maze task, and all hippocampal-dependent learning tasks (Brady, Allan and Caldwell, 2013). PAE PN90-120 male mice demonstrate a slower learning-response in reversal learning task, a predominantly frontal cortex-dependent learning task (Allan, Goggin and Caldwell, 2014). Furthermore, PN90-120 male mice have reduced glucocorticoid receptor nuclear localization in the medial prefrontal cortex (Allan, Goggin and Caldwell, 2014). Glucocorticoid-mediated gene transcription is facilitated using glucocorticoid receptor signaling and specifically required for adaptive and flexible decision making strategies during stressful situations and for learning and

memory (Diorio, Viau and Meaney, 1993; Matsubara *et al.*, 2006). Glucocorticoid signaling facilitated by glucocorticoid receptors regulates the neuronal connections between the medial prefrontal cortex, hippocampus and amygdala and ultimately regulates HPA-axis activation in response to stress by negative-feedback (Diorio, Viau and Meaney, 1993; Matsubara *et al.*, 2006). Therefore, a decrease in Glucocorticoid receptors results in an exaggerated HPA-axis activity, resulting in an increase in cortisol levels (Diorio, Viau and Meaney, 1993). Reduced glucocorticoid receptor mRNA has been reported in the cortex and hippocampal brain regions of major depressive disorder post-mortem brains (Webster *et al.*, 2002; Knable *et al.*, 2004) Moreover, glucocorticoid receptor mRNA is reduced in lymphocytes of patients with major depressive disorder, both while suffering from depression and during remission (Matsubara *et al.*, 2006). High incidence depression (~45%) and Panic Disorder (~21%) is found in children and adults with FASD (Rasmussen *et al.*, 2008), suggesting that the effects on the glucocorticoid receptor and ultimately on the HPA-axis are epigenetic in origin. Taken together, clinical research on major depressive disorder post-mortem brains show a decrease in mRNA glucocorticoid receptor expression in the cortex and hippocampus regions. These are the same regions in which PAE mouse models show a decrease in glucocorticoid receptor nuclear localization.

Offspring of PAE models show slowed neurodevelopment as well as learning and memory deficits in adulthood. Using a similar first third trimester PAE paradigm, Kleiber *et al.* observed significantly slower developmental milestones (negative geotaxis, auditory startle, cliff aversion, and air righting) in PAE offspring when compared to non-PAE controls. Delays in motor coordination, balance and muscle tone is common in infants with FASD (Fried, 1983; Kalberg *et al.*, 2006). PN25-70 PAE offspring demonstrate anxiety-like behaviors in open field activity

assessments and learning and memory deficits in the Barnes maze test when compared to non-PAE controls (Kleiber, Wright and Singh, 2011). Whole brain tissue qPCR studies revealed a down-regulation of *Glra1* and *Grin2c*, involved in the glycine receptor complex and glutamate NMDA receptor complexes, respectively. Interestingly, Glra and Grin gene family sub-units are downregulated in patients with depression, schizophrenia and recently autism (Pilorge, Fassier, le Corronc 2016), providing a further link between PAE and neural developmental/psychiatric disorders.

PAE models show pro-inflammatory signaling and aberrant neuronal development in the hypothalamus, hippocampus and cerebellum, brain regions known to be affected in clinical FASD studies. Research groups are using third trimester chronic and acute PAE studies to assess brain aberrations, behavioral consequences, and gene expression in mice (Volgin, 2008; Coleman *et al.*, 2012; Drew *et al.*, 2015; Smiley *et al.*, 2015). In a chronic high BAC third trimester alcohol exposure study using a 4.0 g/kg ethanol dose (per day), by oral gavage, from postnatal day 4-9, Drew *et al.* found pro-inflammatory cytokines *Il1β* and *Tnfα* mRNA levels upregulated in hippocampus, cerebral cortex, and cerebellum. This PAE paradigm activates microglia to a pro-inflammatory stage causing a further change in microglial morphology in these same brain regions where pro-inflammatory cytokines are expressed. This is significant considering the hippocampus, cerebral cortex, and cerebellum were some of the most affected brain regions in various PAE mouse models and FASD clinical studies (Sowell *et al.* 2008; Parnell *et al.* 2013; Parnell *et al.* 2009). Recent studies suggest that microglia in an uninjured brain are required for proper neuronal synaptic function involved in refinement of brain wiring and synaptic circuitry through synaptic pruning (Paolicelli *et al.*, 2011). Microglia are directly activated by ethanol through *Tlr2* and *Tlr4* signaling in microglia, triggering a cascade of

cytokines, ROS, and NO production (Fernandez-Lizarbe *et al.* 2013). Moreover, ethanol activated pro-inflammatory microglial have been shown to modulate hypothalamus and cerebellum brain regions facilitating the removal of developing hypothalamic and cerebellar (Purkinje) neurons due to the apoptotic insult cause by PAE (Boyadjieva *et al.* 2013; Kane *et al.* 2011). Ethanol has also been shown to cause microglial cell death and also causes a decrease in intracellular levels of *Bdnf* in hypothalamic neurons *in vitro* (Boyadjieva *et al.* 2013; Kane *et al.* 2011). Taken together, PAE in the third trimester is detrimental to the developing fetal brain, producing inflammation and microglial activation that alter the normal course of brain circuitry and produce behavioral outcomes consistent with those seen in clinical FASD diagnosis.

Nitric Oxide Synthase (NOS) produces nNOS, one of three isoforms found almost exclusively expressed in the central and peripheral nervous system (Förstermann and Sessa, 2012). It is a key signaling molecule for proper synaptic plasticity in the brain. Karacay *et al.* studied a varying dose 2.2 g/kg or 4.4 g/kg of ethanol, by ip injection, using chronic PN4-9 administration with either a *nNos*$^{-/-}$ knockout transgenic pregnant female or WT control. PAE *nNos*$^{-/-}$ offspring on C57Bl6x129S6 background show a significant decrease in body weight at PN9-10 and adulthood mice and increased incidence of microcephaly (Karacay, Mahoney, Plume, 2015). Moreover, *nNos*$^{-/-}$ mice demonstrated severe PAE induced cerebral cortex pyramidal neuronal losses compared to WT controls, suggesting brain wiring/connection aberrations (Karacay, Mahoney, Plume, 2015). Furthermore, there is a significant increase of anxiety-like behavior, impaired startle response, and impaired learning and memory (Morris Water Maze), in PN85-90 mice, behavior outcomes that have previously been observed in PAE mouse models and clinical FASD cases (Brady, Allan, and Caldwell 2013; Allan, Goggin, and Caldwell 2014; Clarke and Gibbard 2003). In comparison, only the 4.4 g/kg cohort of WT mice experienced a decrease in body

weight at PN9-10 and had impaired learning and memory deficits (Morris Water Maze) (Karacay, Mahoney, Plume, 2015). Taken together, normal nNos activity seems to have a protective role, while *nNos* mutations worsen brain aberrations and behavioral outcomes in the presence of PAE when compared to PAE WT controls. Interestingly, *Bax* and *tPA* (tissue plasminogen activator) gene mutations (loss of gene activity) protect the brain upon alcohol exposure in PAE mouse models (Young *et al.*, 2003; Noel, Norris and Strickland, 2011).

Coleman *et al.* have observed a reduction in total brain volume (~5%), including reduction in frontal cortex neurons, parvalbumin GABAergic neurons (18%) and pyramidal neurons (15%), in PN82 mice, using an acute PAE model, 2.5 g/kg ethanol dose, by back-injection (sub-cutaneous), at PN7, producing high BAC third trimester alcohol exposure. The hypothalamus, hippocampus, cerebral cortex, corpus callosum, and amygdala were some of the 14 brain regions significantly reduced (the olfactory bulb and cerebellum were reduced but did not reach significance for the study) compared to non-PAE controls (Coleman *et al.*, 2012). Using a similar PAE paradigm, Smiley *et al.* have observed a reduction in total brain volume (~10%), including reduction in frontal cortex neurons, parvalbumin and calretinin GABAergic neurons (~30%), in PN72-89 mice (Smiley *et al.*, 2015). These studies show that an acute exposure to ethanol during third trimester produces significantly reduces brain volume, including a substantial loss of GABAergic and pyramidal neurons in the developing cerebral cortex. The observations have been previously seen in first and second trimester acute as well as chronic PAE, implying that PAE exposure at any time during gestation causes brain aberrations that will inevitably cause abnormal brain function (Sowell *et al.*, 2008).

2.1 Rodent Models: Dosage, Duration, and Gestational Timing of PAE and FASD-like models

PAE rodent model publications have recently reached a critical level, where the experimental parameters of exposure, such as varying dosage, duration, and gestational timing are well enough practiced that the wide array of FASD-like outcomes can be robustly, repeatedly and reliably demonstrated. To analyze the data (Appendix: Table 1), we color-coded FASD-like outcomes within the three general scopes of craniofacial malformations, brain aberrations, and behavioral phenotypes, and then clustered them by the experimental PAE model parameters of gestational timing, dosage and duration. We hypothesized this approach may reveal patterns of PAE model strength, and hopefully, generate new insights to understanding the neurodevelopmental processes underlying FASD (Table 1).

Areas of PAE model strengths become immediately obvious. Severe craniofacial malformations are most robustly expressed using a first trimester acute PAE paradigm. Aberrant behavioral outcomes are best studied using chronic third trimester PAE models. In this regard, the analysis also becomes a tool for many researchers to quickly assess and understand how any PAE model may best suit their own research question. It also quickly reveals the paucity in our understanding of FASD-like outcomes, a clear separation of neurodevelopment and behavioral studies, for example. It further reveals that much of our research in rodent models is biased by a social perception that FASD is a disorder founded in craniofacial or brain malformations that underlie problematic behavior and learning. Consequently, a large spectrum of FASD comorbidities clearly evident in other animal models of PAE and in FASD children and adults is ignored. These obvious strengths and weaknesses identify immediate avenues of opportunity for research initiatives that will have significant impact.

Some other interesting patterns begin to emerge. Both acute and chronic first trimester PAE models clearly indicate that one of the most sensitive windows for craniofacial malformations, the sentinel diagnostic and most recognizable features for FAS, is at early gastrulation. This appears to recapitulate in the mammalian models what has already been well demonstrated in other animal models (Kot-Leibovich and Fainsod 2009; Lovely *et al.* 2016). These PAE studies suggest that a single acute PAE can lead to severe FASD outcomes. In humans, this would be the fifth week of pregnancy – a point where most women may only beginning to suspect they are pregnant. Add to this that the majority of pregnancies in Canada are not planned and that binge drinking is increasingly prevalent among Canadian youth, and one must recognize that the largest prevention strategy – don't drink if you are pregnant – will fail most Canadians. Education and prevention messaging and strategies need to urgently be reassessed to incorporate this reality about the timing of PAE and FASD outcomes.

A second and related pattern to emerge is that the acute PAE in gastrulation, which is associated with severe craniofacial outcomes, seems to correlate with developmental brain abnormalities. This suggests that seemingly disparate neural crest and neuroectodermal cell lineage-derived outcomes may have common developmental or signaling pathways. FAS phenotypes are also observed in chronic low BAC first trimester PAE models spanning conception to gastrulation stages, suggesting that incidence of FASD may be further influenced (additive to alcohol exposure) by genetic modulation, including offspring epigenetic methylation signatures, maternal/offspring genetics and metabolism (Kaminen-Ahola, Ahola, Maga, *et al.*, 2010). It is interesting that having strong robust PAE models show a pattern of the successful use of genetic models to interrogate candidate signaling pathways affected by PAE. PAE models outlined in this review using transgenic mice serve as a reproducible tool to demonstrate that Shh, Glia2,

Cdon, and nNos transgenic mouse models can sensitize or prevent FASD-like outcomes related to craniofacial malformations, brain aberrations, and behavioral deficits. This also demonstrates that incidence and severity of FASD may be further influenced (additive to alcohol exposure) by genetic modulation.

Missing in acute PAE at gastrulation and early neurulation is any pattern of behavioral aberrations in offspring. This may simply reflect that such studies have not been performed or perhaps phenotypic variation in this PAE model prevents behavioral changes from experimental significance(Godin et al. 2010; Scott E. Parnell et al.2009; O'Leary-Moore SK et al. 2010). Regardless, lack of behavioral aberrations is inconsistent with FASD in children, and this is an area that needs to be explored in rodent PAE models.

The genetic patterns observed in genetic knock-out/transgenic PAE mouse models also encourage further examination of cellular changes that may underlie FASD-like pathophysiology. Linking brain aberrations with behavioral deficits may lie in changes at the neural cell level (Caldwell *et al.*, 2008; Allan, Goggin and Caldwell, 2014; Smiley *et al.*, 2015). Furthermore, changes in developing neural cells can lead to alterations in brain wiring or connections associated with the behavioral outcome observed in these models (Kleiber, Wright and Singh, 2011; El Shawa, Abbott and Huffman, 2013; Allan, Goggin and Caldwell, 2014; Karacay, Mahoney, Plume, 2015). Studying these behavior outcomes using these genetic knock-out/transgenic PAE mouse models will allow researchers to further elucidate the molecular/cellular mechanisms of (brain/behavior) FASD outcomes.

Finally, an examination of these patterns suggests tools which could strengthen the use and analysis of PAE models. For example, directly measuring the actual blood alcohol concentration

in the various PAE models would allow much better assessment of outcomes, and in comparisons between PAE models. Secondly, further research is needed to understand the physiological relevance of BAC in the PAE models so as to create better models for PAE in pregnant women (Table 2). All these tools will further allow researchers to choose a respective PAE model with varying dosage, duration, and gestational timing of alcohol exposure. These PAE models will robustly, repeatedly and reliably demonstrate the craniofacial malformations, brain aberrations, and behavioral deficits associated FASD-like outcomes, thus allowing future PAE rodent model research to better elucidate the etiology of FASD and discover a possible cure(s) or treatment for the disorder.

Table 2.1: FASD-Like Outcomes in PAE Mouse Models: Craniofacial Malformations, Brain Aberrations, and Behavioral Deficits seen in PAE Mouse Models varying the Dosage, Duration, and Gestational Timing of Alcohol Exposure.

Exposure Paradigm					Model			Effects									Reference
								Craniofacial			Brain			Behavioral			
	Level	Treatment		Time	Species	Age Assessment	Sex	FD	ED	SH	RV	RA	CA	AD	LD	IC	
1st Trimester Exposure	A	2.9g/kg (2X/day)	Ip	**GD 7**	Mouse C57Bl6	GD 14	M/F										(Sulik et al. 1981)
	A	2.9g/kg (2X/day)	Ip	**GD 7**	Mouse C57Bl6	GD17	M/F										(Godin et al. 2010)
	A	2.9g/kg (2X/day)	Ip	**GD 7**	Mouse 129S6	GD10-19	M/F										(Hong and Krauss 2012)
	A	2.9g/kg (2X/day)	Ip	**GD 7**	Mouse C57Bl6	PN 45	M/F										(Cao et al. 2014)
	A	2.9g/kg (2X/day)	Ip	**GD 7**	Mouse C57Bl6 Shh & Gli2 +/-	GD 17	M/F										(Kletzman et al. 2014)
	A	2.9g/kg (2X/day)	Ip	**GD 7** **GD 8**	Mouse C57Bl6	GD17	M/F										(Lipinski et al. 2012)
	A	2.8g/kg (2X/day)	Ip	**GD 8**	Mouse C57Bl6	GD17	M/F										(Parnell et al. 2009)
	A	2.9g/kg (2X/day)	Ip	**GD 9**	Mouse C57Bl6	GD 17	M/F										(Parnell et al. 2013)
	A	2.9g/kg (2X/day)	Ip	**GD 10**	Mouse C57Bl6	GD 17	M/F										(O'Leary et al. 2010)
	C	10% v/v EtOH	AbL	**GD 0 - 8.5**	Mouse C57Bl6	PD 21-30	M/F										(Kaminen-Ahola et al. 2010)
	C	10% v/v EtOH	AbL	**GD 0 - 8.5**	Mouse C57Bl6	GD 16.5	M/F										(Kaminen-Ahola et al. 2010)
	C	4.2% v/v EtOH	LD	**GD7-16**	Mouse C57Bl6	PN7 PN21	M/F										(Shen et al. 2013)
1st to 2nd Trimester	C	10% v/v EtOH	LD	**GD 0-19**	Mouse C57Bl6	PN60	M/F										(Akers et al. 2011)
	C	4.8% v/v EtOH	LD	**GD 0-19**	Mouse C57Bl6	GD17	M/F										(Anthony et al. 2010)
	C	25% v/v EtOH	LD	**GD 0 - 19**	Mouse CD1	P0-P20	M/F										(El Shawa et al. 2013)
	C	2.0g/kg 4.0g/kg	G	**GD 5 - 19**	Mouse C57Bl6	PD 0-30	M/F										(Cui et al. 2010)
	A	2.5g/kg (2X/day)	G	**PN 7**	Mouse C57Bl6	PN 72-89	M/F										(Smiley et al., 2015)
3rd Trimester	A	2.5g/kg (1X/day)	I-B	**PN 7**	Mouse C57Bl6	PN82	M/F										(Coleman et al. 2012)
	C	2.2g/kg 4.4g/kg 2.2 & 4.4 g/kg	Ip	**PN 4-9**	Mouse F2 129SVJ x C57Bl6 Mouse (nNos -/-)	PD 85-90	M/F										(Karacay et al. 2016)
	C	4g/kg (1X/day)	G	**PN 4-9**	Mouse C57Bl6	PN10	M/F										(Drew et al. 2015)
1st to 3rd Trimester	C	10% v/v EtOH	LD	**GD0-PN6**	Mouse C57Bl6	PN 90-150	M										(Brady et al. 2012)
	C	10% v/v EtOH	LD	**GD0-PN6**	Mouse C57Bl6	PN 40-50	M										(Allan et al. 2014)
	C	5% v/v EtOH	LD	**GD0-PN6**	Mouse C57Bl6	PN 60-90	M										(Caldwell et al. 2008)
	C	10% v/v EtOH	LD	**GD 0 – PN 10**	Mouse C57Bl6	PN 2-21 PN 25-70	M/F										(Kleiber et al. 2011)

Abbreviations:

	FD	Facial Dysmorphologies	VR	Reduced Volume			AL	Anxiety & Depression Like
	ED	Eye defects	RA	Region aberrations			LD	Learning Deficits
	SH	Small head	CA	Cellular anomalies			IC	Impaired Coordination

Table 2.2: PAE Mouse Model BAC Standardization: Variations in dosage depending on delivery or timing (Liquid diet/*ad libitum* or gavage/i.p.) of alcohol exposure in PAE mouse models.

PAE Dosage	PAE Dosage†	BAC (per day) ‡	BAC (per hr) ‡‡	BAC (Human)
4.2% v/v	8.14	1480.00	61.67	
4.8% v/v	9.30	1690.91	70.45	
5.0% v/v	9.69	1761.82	73.41	80mg/dL LDL*
10.0% v/v	19.38	3523.64	146.82	200mg/dL AIBO**
25.0% v/v	48.45	8809.09	367.05	
2.0 g/kg	2.00	363.64	363.64	400mg/dL AID***
2.2 g/kg	2.20	400.00	400.00	
2.5 g/kg	2.50	454.55	454.55	
2.8 g/kg	2.80	509.09	509.09	
2.9 g/kg	2.90	527.27	527.27	
4.0 g/kg	4.00	727.27	727.27	
4.4 g/kg	4.40	800.00	800.00	

† Prenatal Alcohol Exposure (PAE) Dosage: Standardized to grams (g) of ethanol per kilograms (kg) of mouse mass (avg. mouse = 25g). Units: g/kg
‡ Blood Alcohol Concentration (BAC): Total amount of ethanol consumed over a 24 hour period (chronic ad libitum paradigms are higher due to all day voluntary drinking compared to binge acute paradigms (avg. mouse blood conc. = 1.375mL). Units: mg/dL
‡‡ Blood Alcohol Concentration (BAC): Amount of ethanol approximately consumed per hour of the day (binge acute paradigms are administered by i.p., s.c., or oral gavage producing high (peak) BACs as it is in the blood system for an hour (or two) after exposure). Units: mg/dL
* Legal Driving Limit (LDL) in humans (0.08 or 80mg/dL)
** Alcohol Induced Black Out (AIBO) in humans (200mg/dL)
*** Alcohol Induced Death (AID) in humans (400mg/dL)

The purpose of this table was to standardize the PAE dosage paradigms, using the most common PAE dosages discussed in this review. Firstly, PAE dosages were standardized to g/kg (instead of volume of alcohol/distilled water). Mouse mass was standardized to 0.025kg (25g). The PAE dosage was then divided by the amount of blood in the average mouse and provides the Blood Alcohol Concentration Equivalent (per day). The blood alcohol concentration equivalent was then divided by the amount of hours a day alcohol was provided using those paradigms (v/v dosage paradigms are *ad libitum* and all day voluntary drinking. As a result v/v dosages were divided by 24 h where g/kg gastric gavage techniques were divided by 1 h to get the maximum blood alcohol concentration possible in that mouse model paradigm. As a result a 25% v/v alcohol dosage paradigm mimics the 2.0g/kg gastric gavage alcohol dosage paradigm using blood alcohol concentration per hour equivalent.

Chapter 3: Retinoic Acid Deficiency during Gastrulation Induce Craniofacial Malformations in mouse resembling Fetal Alcohol Syndrome

Foreword

Our Gsc:Cyp26A1 mouse model was designed to biochemically mimic alcohol-induced retinoic acid deficiency in the Node during early gastrulation. It is a developmental time point when retinoic acid is required for induction of the neuroectoderm and neural crest cells, cellular signaling, differentiation and subsequent craniofacial development. This chapter is to be published as a research paper describing the characterization of our Gsc:Cyp26A1 mouse model and testing the hypothesis that retinoic acid deficiency (Vitamin A deficiency) at early gastrulation results in FASD-like outcomes in a mammalian model system. FASD is the most common neurodevelopmental disorder in Canada is caused by maternal consumption of alcohol during pregnancy. Craniofacial malformations, brain aberrations, and behavioral deficits are observed in individuals with FASD. Maternal Vitamin A deficiency (retinoic acid deficiency) during pregnancy has also caused craniofacial malformations, brain aberrations, and behavioral deficits reminiscent of those seen in FASD. Here we establish that retinoic acid deficiency in early gastrulation results in craniofacial malformations and brain aberrations that phenocopy PAE induced malformations seen in robust mouse models and developmental aberrations that model FASD outcomes in humans. This work is the first evidence defining a molecular etiology of FASD in a mammalian system. The impact of this work is significant as it establishes solid *in vivo* evidence that (pre-) treatment with Vitamin A is likely to reduce or prevent FASD outcomes in humans.

This chapter reflects a manuscript that is currently in preparation for publication. It represents the greater majority of my Master's thesis body of work, and is considered to be the Materials and Methods, Results, and Discussion sections of my Master's Thesis.

Authors: Petrelli B[1], Oztürk A[1], Pind M[1], Ayele H[1], Fainsod A[2], and Hicks GG[1]

[1] Department of Biochemistry & Medical Genetics; Regenerative Medicine Program, Faculty of Medicine, University of Manitoba, Winnipeg, Canada.
[2] Department of Developmental Biology and Cancer Research, Institute for Medical Research Israel–Canada, Faculty of Medicine, Hebrew University of Jerusalem, Jerusalem, Israel.

Author Contribution: I am the lead author. My contributions to this work are: I performed all experiments detailed in the chapter, performed data analysis and wrote the manuscript. Experimental techniques include: validation of the cassette knock-in, *in vivo* deletion of the neomycin selection cassette in Gsc:Cyp26A1 mice with Cre-recombinase driver mice, deriving *Gsc:Cyp26A1* and *RARE-LacZ* double transgenic mice, designed and performed experimental analysis of RARE-LacZ, craniofacial measurement SEM, cranial nerve immunohistochemistry, maxillary malocclusion MicroCT, and brain MRI experiments. Dr. Arzu Ozturk and Molly Pind engineered the Gsc:Cyp26A1 mouse construction and validated cassette knock-in. Hossaena Ayele assisted in the craniofacial measurement SEM and data analysis. Drs. Abraham Fainsod and Geoff Hicks conceptualized the Gsc:Cyp26A1 mouse and project, I consider both of them mentors.

Abstract

Fetal Alcohol Spectrum Disorder (FASD) is caused by maternal consumption of alcohol during pregnancy affecting 2-5% of the population in Western countries. We have recently determined that acute ethanol exposure overwhelms the aldehyde metabolic enzymes that would normally convert retinaldehyde to retinoic acid (RA). We showed that alcohol exposure during gastrulation reduces RA levels at a time critical for embryogenesis which drives the future craniofacial malformations associated with FAS. Here we describe an early gastrulation directed RA deficiency model genetically designed to biochemically mimic acute alcohol exposure by expressing *Cyp26A1-eGFP* from the endogenous *Goosecoid* (*Gsc*) promoter. $Gsc^{+/Cyp26A1}$ embryos exhibit a reduction of retinoic acid levels during gastrulation and aberrant neurofilament patterning during nervous system formation. Moreover, $Gsc^{+/Cyp26A1}$ E18.5 embryos have FASD Sentinel-Like craniofacial phenotypes, while adult $Gsc^{+/Cyp26A1}$ mice can develop severe craniofacial maxillary malocclusions reminiscent of early gestation prenatal alcohol exposure. Taken together, this RA deficiency model results in developmental changes in neural lineage induction/proliferation, migration patterning, and craniofacial malformations that can be further studied in the context of the molecular etiology of FASD in a mammalian system and support the connection between alcohol exposure and reduced RA signaling.

[Keywords: Retinoic acid, Vitamin A deficiency, Fetal Alcohol Spectrum Disorder (FASD), Craniofacial Malformations, Hindbrain Development, Malocclusion**]**

Introduction

Fetal Alcohol Spectrum Disorder (FASD) is caused by maternal consumption of alcohol during pregnancy. It is the most common cause of neurodevelopmental disorders in children, affecting approximately 1-2% of the population in Canada, United States and Europe (Chudley *et al.*, 2005; Popova *et al.*, 2016). FASD with Sentinel Facial Features (FAS) is the most severe form of FASD and has an incidence of 0.146% worldwide (14.6 per 10000 people) (Popova *et al.*, 2017). There is currently no treatment or cure for FASD, nor is the etiology of the disorder known. Many researchers believe that alcohol dosage (Randall and Taylor 1979; Pierce and West 1986; Bonthius, Goodlett, and West 1988), duration of the alcohol exposure whether acute or chronic, and gestational timing (Anthony *et al.*, 2010; Godin *et al.*, 2010b; Lipinski *et al.*, 2012; Parnell *et al.*, 2013) are important determinants of the induction and severity of the disorder. Other risk factors, such as, maternal genetics and offspring epigenetics (Kaminen-Ahola, Ahola, Maga, *et al.*, 2010), maternal nutrition (Keen *et al.*, 2010), maternal metabolism (Burd, Blair and Dropps, 2012), maternal and offspring stress (Weinberg, 1989; Alberry and Singh, 2016) each to some respect contributes to the severity of FASD outcomes following prenatal alcohol exposure (PAE). Currently, the clinical assessment of FASD includes: FASD with Sentinel facial features and FASD without Sentinel facial features, where Sentinel facial features are distinct craniofacial malformations caused by prenatal alcohol exposure (Cook *et al.*, 2016). Due to their high specificity, these sentinel facial features are used in the clinical diagnosis of FASD, along with neurobehavioral examination and maternal alcohol history (Astley and Clarren, 1996). In general, the severity of facial malformations correlates with the severity in brain defects, specifically forebrain dysmorphologies (DeMyer W, Zeman W, 1964). This holds true for FASD, as

individuals with sentinel facial features tend to have more severe brain aberrations and consequently neurobehavioral anomalies (Chudley *et al.,* 2005; Cook *et al.,* 2016). In order to study a multifaceted disorder like FASD, researchers must start by using an animal model that can replicate the most severe form of the disorder with high penetrance. Secondly, the model should take into consideration that the craniofacial malformations (sentinel facial features) are in many instances of neural crest cell lineage origin (Carlson, 2014). Ideally, the model should test a developmental hypothesis well founded in the literature. In this regard, we based our model on the Vitamin A competition hypothesis (Kot-Leibovich and Fainsod, 2009). This hypothesis suggests that ethanol exposure competitively inhibits to oxidation of retinol (Vitamin A) and retinaldehyde by the appropriate dehydrogenases (DH) that would normally convert retinol to retinoic acid (RA). This occurs because the ethanol clearance and RA production pathways share some of the same dehydrogenase enzymes and the cell shifts to the removal of the impending teratogens, ethanol and acetaldehyde, rather than synthesizing retinoic acid. Unfortunately, retinoic acid is required during early embryogenesis to direct proper neural crest cell patterning and many other developmental processes (Carlson, 2014).

Retinoic acid, one of the biologically active metabolites of Vitamin A, is a diffusible lipophilic molecule that regulates over 3% of genes in the mammalian genome directly (through Retinoic Acid Response Elements, RAREs) and indirectly (by downstream RA target genes) (Balmer and Blomhoff, 2002; Paschaki *et al.*, 2013). All-*trans* Retinoic Acid (ATRA) is required for proper spatial temporal signaling during development, specifically rostral-caudal differentiation (formation) and patterning, and migration of the neural crest and mesoderm cell lineages during gastrulation (Rhinn and Dolle, 2012). Analysis of Vitamin A-deficient quail embryos demonstrated that ATRA regulates anteroposterior (AP) patterning of the neural plate (Halilagic

et al., 2007). Furthermore, ATRA is required for proper migration of neural crest cell lineages from the hindbrain into the frontonasal prominence and branchial arch regions (Bohnsack and Kahana, 2013). The retinaldehyde dehydrogenase family of enzymes (Raldh1, 2, and 3) are responsible for the oxidation of retinol to retinoic acid (Kam *et al.*, 2012). During gastrulation, Raldh2 (Aldh1a2) is the major enzyme family member performing this conversion. Retinoic acid levels are tightly regulated by synthesizing and controlling enzymes like Raldh2, Rdh10 and Dhrs3, but are also controlled from catabolizing enzymes like cytochrome P450 26 subfamily of enzymes (Cyp26A1, Cyp26B1, and Cyp26C1) that catalyze reactions that convert RA into polar metabolites (4-hydroxy- and 4-oxo-RA) rendering them biologically inactive (Ross and Zolfaghari, 2011). Cyp26A1 in particular metabolizes the ATRA, 9-cis-RA, and 13-cis-RA isoforms and prevents inappropriate cell signaling in certain cell populations or in regions like the tail bud of the developing embryo (Pennimpede *et al.*, 2010).

The Vitamin A competition hypothesis predicts that perturbations in RA signaling should result in FASD-like phenotypes. Raldh2 deficient mouse embryos show the extreme effects of Vitamin A (retinoic acid) deficiency in a developing mammalian organism (Niederreither et al. 1999; 2000; 2003). Raldh2 deficient embryos exhibit defective forebrain and optic development, a region where Raldh2 expression is required for proper retinoic acid patterning and frontonasal prominence development (Ribes *et al.*, 2006). Loss of retinoic acid also results in cell death and abnormal craniofacial neural crest distribution that contribute to frontonasal prominence defects (Ribes *et al.*, 2006). Retinoic acid is considered a master signaling regulator during development, perturbation of retinoic acid causes changes to multiple developmental cell signaling pathways which include; homeobox genes (HOX), fibroblast growth factor (FGF), sonic hedgehog (SHH), and paired box genes (PAX). All these pathways are involved in frontonasal prominence

development (Ribes *et al.*, 2006; Kam *et al.*, 2012; Rhinn and Dolle, 2012; Cunningham *et al.*, 2015). Retinoic acid synthesis (RDH10) and retinoic acid receptor gene (RARα/γ) knockout mice, both causing RA deficiency, show aberrations in cranial neural crest cell lineages, craniofacial malformations, and cranium/skeletal defects (Lohnes *et al.*, 1994; Rhinn *et al.*, 2011; Kam *et al.*, 2012; Rhinn and Dolle, 2012). Prenatal alcohol exposure murine models exhibit similar aberrations in cranial neural crest cell lineages, craniofacial malformations, and cranium/skeletal defects (Dunty Jr., Zucker, and Sulik 2002; Lipinski et al. 2012; Godin et al. 2010; Anthony et al. 2010)

We have previously shown in a *Xenopus* FAS model, that a single exposure to alcohol during early gastrulation is sufficient to induce the developmental defects associated with FASD Sentinel facial features (Yelin et al. 2005; 2007). Moreover, supplementation of retinoic acid by Vitamin A or retinaldehyde addition in the *Xenopus* model was sufficient to rescue the developmental defects associated FASD Sentinel facial features (Yelin *et al.*, 2005; Kot-Leibovich and Fainsod, 2009). Acute ethanol exposure overwhelms the aldehyde metabolic enzymes that would normally convert retinol (Vitamin A) to retinoic acid (RA) (Kot-Leibovich and Fainsod, 2009). We hypothesize that ethanol exposure reduces RA levels during critical developmental stages, i.e. early gastrulation, and this aberration induces the craniofacial malformations associated with FAS. We chose to test this hypothesis directly in a mammalian system by designing a genetic model that would biochemically mimic the reduced RA levels due to acute ethanol exposure, at the right time, early gastrulation, and in the right place, the Spemann Mangold organizer. To create this model, we inserted a Cyp26A1-eGFP expression cassette into exon 2 of the endogenous *Goosecoid* (*Gsc*) gene. The *Gsc* promoter dictates spatial-temporal expression to the embryonic organizer at the start of gastrulation in mouse embryos.

Cyp26A1 degrades the endogenous RA in these cells, biochemically mimicking the alcohol-induced competitive inhibition of Raldh2 and resulting in RA-deficiency and perturbation of neural crest cell lineage induction, proliferation, and migration.

Results

Generation of Gsc$^{+/Cyp26A1}$ transgenic mice

The mouse *Gsc* gene is encoded by three exons and is expressed in the embryonic organizer (node) during gastrulation (Blum *et al.*, 1992). *Gsc*-null (homozygous) mice are neonatal lethal due to palate malformations making the pups unable to suckle milk from the dame (Rivera-pérez *et al.*, 1995). *Gsc* heterozygous mice are viable, without palate malformations and indistinguishable (morphologically) from their WT littermates (Rivera-pérez *et al.*, 1995). To take advantage of that well studied transgenic mouse, Gsc$^{+/Cyp26A1}$ transgenic knock-in mouse strains were constructed using the same targeting site used to create the *Gsc*-null mutations in Behringer's model. We constructed a donor template with approximately 500bp homology arms flanking the Cyp26A1-eGFP cassettes into exon 2 of a *Gsc* allele (Fig. 1A). Two heterozygous Gsc$^{+/Cyp26A1}$ strains on a C57BL/6N background were constructed differing by the translation element used for Cyp26A1 cDNA expression. The Gsc$^{+/Cyp26A1(G12)}$ strain contains an T2A-Cyp26A1-T2A-eGFP cassette and the Gsc$^{+/Cyp26A1(H4)}$ strain contains an IRES-Cyp26A1-T2A-EGFP cassette. It is expected that the T2A construct would be more efficiently translated (Cyp26A1) than the IRES construct (Kim *et al.*, 2011). Thereby, generating models that may differ in the level of RA deficiency (Fig. 1B). The constructs were sequence validated across all junctions and functional elements (Fig. 1C) and correct targeting of *Gsc* was confirmed by

Southern blot analysis (data not shown). $Gsc^{+/Cyp26A1}$ mice were later mated with C57BL/6N Cre-recombinase mice (REF) to delete the downstream β-actin promoter driven Puro antibiotic selection marker cassette (Fig. 1B). $Gsc^{+/Cyp26A1}$ mice should express Cyp26A1 in the definitive endoderm at early gastrulation, resulting in retinoic acid deficiency and subsequent perturbation of neural crest cell induction.

$Gsc^{+/Cyp26A1}$ mice are born fully viable, but at reduced frequency compared to WT litter mates, 0.66:1 (n=351) and 0.88:1 (n=233) for $Gsc^{+/Cyp26A1(G12)}$ and $Gsc^{+/Cyp26A1(H4)}$ strains, respectively (Fig. 1D). The reduced frequency observed for the G12 strain supports the expectation that the T2A-translated Cyp26A1 may be more RA-deficient and leads to more severe phenotypes, compared to the H4 strain. That there is a difference between the two otherwise exactly the same strains suggest the *Gsc*:Cyp26A1 is biologically active *in vivo* and a strong likelihood of discernable phenotypes in the majority of embryos remaining. The appearance of reabsorption sites at E8.5 in $Gsc^{+/Cyp26A1}$ pregnancies suggests that some heterozygous mutants die during early-mid gastrulation (data not shown). Male to Female progeny numbers in $Gsc^{+/Cyp26A1}$ mutants and WT littermates in both strains were obtained at an expected frequency of near 1:1 (Fig. 1D).

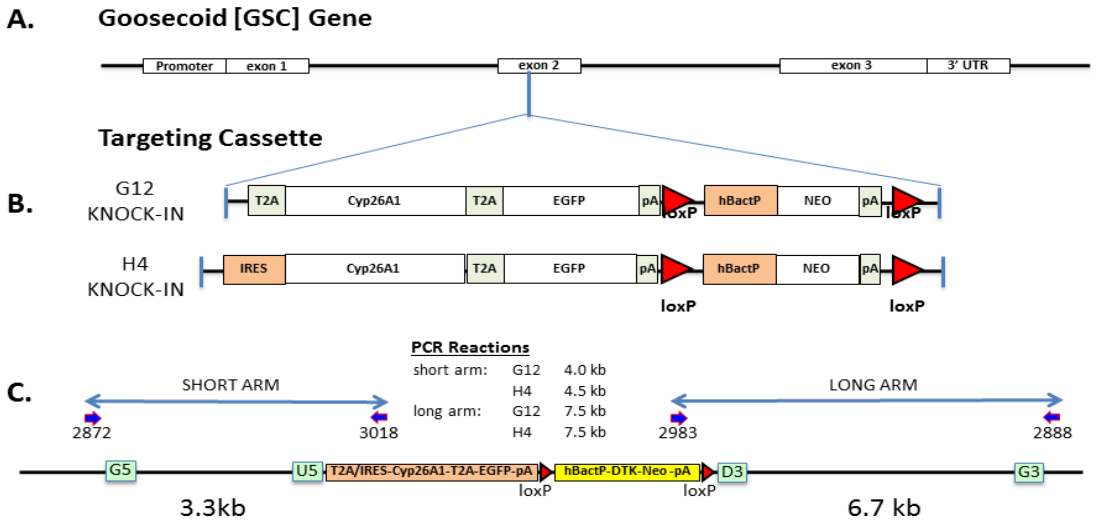

D.

Gsc:Cyp26A1 F1 Generation			
Strain	**Genotype**	**# of Offspring**	
H4 (IRES)	**$Gsc^{+/Cyp26A1}$**	**109**	**WT : Cyp26A1/+ †**
	$Gsc^{+/+}$ (WT)	**124**	**1 : 0.88**
	Total	**233**	
G12 (T2A)	**$Gsc^{+/Cyp26A1}$**	**140**	**WT : Cyp26A1/+ †**
	$Gsc^{+/+}$ (WT)	**211**	**1 : 0.66**
	Total	**351**	
Total Gsc:Cyp26A1 Offspring		**208**	

† Mendelian Ratio between $Gsc^{Cyp26A1/+}$ mice and WT littermate mice within the same strain

Figure 3.1. Gsc:Cyp26A1-eGFP Gene Targeting Design and Mouse Derivation. (A) The Gsc:Cyp26A1-eGFP cassette was targeted to exon 2 of the endogenouse *Gsc* gene by homologous recombination. (B) Cyp26A1 was used to catabolize RA and all RA isoforms in cells expressing Gsc. eGFP is a co-expressed fluorescent marker used to identify these cells in *in vitro* and *in vivo* studies. The cassette was constructed with two cyclin T2A peptide-bond-skipping translation elements to translate both the Cyp26A1 and eGFP gene products as individual proteins when the Gsc promoter was activated. Neomycin is a mammalian selection marker for gene targeting, which was later removed *in vivo* by crossing with a Cre mouse. The G12 strain uses a T2A translational element for Cyp26A1. The H4 strain uses an IRES translational element for Cyp26A1. (C) All targeting steps in ES and C57BL/6N mice were sequence validated to ensure correct recombination events and intact functional elements. (D) F1 Gsc:Cyp26A1 mice were born healthy, but at reduced frequency, as compared to WT littermates.

Activin A induces eGFP expression in Gsc$^{+/Cyp26A1}$ embryoid bodies

To validate that expression of Cyp26A1-eGFP is under the control of the *Gsc* promoter we performed embryoid body assays with and without Activin A and FGF. *Gsc* is specifically expressed in the definitive endodermal germ layer of the developing embryo. To induce *Gsc* expression *in vitro*, embryoid bodies (EB) assays were used to replicate the early developmental cell signaling interactions required to initiate definitive endoderm induction. Activin A is a well-established inducer of *Gsc* gene expression, particularly during embryo and embryoid body differentiation (Blum *et al.*, 1992; Soto-Gutiérrez *et al.*, 2007). Gsc$^{+/Cyp26A1}$ embryonic stem cells were cultured under embryoid body assay conditions, with or without 100 ng/mL Activin A and 100 ng/mL FGF-2 for 5 days, as described (Soto-Gutiérrez *et al.*, 2007). *Gsc$^{+/Cyp26A1}$* embryoid bodies treated with Activin A and FGF-2 clearly expressed eGFP, compared to embryoid bodies without Activin A and FGF, or embryoid bodies from WT ES cells (Fig. 2A). This demonstrates eGFP is inducibly expressed in cells under conditions that induce the *Gsc* promoter. To confirm our embryoid body assay does initiate definitive endoderm induction, we performed immunohistochemistry using Sox17 as a marker for definitive endoderm. Gsc$^{+/Cyp26A1}$ embryoid bodies with Activin A and FGF-2 supplementation show definitive endoderm marker (Sox17) expression, the cell lineage where *Goosecoid* is actively expressed during early gastrulation (Fig. 2B).

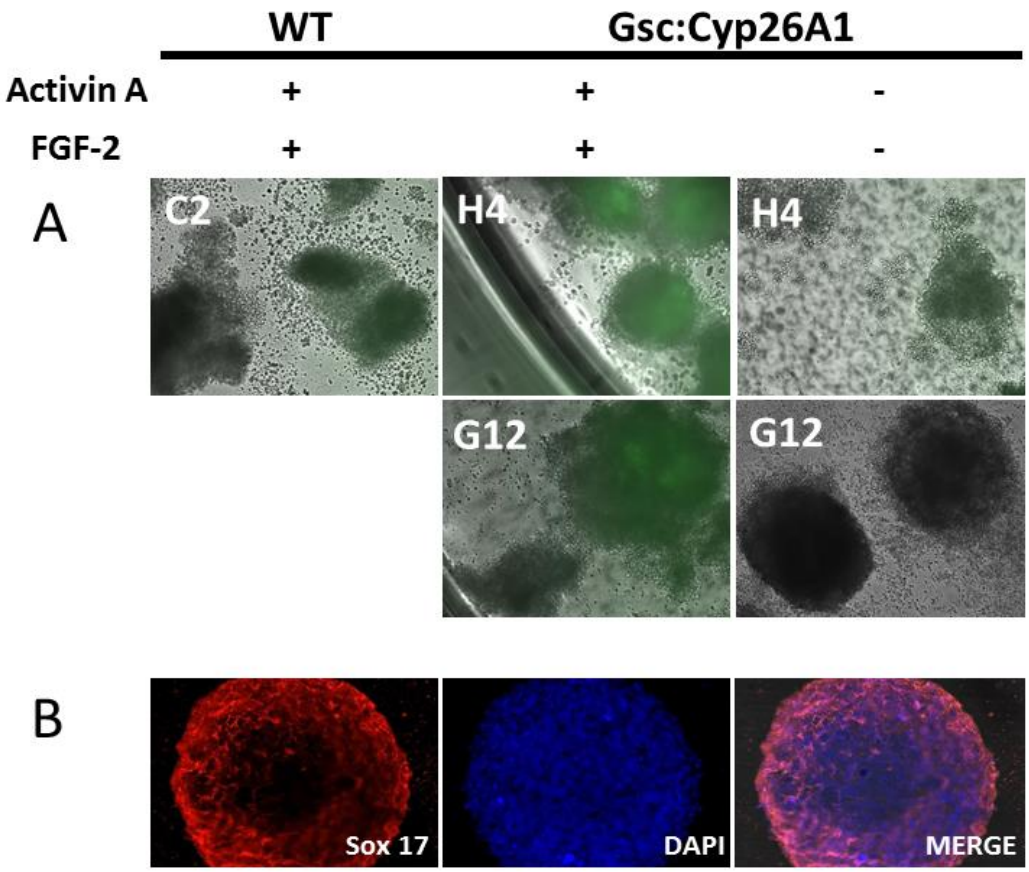

Figure 3.2. Gsc:Cyp26A1-eGFP is Expressed in Embryoid Bodies Induced with Activin A and Fibroblast Growth Factor (FGF). (A) Embryoid body (EB) formation was used to generate definitive endoderm germ cells *in vitro*. Activin A and FGF-2 was used to induce *Gsc* gene expression, including Cyp26A1-eGFP expression from the targeted *Gsc* allele. Results clearly demonstrate Gsc:Cyp26A1-eGFP is inducible under these conditions by eGFP expression in Activin A treated cells (middle panels), but not in untreated or EBs generated from wild-type ES cells. (B) Sox17 immunocytochemistry was performed on embryoid bodies to confirm definitive endoderm cell induction.

E8.5 Gsc$^{+/Cyp26A1}$- RARE-Lac-Z embryos show reduced RA activity

To functionally validate our *Gsc:Cyp26A1-eGFP* cassette *in vivo, Gsc$^{+/Cyp26A1}$* mice were crossed with *RARE-hsp68-lacZ* transgene mice and E8.5 embryos were assessed for RA activity patterning by LacZ expression (Rossant et al. 1991). *Gsc$^{+/Cyp26A1}$ -RARE-LacZ* embryos have a marked reduction of RARE-LacZ expression in the frontonasal prominence region (developing forebrain) of the embryo compared to WT littermates (Fig. 3A-B). This data indicates Cyp26A1-induced RA deficiency is indeed generated *in vivo*. In addition, the patterning of the RARE-LacZ activity in the frontonasal prominence was altered compared to WT *RARE-LacZ* embryos (Fig. 3A-B, arrowheads). The frontonasal prominence region develops into the face, neck and brain, all of which require tightly regulated retinoic acid expression (Bohnsack et al., 2010, Rhinn et al. 2012). Perturbations in retinoic acid signaling in the frontonasal prominence region will have developmental consequences for proper craniofacial morphogenesis (Ribes et al. 2005). In some cases, we observed *Gsc$^{+/Cyp26A1}$ -RARE-LacZ* embryos with severely reduced LacZ expression in the frontonasal prominence (Fig. 3C, arrowheads). These embryos with severely perturbed LacZ expression/retinoic acid activity may represent the embryos we assume would be reabsorbed. RARE-LacZ expression was not affected in the somites, lateral mesoderm derivatives, and trunk region of E8.5 Gsc$^{+/Cyp26A1}$ embryos compared to their WT siblings (Fig. 3 D-E), indicating that the effects of *Gsc:Cyp26A1-eGFP* are only seen in tissues derived from cells where the Cyp26A1 cassette was activated.

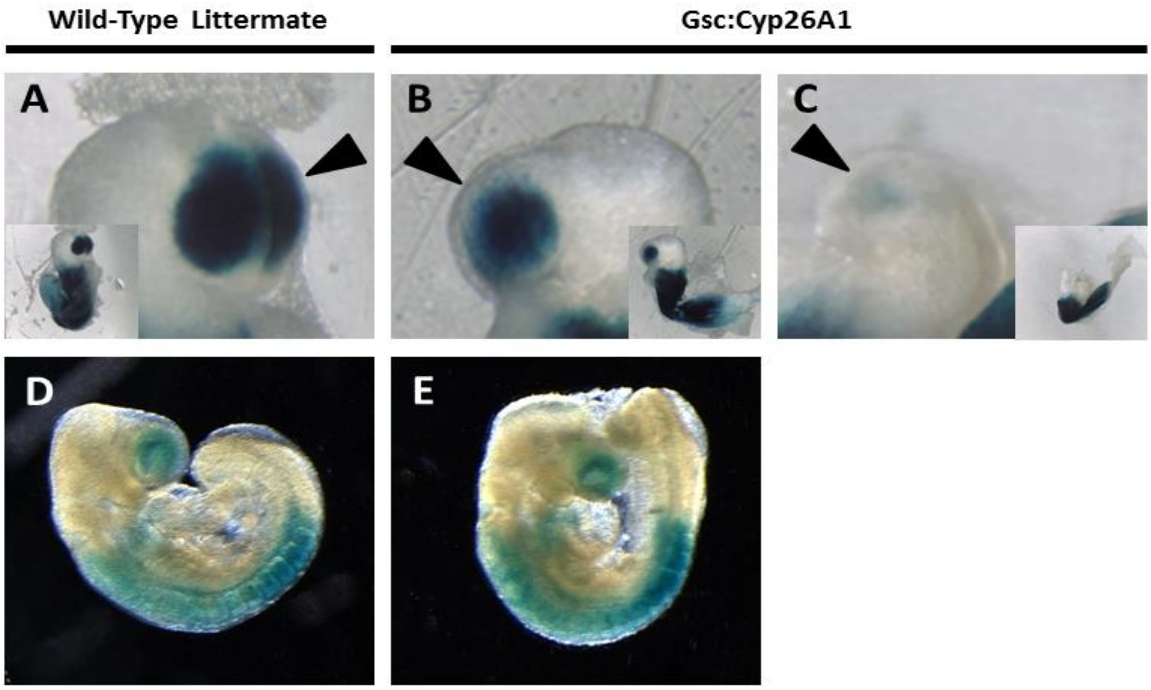

Figure 3.3. Gsc:Cyp26A1 E8.5 Embryos Have a Reduction in Retinoic Acid Activity/RARE-LacZ Expression. (A-C) Gsc:Cyp26A1$^{+/-}$ mice were crossed with RARE-LacZ$^{+/+}$mice containing a transgene reporter for intracellular RA levels. Gsc:Cyp26A1$^{+/-}$ x RARE-Lac-Z$^{+/-}$ embryos demonstrate both a reduction in Retinoic Acid activity/RARE-LacZ expression (B and C, lighter blue X-gal staining) in the frontonasal prominence region (Neural Crest Cell derived lineage; black arrow). WT littermate embryos (Gsc:Cyp26A1$^{+/+}$ x RARE-Lac-Z$^{+/-}$) develop proper frontonasal prominence formation and RA normal levels (A). This data shows Gsc:Cyp26A1 embryos have reduced retinoic acid activity in tissues known to express *Gsc*.. (D-E) Patterns of RARE-Lac-Z activity in Gsc:Cyp26A1$^{+/-}$ x RARE-Lac-Z$^{+/-}$ embryos are normally expressed in non-*Gsc*-transcribed tissues (E) compared to WT siblings (D). All embryos were gathered at E8.5 (A-E). The RARE-LacZ mouse has a Retinoic Acid Response Element (RARE) fused to a LacZ (β-galactosidase) reporter gene.

8.5 Gsc$^{+/Cyp26A1}$ embryos have morphological and developmental aberrations

E8.5 *Gsc$^{+/Cyp26A1}$-RARE-LacZ* embryos not only show a reduction in RARE-LacZ expression in the frontonasal prominence region but this induced RA deficiency also results in observable malformations in the developing frontonasal prominence (forebrain region) compared to wildtype littermates (Fig. 4 A-B). The majority of E8.5 Gsc$^{+/Cyp26A1}$ embryos share a common phenotype (Fig. 4 C-D); however, some E8.5 Gsc$^{+/Cyp26A1}$ embryos have malformations with varying degrees of severity in addition to being developmentally delayed (E7.75-8.0 in some cases, as determined by size, not turned and a smaller number of somites; Fig. 4 E-F). Normally embryos delayed more than one embryonic day would undergo reabsorption, mostly likely the reason why in the Gsc$^{+/Cyp26A1}$ transgenic model, the Mendelian frequency was not 1:1 (Flores et al., 2014). E8.5 Gsc$^{+/Cyp26A1}$ embryos also have malformed, non-bilateral frontonasal prominence lobes compared to WT littermates (Fig. 4C and F, Fig. 3B, arrowheads). Gross morphological malformations were not seen in the heart, somites, lateral mesoderm, or trunk of (similar sized) Gsc$^{+/Cyp26A1}$ E8.5 embryos compared to WT Littermates.

Developmentally regulated RA activity returns to normal expression by E9.5-11.5 Gsc$^{+/Cyp26A1}$ embryos

Reduced RA activity should not be detectable after E9.0 as both, the *Gsc*-driven cassette expression and residual Cyp26A1 mRNA and protein will no longer be present (Tay *et al.*, 2010). RA activity, as measured by RARE-LacZ expression, should exhibit a normal pattern in Gsc$^{+/Cyp26A1}$ embryos. E9.5-11.5 *Gsc$^{+/Cyp26A1}$-RARE-lacZ* embryos do indeed show normal RA activity patterns, indicated that the *Gsc:Cyp26A1* is not expressed. Surprisingly, Gsc$^{+/Cyp26A1}$ embryos do not show overt signs of development malformations (Fig. 5A-F), nor a reduction of

size in the frontonasal prominence region at E9.5 (Fig. 5A-B), as was previously seen at the E8.5 timepoint. $Gsc^{+/Cyp26A1}$ embryos appear have normal RARE-lacZ expression patterns at the E10.5 and E11.5 timepoints, compared to WT littermates (Fig. 5C-F). The normal RARE-lacZ pattern suggests that RA signaling is back to normal by E9.5, but it does not rule out downstream effects and outcomes resulting from earlier perturbations that may be expressed at either the cellular level or later in development.

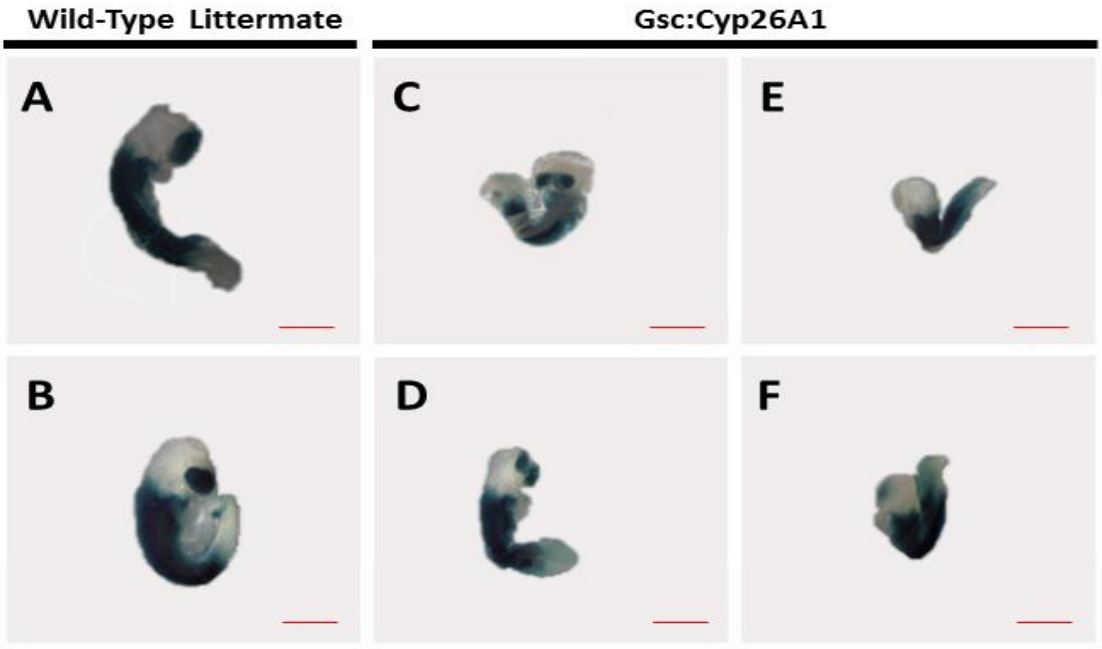

Figure 3.4. GSC:Cyp26A1 E8.5 Embryos Have Aberrations in Retinoic Acid Dependent Embryonic Patterning. Gsc:Cyp26A1 embryos (C-D) show changes in morphology of the frontonasal prominence region (blue stained region in forebrain) compared to WT siblings (A-B). In rare cases (~1 in 20 embryos) Gsc:Cyp26A1 embryos have a frontonasal prominence region devoid of RA activity, a severely malformed craniofacial region, and are slightly developmentally delayed (E-F). These are tissues neural crest cell in origin and will make the future face and forebrain.

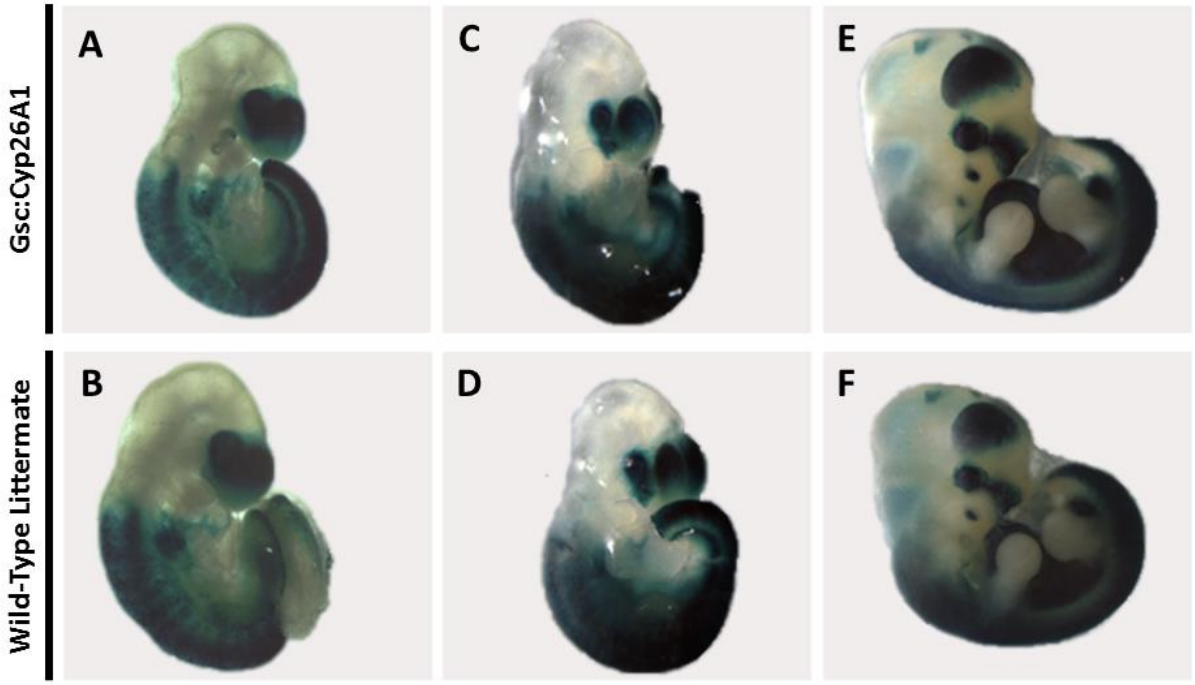

Figure 3.5. E9.5-11.5 Gsc:Cyp26A1 Embryos Show No Distinct Changes in RARE-LacZ Patterning. E9.5-11.5 Gsc:Cyp26A1 embryos (A, C, and E) no longer show distinct changes in embryonic patterning, gross morphology and intensity of RARE-LacZ expression compared to WT littermates (B, D, and F).

$Gsc^{+/Cyp26A1}$ E10.5 Embryos show aberrant cranial nerve patterning

Developmental effects resulting from RA deficiency at gastrulation can been at later stages of brain development. Previous studies showed that perturbation of retinoic acid during gastrulation can cause malformations in the developing cranial nerves, specifically cranial nerves V thru XII (Niederreither et al. 2003). $Gsc^{+/Cyp26A1}$ embryos show either a complete loss of the IX cranial nerve, a loss of the dorsal root of the IX cranial nerve, slender dorsal root fibers, or a fusion of the IX^{th} to X^{th} cranial nerves when compared to WT littermates (Fig. 6A-D). $Gsc^{+/Cyp26A1}$ E10.5 embryos show decreased overall staining of nerve fibers in the cranial nerves and hindbrain regions, specifically cranial nerves VII, VIII, IX, and X (Fig. 6A-D). $Gsc^{+/Cyp26A1}$ E10.5 embryos

have slender dorsal root fibers innervating the frontonasal prominence and branchial arch regions in cranial nerves V-XII when compared to WT littermates (Fig. 6B and D). Additionally, $Gsc^{+/Cyp26A1}$ E10.5 embryos show asymmetric abnormalities in cranial nerve patterning when comparing the right and left sides of the same embryo.

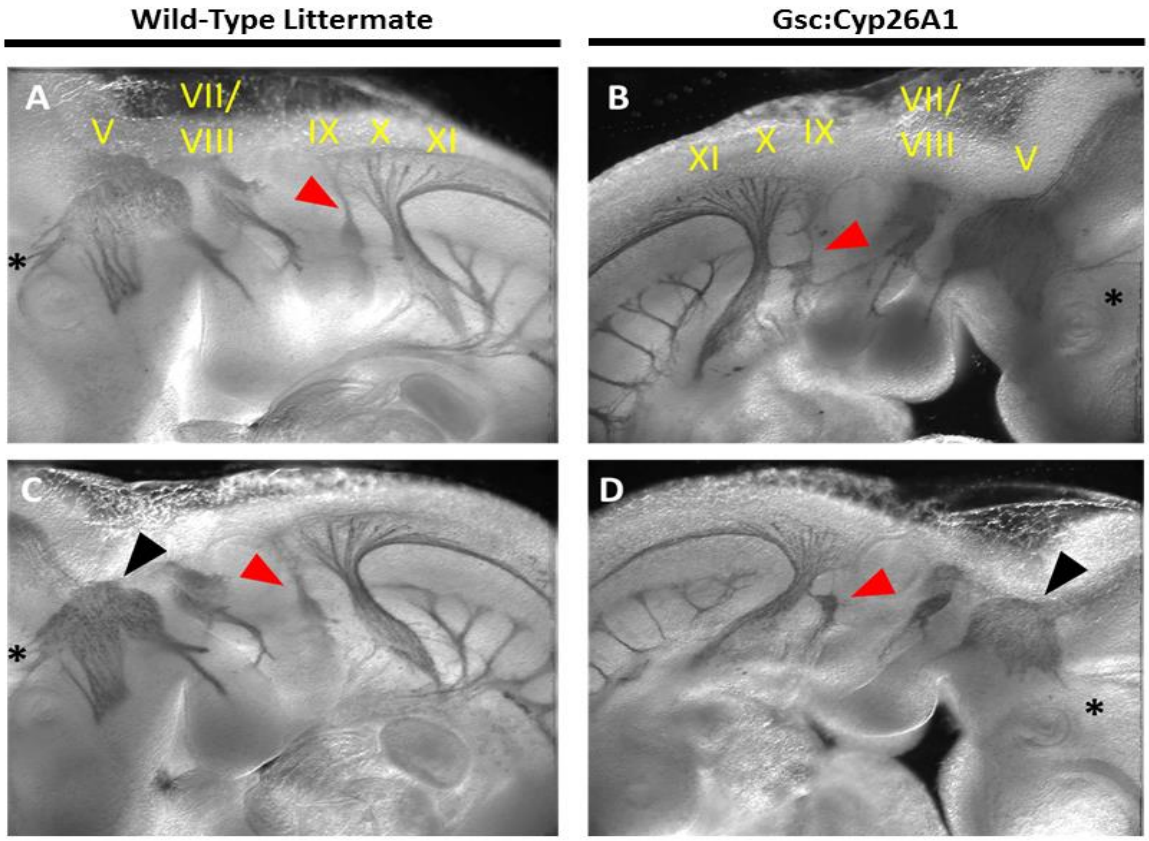

Figure 3.6. GSC:Cyp26A1 E10.5 Embryos Have Aberrant Neural Crest Cell Migration in the Developing Cranial Nerves of Branchial Arches. GSC:Cyp26A1 E10.5 embryos show a dysregulated cranial nerve patterning in the developing forebrain and branchial arches derived from the neural crest cell lineage mitigated by retinoic acid induced Hox genes (B and D). GSC:Cyp26A1 E10.5 embryos have decreased neural crest cell migration in cranial nerves V (black arrows), VII, VIII, X, XI, and specifically IX (red arrows). WT Littermates demonstrate proper cranial nerve patterning in the developing forebrain and branchial arches; the cranial nerves are migrating as expected (A and C). Notice that cranial nerve V does not innervate the optic vesicle in either of the Gsc:Cyp26A1 embryos, but correctly innervates the optic vesicle in WT littermate embryos (black asterisk). These result demonstrate that the GSC:Cyp26A1 model results in aberrant neural crest cell proliferation and migration.

$Gsc^{+/Cyp26A1}$ E18.5 Embryos have FASD Sentinel-Like Craniofacial Phenotype

We demonstrate that E18.5 $Gsc^{+/Cyp26A1}$ embryos develop an FASD sentinel feature craniofacial phenotype. Moreover, $Gsc^{+/Cyp26A1}$ mice have an 88% penetrance of FASD craniofacial phenotypes (Supp. Fig. 1). Scanning Electron Microscopy analysis of $Gsc^{+/Cyp26A1}$ embryos identified comparable prenatal alcohol exposure (FASD Sentinel-like) craniofacial malformations as found in previous PAE models (Anthony *et al.*, 2010)(Godin et al. 2009). $Gsc^{+/Cyp26A1}$ embryos had a larger philtrum-lip length ratio compared to WT littermates (sign.= 2 litters, trend.= 4 litters) (Fig. 7A and C). $Gsc^{+/Cyp26A1}$ embryos had a smaller bigonial line length compared to WT littermates (sign.= 2 litters, trend.= 3 litters) (Fig. 7B and C). $Gsc^{+/Cyp26A1}$ embryos had a smaller whisker pad length compared to WT littermates (sign.= 4 litters, trend.= 1 litters) (Fig.7B and C). $Gsc^{+/Cyp26A1}$ embryos had a smaller frontal snout area compared to WT littermates (sign.= 2 litters, trend.= 4 litters) (Fig. 7D). The mean for each of the 4 craniofacial measurements for both $Gsc^{+/Cyp26A1}$ and WT littermates in each individual litter are shown in (Supp. Table 1). 4 craniofacial measurements (Supp. Fig. 2): philtrum-lip ratio, bigonial line, whisker pad length and frontal snout area were found to exhibit significant differences in nearly all litters (N=7 litters; n=69 embryos). The other 5 measurements: midfacial depth, lowerfacial depth, neck to edge of mandible, and side snout area were trending in some of the 8 litters examined (Supp. Table 2). We assessed many other craniofacial measurements that may be linked to neural crest development, but found no trending patterns between $Gsc^{+/Cyp26A1}$ and WT Littermate embryos. It should be noted that taking advantage of the SEM imaging it was possible for the first time to measure the frontal and side snout areas of the E18.5 embryos, this measurement was not possible in 2D craniofacial analysis.

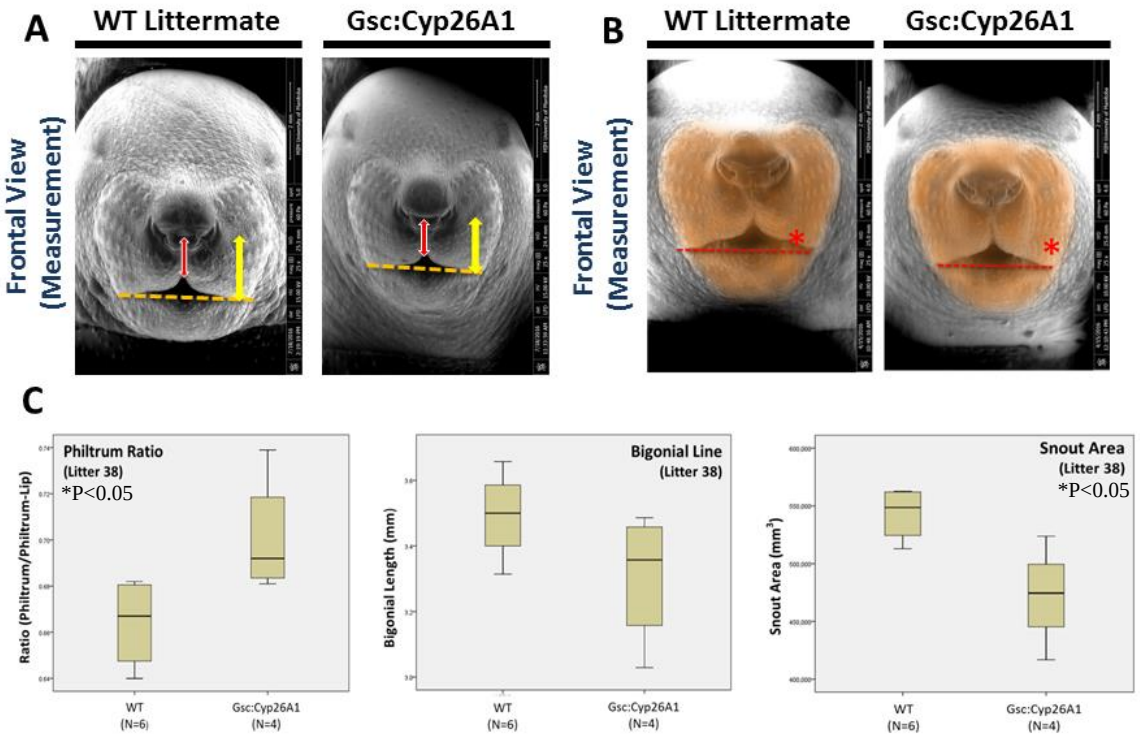

Figure 3.7. Gsc:Cyp26A1 E18.5 Embryos Have Fetal Alcohol Syndrome (FAS)-like Craniofacial Malformations. (A) Gsc:Cyp26A1 E18.5 Embryos have a less defined, flatter maxillary formation resulting in a larger philtrum/philtrum-lip ratio compared to WT littermates (red arrow length/yellow arrow length). For comparison, WT littermates E18.5 embryos have a more defined, normal protruding maxillary formation resulting in a smaller philtrum/philtrum lip ratio. (B) Gsc:Cyp26A1 E18.5 embryos have a narrower bigonial line width (red dashed line, asterisk marks the comparative length of Gsc:Cyp26A1 bigonial line width on a WT sibling). The orange overlay defines a smaller snout area in Gsc:Cyp26A1 E18.5 embryos. For comparison, WT E18.5 embryos have a wider bigonial line width and larger snout area. (C) Craniofacial measurements for individual embyros of a representative litter are shown. Observed differences for each phenotype reach significance within almost all of the 8 litters examined. *P<0.05

$Gsc^{+/Cyp26A1}$ P60-75 mice have high incidence of Craniofacial Maxillary Malocclusions

We demonstrate that $Gsc^{+/Cyp26A1}$ mice developed severe postnatal craniofacial maxillary malocclusions (Fig. 8). $Gsc^{+/Cyp26A1}$ mice (n=10; ages 8-10 weeks), WT littermates (n=4; ages 8-10 weeks), and C57BL6/N In House Colony (University of Manitoba) malocclusion mice (n=3; ages 4-10 weeks) had all undergone MicroCT analysis. The WT littermates and C57BL6/N House (University of Manitoba) Colony malocclusion mice were used as negative controls for the experiment, respectively (Table 1). We demonstrate that craniofacial malocclusions and pre-maxillary twisting is not found in the WT littermate cohort (0 malocclusions; n=120, Table 1). Incidence of craniofacial malocclusions in C57BL6/N colonies are 0.04% (Jax Laboratory) and 0.32% (C57BL6/N In House Colony, University of Manitoba), (Table 1). $Gsc^{+/Cyp26A1}$ mouse cohort had a 12.5% overall incidence of craniofacial malocclusions and pre-maxillary twisting between the G12 and H4 strains (11 malocclusions; n=88) (Table 1; Fig. 8). $Gsc^{+/Cyp26A1}$ mice developed maxillary malocclusions as a result of the premaxillary (nasal) bone twisting (Twigg *et al.,* 2009). When comparing the cranium measurements of $Gsc^{+/Cyp26A1}$ mice to control cohorts, WT littermate and C57BL6/N In House Colony malocclusion mice, $Gsc^{+/Cyp26A1}$ demonstrated a significant increase in the overall width of the cranium. P60-75 $Gsc^{+/Cyp26A1}$ mice have a significantly wider nasal, frontal, and interparietal bone measurements ($p<0.05$) compared to WT littermate mice and a trending result compared to C57Bl6/N In House Colony malocclusion mice (Fig. 9A). $Gsc^{+/Cyp26A1}$ mice have a significantly wider L-R anterolateral bone measurement ($p<0.01$), compared to WT littermate mice and a trending result compared to C57BL6/N In House Colony malocclusion mice (Fig. 9A). We followed up the initial cranium MicroCT width and length measurements with 11 Maxillary and Mandible Length measurements, using the same three cohorts of mice (Supplemental Fig. 2). $Gsc^{+/Cyp26A1}$ mice have a significantly larger upper

incisor height ($p<0.001$), as expected compared to WT littermate mice due to the maxillary malocclusion (Supplemental Fig. 3). $Gsc^{+/-}$ mutant mice have not been documented to develop craniofacial maxillary malocclusions at P60 to 75 (Rivera-pérez *et al.*, 1995). Nor do vitamin A/retinoic acid deficient P60-75 mouse models show craniofacial maxillary malocclusions as seen in our model. Interestingly, first-trimester PAE mice were shown to have wider cranium measurements (a trending result) compared to non-PAE mice (Kaminen-Ahola, Ahola, Maga, *et al.*, 2010). Moreover, $Gsc^{+/Cyp26A1}$ craniofacial malocclusions and pre-maxillary twisting phenotypes resemble the pre-maxillary twisted snouts of first-trimester PAE mice (Kaminen-Ahola, Ahola, Maga, *et al.*, 2010). Taken together, the increased incidence and severity of craniofacial malocclusions in $Gsc^{+/Cyp26A1}$ mice is a true phenotype when compared to WT littermates and C57BL6/N In House Colony malocclusion mice.

Table 3.1: $Gsc^{+/Cyp26A1}$ P60 Mice Have Severe Craniofacial Malocclusions

	$Gsc^{+/Cyp26A1}$ *	WT Littermates*	C57Bl6 In House Colony†
G12	7/44 (15.9%)	0/70 (0.0%)	11/3733 (0.32%)
H4	4/44 (9.1%)	0/50 (0.0%)	
Total	11/88 (12.5%)	0/120 (0.0%)	11/3733 (0.32%)

* C57Bl6 Background † University of Manitoba C57Bl6 Mouse Facility (House) Colony

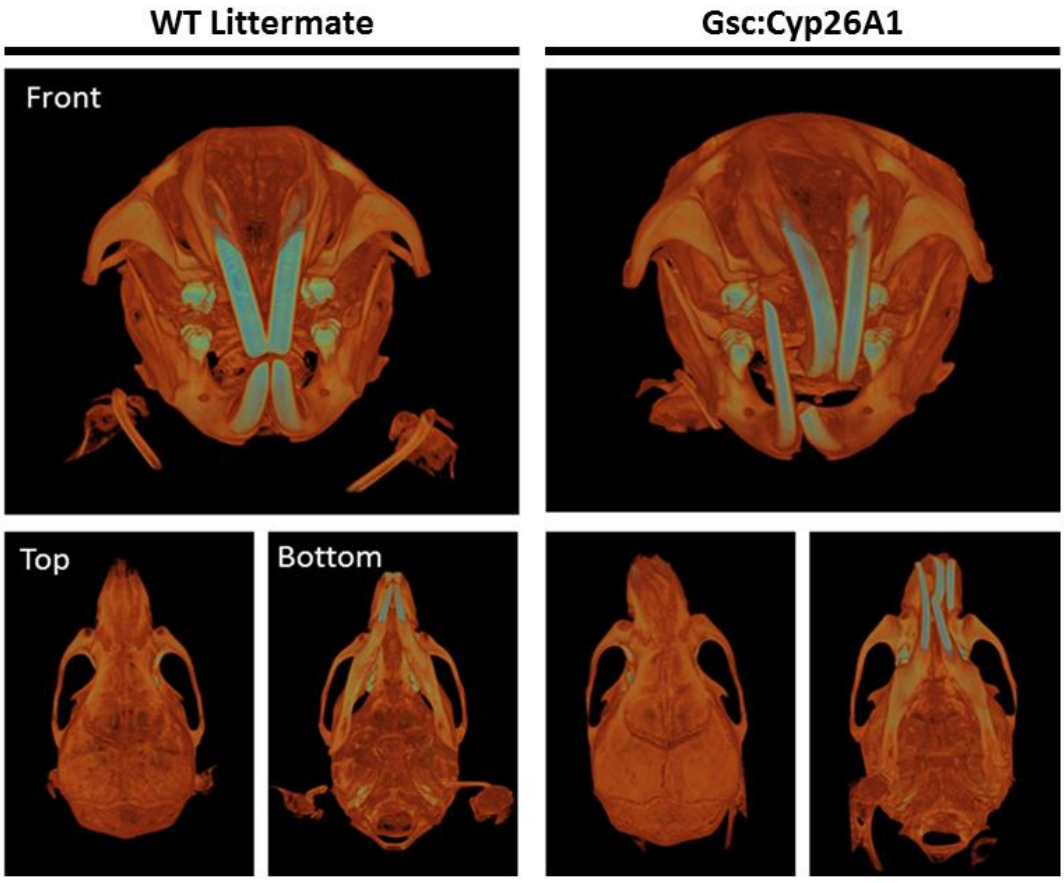

Figure 3.8. GSC:Cyp26A1 P60 Mice Have Severe Craniofacial Malocclusions. GSC:Cyp26A1 P60 mice (Panel B, Top View) demonstrate a curvature in the maxillary process (specifically the pre-maxillary component) when compared to WT littermates (Panel A, Top View). GSC:Cyp26A1 P60 mice (Panel B, Bottom View) do not have a curvature of the mandibular component, the mandible is straight when compared to the skull as seen in WT littermates (Panel A, Bottom View). The curvature to the maxillary component can be seen to impact the natural grinding of the incisors, ultimately causing a severe malocclusion in Gsc:Cyp26A1 mice (Panel B, Front View); the incisors grind normally in WT littermate mice (Panel A, Front View).

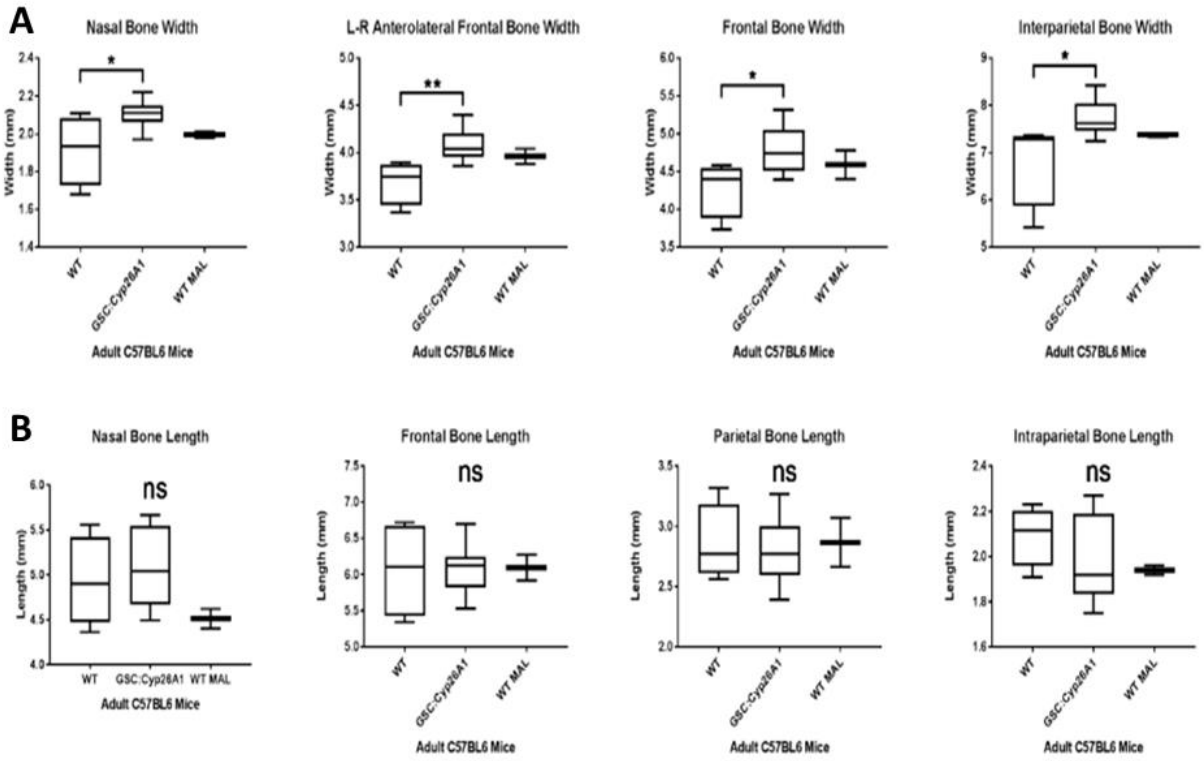

Figure 3.9. GSC:Cyp26A1 P60 Mice Have a Wider Cranium Compared to WT Littermates. (A) GSC:Cyp26A1 P60 mice show a statistically significant wider cranium in all 4 major skull region width measurements (Nasal Bone, L-R Anterolateral Frontal Bone, Frontal Bone, and Intraparietal Bone Widths). GSC:Cyp26A1 P60 mice exhibit the greatest statistical significance in the L-R Anterolateral Frontal Bone width measurement, this is the fusion point between the maxillary and pre-maxillary components of the cranium and where the curvature originates causing the malocclusions. (B) GSC:Cyp26A1 P60 mice do not demonstrate any statistically significant longer cranium in any of the 4 major skull region length measurements. Interestingly, the intraparietal bone length measurement was shorter, but only trending compared to WT littermates (B - Intraparietal Bone Length). *P<0.05, **P<0.01

$Gsc^{+/Cyp26A1}$ P180 mice have Reduced White Matter (Axonal) Bundle Volumes

100uM Magnetic Resonance Imaging of 180 day $Gsc^{+/Cyp26A1}$ adult mice and cage matched wildtype littermates has shown significant changes in volume of the Anterior Commissure bundle tract (Fig. 10). $Gsc^{+/Cyp26A1}$ G12 strain mice particularly exhibit a reduction in Anterior Commissure bundle tract volume compared to WT Littermates in two litter pairs G12 and G9 by 31% and 34%, respectfully. $Gsc^{+/Cyp26A1}$ H4 strain mice exhibit an increase in Anterior Commissure bundle tract volume compared to WT Littermates in litter pair H6 by 4%. $Gsc^{+/Cyp26A1}$ strain mice also have an increase in Corpus Callosum bundle tract volume compared to WT littermates in all three litter pairs G12, G9, and H6 by 7%, 6%, and 3%, respectfully. Hippocampal volume was increased in all three $Gsc^{+/Cyp26A1}$ mice litter pairs G12, G9, and H6 compared to WT littermates, by 2%, 8%, and 3%, respectfully. Total Brain, Corpus Callosum, and Hippocampus regions showed trending but not significant differences in volume between $Gsc^{+/Cyp26A1}$ mice and WT littermates. Anterior Commissure bundle tract volume is different among the Gsc:Cyp26A1 strains, producing a severe result in the G12 strain.

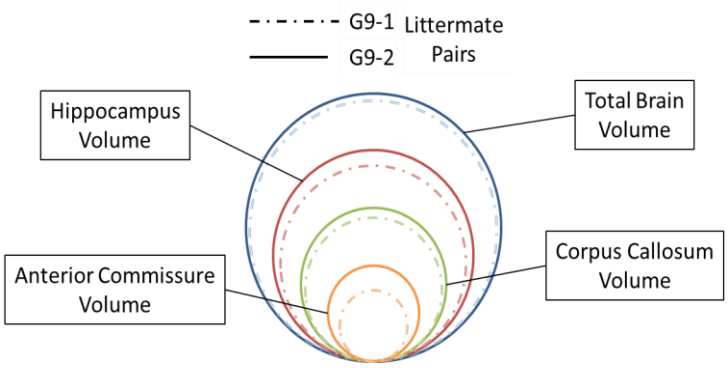

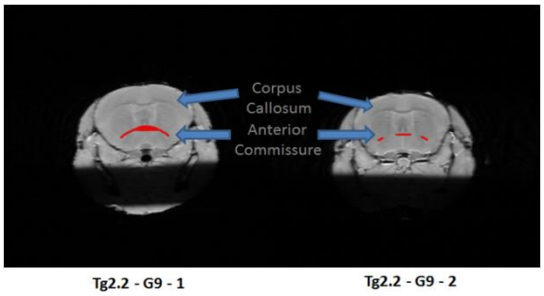

GSC:Cyp26A1 MRI Pilot Study Litter Pair #1	Litter Pair (Female)		% Change
	G9-1	G9-2	
TB Volume (mm^3)	467.45	481.52	3%
HP Volume (mm^3)	30.44	32.81	8%
CC Volume (mm^3)	6.79	7.22	6%
AC Volume (mm^3)	1.28	0.96	34%

GSC:Cyp26A1 MRI Pilot Study Litter Pair #2	Litter Pair (Female)		% Change
	G12-1	G12-2	
TB Volume (mm^3)	465.92	435.59	7%
HP Volume (mm^3)	32.66	32.00	2%
CC Volume (mm^3)	7.01	7.52	7%
AC Volume (mm^3)	1.46	1.12	31%

GSC:Cyp26A1 MRI Pilot Study Litter Pair #3	Litter Pair (Female)		% Change
	H6-1	H6-2	
TB Volume (mm^3)	478.27	466.83	2%
HP Volume (mm^3)	31.89	32.93	3%
CC Volume (mm^3)	7.77	7.54	3%
AC Volume (mm^3)	1.28	1.33	4%

Figure 3.10. Adult Gsc:Cyp26A1 Brains Have Smaller Anterior Commissure Volume. An MRI study was performed on three 180-day Gsc:Cyp26A1 and WT female littermate pairs. Sequential 100uM MRI scans of the brain for each of the mice was performed and analysis was blinded to genotype in each pair. Volume plot is used as a visual aid to reflect changes in brain region volume between mouse litter pairs (not to scale). 100uM MRI section shows reduction in anterior commissure area (red trace) in litter pair #1 mice. Tables contain volume measurements and percent changes within each litter pair. Reduction in anterior commissure volume is highlighted with red box. TB: Total Brain, HP: Hippocampus, CC: Corpus Callosum, AC: Anterior Commissure. Gsc:Cyp26A1 Females: G9-2, G12-2, and H6-1. WT Littermates: G9-1, G12-1, and H6-2.

Discussion

It is has been shown that retinoic acid deficiency in a mammalian model causes developmental malformations in neural crest cell migration and proliferation (Niederreither *et al.*, 2003). Furthermore, prolonged gestational retinoic acid deficiency causes a plethora of malformations including: limb deformities, organogenesis aberrations, and craniofacial/brain malformations, to name a few (Sulik KK, Cook CS, 1988; Cunningham, Zhao and Duester, 2011; Lee *et al.*, 2012). Here we provide evidence that our *Gsc:Cyp26A1* mouse model demonstrates craniofacial malformations and developmental brain aberrations due to spatial-temporal reduction of retinoic acid at gastrulation. Interestingly, alcohol exposure during gastrulation causes similar migration and proliferation aberrations in neural crest cell lineages in mouse models (Dunty Jr., Zucker and Sulik, 2002). It has been demonstrated in *Xenopus* models using biochemical evidence that alcohol competes for the retinaldehyde dehydrogenase 2 (Raldh2) activity, which reduces retinoic acid formation and expression of retinoic acid for downstream pathway signaling during gastrulation (Kot-Leibovich and Fainsod, 2009). There is high incidence of malformations such as microcephaly and reduced axial length, and craniofacial defects in embryos exposed to ethanol (Yelin *et al.*, 2005, 2007). These same malformations are also seen in embryos deficient for retinoic acid during gastrulation, resembling the phenotypic anomalies in embryos exposed to ethanol and in individuals affected by FASD (Kot-Leibovich and Fainsod, 2009). The *Xenopus* studies provide evidence that early molecular changes to the retinoic acid synthesis pathway would biochemically mimic exposure to ethanol at gastrulation, making this a useful model system for studying FASD.

We demonstrate that retinoic acid perturbation during early gastrula causes defective patterning in cranial and hindbrain nerves. The glossopharyngeal cranial nerve (IX) in particular seems to be the most affected in Gsc:Cyp26A1 embryos, as many of the embryos have no dorsal root and a reduction in ventral fibres. Furthermore a few of the embryos had fused IX-X cranial nerves, whereby cranial nerve IX buds ventrally from the X cranial nerve. These Gsc:Cyp26A1 aberrant glossopharyngeal nerve phenotypes are reminiscent of *Nkx 2.2* and *Nkx 2.9* knock-out mice, which show reduction/loss of dorsal root fibers and IX/X cranial nerve fusion (Pabst *et al.*, 2003; Jarrar *et al.*, 2015). These aberrant glossopharyngeal nerve phenotypes are further reminiscent of early gastrulation alcohol exposed embryos which also show reduction/loss of dorsal root fibers and IX/X cranial nerve fusion (Dunty Jr., Zucker and Sulik, 2002). *Nav2* knock-out mice also exhibit reduction/loss of dorsal root fibers and IX/X cranial nerve fusion in 60% of offspring (McNeill et al. 2010), comparable to those glossopharyngeal nerve phenotypes found in Gsc:Cyp26A1, *Nkx 2.2*, *Nkx 2.9*, and PAE embryos. *Nav2* is an atRA-responsive gene and is tightly regulated by RA expression, moreover it is required for proper neurite outgrowth in murine and human neuroblastoma cell models (Muley *et al.*, 2008; McNeill *et al.*, 2010). The loss of RA signaling in our Gsc:Cyp26A1 model may cause downstream genes like *Nav2* to be perturbed and result in reduced neurite outgrowth, specifically in the neural crest derived glossopharyngeal dorsal root nerves. The role of RA in neural crest cell migration and proliferation is further elucidated in *Hoxa3* null embryos, as those embryos share similar glossopharyngeal nerve phenotypes to *Nav2* knock-out embryos. *Hoxa3* null embryos exhibit both the reduction/loss of dorsal root fibers and IX/X cranial nerve fusion (Watari *et al.*, 2001). *Hoxa3* is a direct downstream RA target and is involved in regulating cell migration in the dorso-ventral direction at rhombomeres 5 and 6 (R5 and 6). The glossopharyngeal (IX) nerve is derived

from R6 (Watari *et al.*, 2001). Taken together, RA deficiency during early gastrula stages is sufficient to dysregulate RA downstream gene cascades in cranial nerve migration and proliferation/outgrowth resulting in phenotypes seen in PAE models.

Our Gsc:Cyp26A1 mouse model demonstrates that perturbation of RA production at gastrulation, causes craniofacial malformations which resembles mouse prenatal alcohol exposure phenotypes. It has been well documented that PAE causes craniofacial malformations including microcephaly in murine models and in FASD individuals, but what might not be as common are craniofacial malformations caused by maternal Vitamin A deficiency (RA deficiency) whereby microcephaly is a common phenotype (Clagett-Dame and Deluca, 2002). Although not as well documented, prenatal Vitamin A deficiency causes craniofacial malformation in newborns and resembles the defects seen in FASD newborns. Vitamin A deficiency in murine models has not been well studied especially retinoic acid deficiency at early gastrulation. Gsc:Cyp26A1 RARE-LacZ expression demonstrated that RA expression in the frontonasal prominence at E8.5 was perturbed compared to WT littermates. Although it known that *Gsc* is no longer expressed after E6.8 until E10.0, it demonstrates that RA deficiency at early gastrulation did indeed cause a dysregulation in the retinoic acid downstream gene cascade and caused the craniofacial malformations and cranial nerve aberrations observed in our Gsc:Cyp26A1 mouse model.

We further demonstrate using scanning electron microscopy that E18.5 Gsc:Cyp26A1 embryos did indeed have a statistically significant: larger philtrum to lip ratio, a smaller frontal nasal area, and a smaller bigonial width within their respective litters compared to wild-type littermates. This is the first time a retinoic acid deficiency model has been assessed for craniofacial malformations using scanning electron microscopy, but it demonstrated similarities to craniofacial malformations in PAE models (Sulik and Johnston, 1983; Anthony *et al.*, 2010). A

smaller bigonial width has been shown to be a significant measurement in models where ethanol was administered chronically starting at gastrulation (E7.0) and acutely during gastrulation (E7.0 and E8.5) (Anthony et al. 2010; Lipinski et al. 2012, respectively). With the bigonial width measurement being statistically significant in our study we demonstrated that retinoic acid deficiency at gastrulation does indeed resemble a PAE phenotype. Additionally our study found two other statistically significant measurements; philtrum to lip ratio and frontal snout area to further demonstrate changes in maxillary formation in E18.5 Gsc:Cyp26A1 embryos. The Philtrum to Lip ratio measurement takes into consideration that the length of the philtrum over the length of the bottom of the nose to the top of the mandible (Lip) (ratio) is larger in Gsc:Cyp26A1 than in wild-type littermates. Even though the philtrum length measurement is not larger in Gsc:Cyp26A1 than wild-type littermates as seen in other PAE models (Sulik and Johnston 1983; Parnell et al. 2009; Lipinski et al. 2012), the maxillary region in the E18.5 Gsc:Cyp26A1 embryos is affected. Particularly, the maxillary region is narrower and longer in Gsc:Cyp26A1 embryos as seen in PAE models (Sulik and Johnston 1983; Parnell et al. 2009), and the maxillary region is where midface hypoplasia occurs in FASD individuals (Moore *et al.*, 2002; Naidoo *et al.*, 2006). One of our initial experiments was to bin Gsc:Cyp26A1 x WT (C57Bl6) littermates as either being mutant (Gsc:Cyp26A1) or normal (WT littermate) in a blinded arrangement where genotypes would not be known till at the time of weening. We found qualitatively, that 88% of our Gsc:Cyp26A1 PN1 mice had a discernable craniofacial phenotype compared to their WT littermates. In order to capture this discernable craniofacial phenotype, as a smaller snout (face) region in mice we choose to take an area measurement to replicate our findings in a quantitative manner. The frontal snout area measurement further demonstrates that the entire snout region of Gsc:Cyp26A1, which includes the maxillary region (and mandible

region) is smaller when compared to wild-type littermates. This phenotype is seen in other early gastrulation PAE models whereby the overall area of the affected embryos snout (and cranium) is smaller when compared to non-affected littermates (Sulik and Johnston 1983; Godin et al. 2010). Our model fully demonstrates that the snout (and cranium) area changes are in fact due to retinoic acid deficiency and dysregulation in the cascade of downstream RA responsive genes. This will be the first ever model of FAS (due to retinoic acid deficiency) to assess the behavioral deficits we have observed in our Gsc:Cyp26A1 model.

Gsc:Cyp26A1 mice exhibit maxillary malocclusions which resemble those of early gastrulation prenatal alcohol exposure mice. It has been well documented that Vitamin A deficiency causes maxillary malocclusions in murine models and in humans (as VAD), but what might not be commonly reported are maxillary (dental) malocclusions, a known and usually overlooked co-morbidity caused by maternal PAE (Streissguth, Clarren and Jones, 1985; Popova *et al.*, 2016). In mice, prenatal alcohol exposure prior to and at early gastrulation causes maxillary malocclusions, but more specifically a curvature of the premaxillary region of the cranium in adult mice (>P30) (Kaminen-Ahola, Ahola, Maga, *et al.*, 2010). We demonstrate that Gsc:Cyp26A1 mice develop analogous maxillary malocclusions to those early gastrulation PAE model mice in Kaminen-Ahola et al.'s study, moreover our model also exhibits increases in cranium width as seen with the PAE mice in their study. It can be suggested by this data that our early gastrulation retinoic acid deficiency model is quite similar to an early gastrulation PAE model. Unfortunately many PAE studies do not study adult mice for craniofacial malformations, including maxillary studies focused on maxillary and pre-maxillary regions during development and into adulthood we would find higher incidences of craniofacial malformations in murine models.

Gsc:Cyp26A1 mice further exhibit brain volume changes, specifically a decrease in volume of the anterior commissure bundle tract, a phenotype seen in PAE mouse models (Higashiyama *et al.*, 2007; Cao *et al.*, 2014) (Fig. 10). The anterior commissure bundle tract has also been affected in clinical FASD cases, usually presenting in more clinically severe FAS cases (Coulter *et al.*, 1993). It has been well documented that PAE causes brain volume, brain region morphology/shape, and neuronal cell changes in murine models and in humans (as FASD) (Godin et al. 2010; Parnell et al. 2009; El Shawa, Abbott, and Huffman 2013; Cui et al. 2010; Allan, Goggin, and Caldwell 2014), but there are virtually no papers that demonstrate brain aberrations due to only maternal Vitamin A or retinoic acid deficiencies during pregnancy (Clagett-Dame and Deluca, 2002). There have been studies in murine models that show Vitamin A deficiency but this is usually secondary effect to another teratogen, an example being alcohol (Feltes *et al.*, 2014). Interestingly there has been a medical case report demonstrating a reduction in retinol and retinyl-esters levels in blood serum of PAE newborns (Goez, Scott and Hasal, 2011). Our model serves as the first enzymatic metabolizing model of retinoic acid deficiency at early gastrulation. The links between retinoic acid deficiency and PAE at gastrulation are quite interesting allowing for future sensitized $Gsc^{+/Cyp26A1}$ studies. Taken together, our data provide *in vivo* evidence that strongly supports retinoic acid deficiency as a major molecular etiology of craniofacial malformations and brain aberrations associated with FASD outcomes. The findings suggest Vitamin A supplementation may significantly reduce or prevent FASD outcomes in children with PAE. Further studies exploring the protective effects of Vitamin A in PAE mouse models will need to be done before a therapeutic clinical application of Vitamin A can be performed. This mammalian model of FAS will be the first to test FAS behavioral deficits,

leading to more effective prevention strategies and reducing the burden of this disorder on children, their families, and society.

Methods

Generation of $Gsc^{+/Cyp26A1}$ mouse as a novel transgenic mammalian model

Gsc targeting and genotype analysis. We isolated a (size kb) *Gsc* genomic clone from a mouse C57bl6 genomic library using a 5' complementary DNA probe. The targeting construct contained 18kb of genomic DNA with a T2A-Cyp26A1-T2A-eGFP-LOX-hBacP-ΔTK/NEO-LOX (G12) or IRES-Cyp26A1-T2A-eGFP-LOX-hBacP-ΔTK/NEO-LOX (H4) cassette inserted in an antisense orientation using U5 and D3 homologous recombination sites located in the second exon of the *Gsc* gene. This construct disrupts the *Gsc* coding sequence after aa355, deleting the homebox region downstream of the insertion site. After electroporation in ES cells and positive/negative selection, eight targeted cell clones were identified, ES cells were genotyped by Southern-blot analysis using *Nsil* restriction site and 3' Cyp26A1 probe that hybridizes to a 9.3kb (G12, T2A) and 9.8kb (H4, IRES) for the targeted allele. Mouse ear punch, embryonic yolk sac, and embryonic tail DNA was genotyped by PCR using 2 primers: a sense primer located in exon 1 and an antisense primer located in exon 2 of Cyp26A1, producing 2 amplification products. The first PCR product for the mutant allele creates an amplification product ~460bp representing *Cyp26A1* cDNA that is present only in the transgene. The second PCR product creates an amplification product ~750bp for both endogenous *Cyp26A1* alleles, considered a WT allele band.

Embryoid body assay

$Gsc^{+/Cyp26A1}$ cells from both strains G12 and H4 were used for the embryoid body (EB) experiments. Parental C2 embryonic stem cells were used as controls for the EB experiments. Cells were thawed from frozen (1,000,000 cells/per vial) stocks and plated in 2 wells (of a 6 well plate) at approximately 500,000 cells per well on an adherent layer of MEFs. When cells achieved a confluency of 80% approximately 48 h post-plating, the cells were passaged to a 10cm adherent cell culture plate on an adherent layer of MEFs. When cells achieved a confluency of 80%, the cells were trypsinized from the 10cm plate and washed by centrifugation twice with 5mL DMEM. Cells were then split over 2-10cm adherent cell culture plates (in approximately 10mL of medium) for a 1 h incubation period without a MEF adherent layer, to obtain only ES cells and remove any remaining MEFs from the cell suspension. Cell suspensions were then collected after the 1 h incubation period and cells are washed by centrifugation with 5mL DMEM. Cells were then counted and diluted to a concentration of 50,000 cells/per mL in DMEM. 50,000 cells (1mL) were placed in each well of a ultra-low density attachment 6 well plate and supplemented with 100ng/mL of Activin A and 100ng/mL of Basic Fibroblast Growth Factor (FGF-2). A 6 well plate would normally have 2 wells for each the C2, G12, and H4 lines, only one of those wells would be supplemented with Activin A and FGF-2, the other would be a control). The plate would be placed in an incubator at 5% CO_2 and 37°C. Media was changed daily for 5 days as per Nature protocol (Soto-Gutierrez et al., 2007). EBs in ultra-low density plate would be moved to glass bottom cell culture chambers prior to imaging for fluorescent eGFP expression to reduce additional background signal (from plastics). Fluorescent Microscopy imaging was performed on a Leica MZ16FA stereozoom microscope with an eGFP FluoIII filter changer, a 1X optical lens and 1.2 MP Leica DC500.

Embryo dissection and fixation

A pregnant female mouse (either WT (female) mated with Gsc:Cyp26A1 (male) or Gsc:Cyp26A1 (female) mated with WT (male)) on day E8.5, 9.5, 10.5, 11.5 or 18.5 dpc (days post coitum) was sedated using Isofluorane anesthetic and subsequently sacrificed using cervical dislocation. The abdomen was washed with 70% ethanol and the abdominal cavity was dissected and uterine horns exposed. Uterine horns were then removed using surgical scissors and washed in sterile PBS in a 10cm cell culture plate. Each embryo was dissected from the uterine wall and placenta, yolk sacs with embryo were removed for days E8.5, E9.5, E10.5, and E11.5 using fine (55) forceps in sterile PBS. The yolk sac was then removed from around the embryo, care was taken to not damage the embryo, but remove as much of the yolk sac as possible to use as genomic DNA for genotyping. This was difficult for E8.5 and E9.5 embryos as the yolk sac attaches to the truck of the embryo that is only a few cell layers thick at this point in development. For 18.5 dpc embryos, each embryo was dissected from the uterine wall and placenta, using fine surgical scissors and (5) forceps in sterile PBS. Approximately ~0.5cm of the latter portion of the embryo's tail was taken as genomic DNA for genotyping. E8.5-E11.5 dissected embryos were each placed in a well of a 4-well cell culture dish in approximately 0.5mL of chilled sterile PBS (placed at 4°C for no longer than 2 h until fixation). A Dissection Microscope (Leica MZ6) was used to dissect the E8.5-11.5 embryos from the yolk sacs.

E8.5-11.5 embryos were then fixed overnight (12-16 h) in freshly prepared (<24h) 4% paraformaldehyde at 4°C. After overnight fixation E8.5-11.5 embryos were placed in 0.5mL sterile PBS at 4°C until used for experiments or imaging purposes. E18.5 dissected embryos were each placed in a 15mL conical tube in approximately 5mL of a 2% paraformaldehyde-2% glutaraldehyde mixture solution for fixation (required for SEM imaging, Section 2.11). E18.5

embryos were kept in the fixation mixture solution until SEM imaging (usually performed within 1-2 weeks), if the fixation solution darkened within 2-3 days, the 2% paraformaldehyde-2% glutaraldehyde fixation mixture was changed (occasionally occurred due to large amount of amniotic fluid in the conical tubes during fixation).

RARE-LacZ embryo expression assay

A pregnant female Gsc:Cyp26A1 mouse mated with male RARE-LacZ mouse on day E8.5, 9.5, 10.5, 11.5 dpc (days post coitum) was sedated using Isofluorane anesthetic and subsequently sacrificed using cervical dislocation. Embryos at their respective dpc were dissected from the dams as per "embryo dissection section" above. After dissection E8.5-11.5 embryos were then processed using a β-galactosidase staining protocol (obtained from the Rivera lab; University of New Mexico, and adapted from the original Behringer lab protocol). Embryos in sterile PBS at 4°C were placed in a fixation solution (0.2% Glutaraldehyde, 2% Formalin, 5mM EGTA and 2mM $MgCl_2$ in 0.1M Phosphate buffer pH 7.3) for a specific amount of time depending on their dpc (10' → E8.5-9.5, 15' → E10.5-12.5). Embryos were then removed from the fixation buffer and placed in a rinse solution (0.1% Na-deoxycholate, 0.2% IGEPAL, 2mM $MgCl_2$ in 0.1M Phosphate buffer pH 7.3) for 3 consecutive – 30 minute rinses. Embryos were then stained overnight at 37°C in a X-gal stain (1mg/mL X-gal, 5mM Potassium ferricyanide, 5mM Potassium ferrocyanide in 0.1M Phosphate buffer pH 7.3). Embryos were washed 3 consecutive times in Sterile PBS to remove yellow coloration from X-gal staining. Embryos were then photographed and stored in 70% ethanol for 2 months. Stereo Microscopy imaging was performed on a Leica MZ16FA stereozoom microscope with a 1X optical lense and 1.2 MP Leica DC500 or 6MP Zeiss Axiocam 512 Color camera.

Whole-mount immunohistochemistry

A pregnant female mouse (either WT (female) mated with Gsc:Cyp26A1 (male) or Gsc:Cyp26A1 (female) mated with WT (male)) on day E10.5 dpc was sedated using Isofluorane anesthetic and subsequently sacrificed using cervical dislocation. Embryos at E10.5 dpc were dissected from the dams as per "embryo dissection section" above. After dissection E10.5 embryos were then processed using a Whole mount Immunohistochemistry staining protocol (obtained from the Marzban lab; University of Manitoba). The whole mount technique allows embryos to be fixed in their normal structural (3D) confirmation while allowing the tissue to become semi-transparent, allowing for staining using immunological techniques (IHC). This is different than standard (2D) IHC that uses tissue sections ranging from 5um to 100um in thickness and staining using immunological techniques. Whole mount Immunohistochemistry (IHC) neurofilament (cranial nerve) staining was performed as described (Marzban et al. 2008, Joyner and Wall 2008). The whole mount IHC neurofilament antibody used was a Goat Anti-Mouse IgG with HRP conjugate (AP308P; EMD Millipore). Stereo Microscopy imaging was performed on a Leica MZ16FA stereozoom microscope with a 1X optical lens and 6MP Zeiss Axiocam 512 Color camera.

Scanning Electron Microscopy, Micro-CT and MRI imaging

Scanning Electron Micrography (SEM) was performed on the FEI Quanta 650 FEG a variable pressure field emission scanning electron microscope for high-resolution imaging (SE, BSE) with low-vacuum capabilities. Fixed E18.5 embryos as per "embryo dissection section" above were used for SEM to gather craniofacial measurement analysis. E18.5 embryo (SEM) craniofacial measurements were adapted from Anthony et al. 2010 and Lipinski et al. 2012

publications. SEM parameters: Detection Unit: LFD, Magnification: 25X, HV: 15.00kV, Chamber Pressure: 60Pa, Spot: 5.0. Embryos were not left in the unit for more than 15 minutes, nor were they imaged more than 2 times, non-consecutively (only subjected to changes in pressure twice). Micro Computed Tomography (MicroCT) was performed on the SkyScan 1176 x-ray microtomography system equipped with a large format 11 megapixel x-ray camera. Dead/non-fixed P60-75 mice were used for MicroCT to gather craniofacial measurements and assess malocclusions. P60-75 mouse craniofacial measurements were adapted from Kawakami and Yamamura 2008 and De Carlos et al. 2012. Micro CT Parameters: Resolution: 9um and HV: 50kV. Magnetic Resonance Imaging (MRI) was performed on the Bruker 7T MRI scanner system. Dead/transcardially perfused (with a 1:10 mixture buffered formalin) P180 mice and later immersed in buffered formalin for 72 h were used for MRI to assess brain aberrations. MRI scan parameters: matrix size=256 × 256 × 256, FOV = 2.56 × 2.56 × 2.56 mm3, flip angle = 0°, scan time= 12.5-13 h.

Supplemental Table 3.1: The 4 craniofacial measurements (means) in the 7 Gsc:Cyp26A1 E18.5 Embryo Litters Compared to WT Littermate Embryos

Craniofacial Measurement	Gsc:Cyp26A1	WT Littermate	
Bigonial Line Length	3.35mm	3.43mm	Litter 21
Whisker Pad Length	4.49mm	4.63mm	
Philtrum to Lip Ratio	0.638	0.622	
Frontal Snout Area	501546 AU	558264 AU	
Craniofacial Measurement	Gsc:Cyp26A1	WT Littermate	
Bigonial Line Length	3.18mm	2.8mm	Litter 34*
Whisker Pad Length	4.27mm	3.69mm	
Philtrum to Lip Ratio	0.67	0.65	
Frontal Snout Area	442818 AU	438684 AU	
Craniofacial Measurement	Gsc:Cyp26A1	WT Littermate	
Bigonial Line Length	2.99mm	2.99mm	Litter 35
Whisker Pad Length	3.94mm	4.17mm	
Philtrum to Lip Ratio	0.711	0.725	
Frontal Snout Area	394769 AU	407715 AU	
Craniofacial Measurement	Gsc:Cyp26A1	WT Littermate	
Bigonial Line Length	3.31mm	3.52mm	Litter 38
Whisker Pad Length	4.38mm	4.62mm	
Philtrum to Lip Ratio	0.701	0.66	
Frontal Snout Area	472383 AU	545156 AU	
Craniofacial Measurement	Gsc:Cyp26A1	WT Littermate	
Bigonial Line Length	3.09mm	3.14mm	Litter 48
Whisker Pad Length	3.89mm	4.15mm	
Philtrum to Lip Ratio	0.727	0.708	
Frontal Snout Area	396576 AU	434033 AU	
Craniofacial Measurement	Gsc:Cyp26A1	WT Littermate	
Bigonial Line Length	3.06mm	3.23mm	Litter 41
Whisker Pad Length	4.07mm	4.05mm	
Philtrum to Lip Ratio	0.674	0.518	
Frontal Snout Area	423971 AU	443939 AU	
Craniofacial Measurement	Gsc:Cyp26A1	WT Littermate	
Bigonial Line Length	3.70mm	3.68mm	Litter 16
Whisker Pad Length	4.58mm	4.62mm	
Philtrum to Lip Ratio	0.491	0.507	
Frontal Snout Area	555161 AU	564516 AU	
*Only one Gsc:Cyp26A1 Embryo in Litter 34			

# Litter	Total # mice	Wild Type		Gsc:Cyp26A1		Genotype
		Normal	FAS	Normal	FAS	Assessed Phenotype
6	31	14	0	2	15	

100% (14/14) of wild-type mice were assessed as a normal Cranial Facial phenotype.

88% (15/17) of mutant mice assessed had a discernable FAS phenotype.

Supplemental Figure 3.1: Blinded Analysis of Gsc:Cyp26A1 Mice Demonstrates FAS Phenotype Evident in F1 Generation. A blinded assessment was performed on 6 litters of mice (n=31) to determine the phenotype and whether an F1 generation pup (P1) was indeed FAS-like or WT using the FAS criteria. After Weaning (P21), mice were genotyped and results compared to the assessment made by the laboratory technician. 100% of mice assessed as WT were all genotyped WT (14/14), while 88% of mice assessed phenotypically as FAS, were genotyped as Gsc:Cyp26A1-eGFP (15/17). Therefore, the Gsc:Cyp26a1-eGFP mouse model has an 88% phenotypic penetrance of FAS.

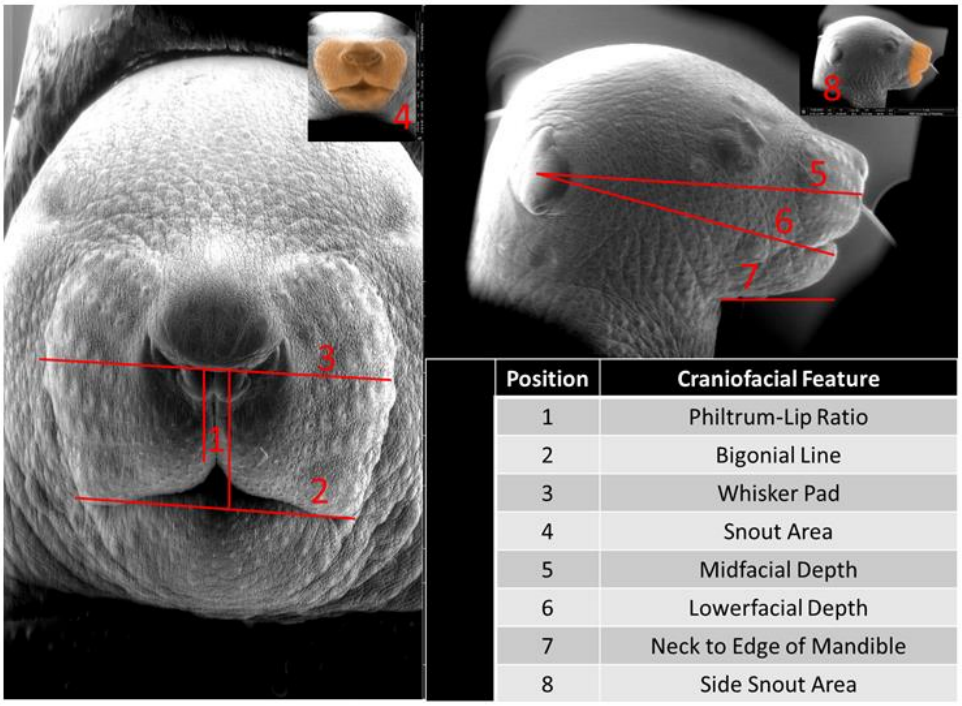

Position	Craniofacial Feature
1	Philtrum-Lip Ratio
2	Bigonial Line
3	Whisker Pad
4	Snout Area
5	Midfacial Depth
6	Lowerfacial Depth
7	Neck to Edge of Mandible
8	Side Snout Area

Supplemental Figure 3.2: Craniofacial Measurements Used for E18.5 Embryo Facial Analysis (adapted from Anthony et al., 2010 and Lipinski et al. 2012). Gsc:Cyp26A1 and WT littermate E18.5 embryo SEM frontal and side view pictures were used for quantitative measurements, including the snout and side snout areas.

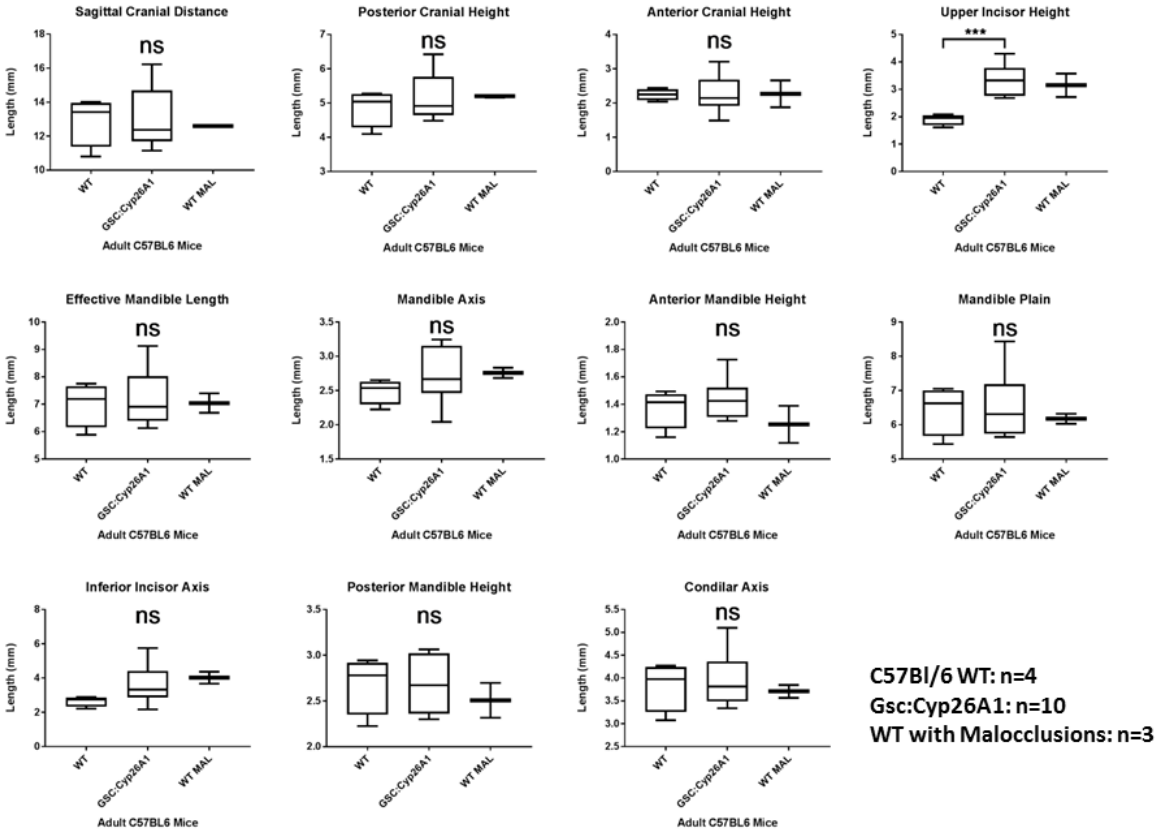

Supplemental Figure 3.3. GSC:Cyp26A1 P60 Mice Have Large Upper Incisors, But Do Not Have Any Length or Height Variations in the Cranium or Mandible Regions. GSC:Cyp26A1 P60 mice had only one statistical significant length or height measurement. It was the upper incisor height, which was expected due to the twisted snout that resulted in a maxillary malocclusion and longer incisors. Therefore, this measure actually served as an internal control for the length and height measurements. Trending results in the inferior incisor axis, posterior cranial height and mandible axis were observed in Gsc:Cyp26A1 mice. Interestingly, Gsc:Cyp26A1 mice had a distinctively larger trending anterior mandible height compared to WT mice. ***P<0.001

Chapter 4: Conclusion: Significance and Future Directions

The Gsc:Cyp26A1 transgenic mouse is the first known model demonstrating RA deficiency as a major etiology of FASD-like outcomes in a mammalian model. We have provided strong evidence that the Gsc:Cyp26A1 transgenic mouse is a robust model demonstrating the long-term developmental effects of retinoic acid deficiency at early gastrulation. The similarities in FASD-like outcomes found between PAE mouse models in the literature and the Gsc:Cyp26A1 transgenic model is remarkable. The craniofacial malformations observed in the Gsc:Cyp26A1 mouse model also recapitulate of the defects found in Fainsod's *Xenopus* studies of alcohol exposure during early gastrulation. Our mouse model produces similar phenotypic outcomes that are also found in Vitamin A Deficiency (VAD / RA deficiency) mouse models at gastrulation. The similarities in craniofacial malformations between PAE, VAD, and the Gsc:Cyp26A1 mouse models suggests that reduced levels of RA during gastrulation drives FASD-like phenotypes. Moreover, RA catabolism or competitive inhibition of Raldh2 by ethanol, and the resulting drop in RA production can alone explain the FASD-like outcomes.

PAE mediated retinoic acid deficiency may be the underlying mechanism of cranial NCCs survival and migration impairments and subsequent craniofacial malformations. There have been many studies that demonstrate that RA teratogenicity, either RA excess or deficiency at gastrulation, causes craniofacial malformations (Abu-Abed *et al.*, 2001; Kam *et al.*, 2012; Lee *et al.*, 2012). As previously described, PAE at gastrulation also cause craniofacial malformations reminiscent of those found in RA teratogenicity studies. Retinoic acid is required for proper survival and migration of neural crest cells (NCCs), specifically the prosencephalon and mesencephalon cranial neural crest cells which ultimately form the bone, cartilage, and

peripheral nerves of the developing face(Bronner and LeDouarin, 2012; Gong, 2014; Chawla *et al.*, 2016). The rhombencephalon cranial neural crest cells form the pharyngeal arches in the developing embryo, which form parts of the future larynx, pharynx, thymus, lungs, and heart (Bronner and LeDouarin, 2012; Gong, 2014; Chawla *et al.*, 2016). RA Teratogenicity at early developmental time points will cause altered cellular signaling and impact the survival and migration of these NCCs. Moreover, the epigenetic signatures in these NCCs and progenitor stem cell lineages will also be impaired, affecting future cell types. Thus, RA deficiency at gastrulation affects the NCCs that will form the future craniofacial and thoracic regions in a developing embryo. E8.5 Gsc:Cyp26A1 embryos show impaired RA expression and cellular signaling in the developing forebrain (prosencephalon) region, where cranial NCCs will form the bone, cartilage, and peripheral nerves of the developing face. Moreover, E10.5 Gsc:Cyp26A1 embryos show impaired patterning in cranial nerves V thru XI, which are derived from cranial NCCs and ectodermal placode cells. Furthermore, E18.5 Gsc:Cyp26A1 embryos demonstrate significantly smaller facial measurements (Bigonial Line, Whisker Pad, Frontal Snout Areas) compared to WT Embryos, suggesting altered cellular signaling and impact on the survival of cranial NCCs. Interestingly, the phenotypes observed in Gsc:Cyp26A1 E8.5, 10.5 and 18.5 embryos were already established in PAE mouse model studies where alcohol was provided to dams at early gastrulation or throughout pregnancy. As hypothesized, this suggests that PAE mediated retinoic acid deficiency may be the underlying mechanism of cranial NCCs survival and migration impairments and craniofacial malformations.

Establishing the Gsc:Cyp26A1 RA deficiency model as an *in vivo* model of FASD opens up the possibility to assess whether changes in epigenetic signatures of PAE/FASD-like outcomes and downstream ethanol/retinoic acid affected signaling pathways may be clinically relevant as

FASD biomarkers. The observed craniofacial malformations in the *Gsc:Cyp26A1* model suggest that mice have underlying aberrant cellular signaling and epigenetic remodeling in craniofacial tissues. Gsc:Cyp26A1 P60 (adult) mice also have a high incidence of craniofacial malocclusions. Moreover, these malocclusions are caused by a curvature of the maxillary component of the skull, derived from cranial NCCs from the forebrain (prosencephalon) (Bronner and LeDouarin, 2012). The Gsc:Cyp26A1 model is the first known RA deficiency model at early gastrulation to show incidence of maxillary malocclusions. Intriguingly, this suggests that the maxillary malocclusions might be due to epigenetic modulation, as the snout does not fully develop until well after weaning. Interestingly, Kaminen-Ahola *et al's* PAE paradigm using a chronic E0.5-E8.5, *ad libitum* (voluntary), 10% v/v alcohol exposure shows a maxillary malocclusion in P30 (adolescent) mice that is reminiscent of those observed in the Gsc:Cyp26A1 model. The PAE paradigm encompasses the early gastrulation period (E6.5-7.0), suggesting that PAE mediated retinoic acid deficiency may be the underlying mechanism of maxillary malocclusions (Kaminen-Ahola, Ahola, Maga, *et al.*, 2010). Moreover, Kaminen-Ahola *et al.'s* PAE study showed that epigenetic changes were found in agouti mice, further suggesting that retinoic acid deficiency may cause epigenetic changes to some degree as seen in this PAE paradigm (Kaminen-Ahola, Ahola, Maga, *et al.*, 2010). The Gsc:Cyp26A1 model of retinoic acid deficiency (mimicking alcohol exposure) at early gastrulation demonstrates PAE model phenotypes. PAE/FASD researchers were once not able to gather reproducible data from these types of PAE questions due to the varying dosage, duration, and gestational timing of alcohol exposure in PAE mouse models. The Gsc:Cyp26A1 mouse provides a testable robust, reliable, and reproducible model, demonstrating FASD-like outcomes.

The Gsc:Cyp26A1 model provides substantial craniofacial FASD-like outcomes, but the model is also capable of studying embryonic development and viability. The Gsc:Cyp26A1 model was created to biochemically mimic alcohol exposure and much thought and planning went into the use of Cyp26A1 and its enzymatic activity. An early design concern was the level of expression of Cyp26A1. We needed enough Cyp26A1 to produce a phenotype, but needed to balance a tipping point of overexpression that might lead to non-viable mice. Two Gsc:Cyp26A1 lines (G12 and H4) were constructed as a strategy to "fine tune" Cyp26A1 expression levels with phenotypic outcomes. One line (G12) utilizes a T2A (self-cleaving peptide regulation) element that is more efficient in producing (Cyp26A1) protein compared to an IRES (translation initiation regulation) element that is used in the other line (H4) (Kim *et al.* 2011). One would expect a 1:1 (WT:*Gsc:Cyp26A1*) ratio for offspring (in WT x Het matings), yet Gsc:Cyp26A1 G12 line and H4 line are 1:0.66 and 1:0.88, respectively. This experimental observation supports the prediction that Cyp26A1 activity varies between lines; and luckily, we are in the "sweet zone" for Cyp26A1-induced RA deficiency – not to little, not too much. That there is some embryonic lethality in the Gsc:Cyp26A1 model suggests that RA deficiency at early gastrulation can induce a severe phenotype causing embryonic lethality. Assessments of litters gathered for E8.5 and E10.5 experiments show that embryos arrest at or just after E8.5. Early embryo lethality in both PAE and VAD (retinoic acid deficiency) mouse models is well documented and suggests that retinoic acid deficiency at gastrulation may be one of the mechanisms causing this phenotype (Sulik, Johnston and Webb, 1981; Sulik and Johnston, 1983; Niederreither *et al.*, 2000; Rhinn *et al.*, 2011; Rhinn and Dolle, 2012). Interestingly, heavy or binge alcohol exposures during the first trimester (of pregnancy) has a significantly increased risk of spontaneous abortion (miscarriage) in humans (Bailey and Sokol, 2011). Cell signaling at pre-gastrulation requires

defined RA concentrations, so much so that during blastocyst development (E3.5-5.5, pre-implantation) embryonic Cyp26A1 and Cyp26C1 are expressed, stopping maternally derived (extracellular) RA from entering the blastocyst (Kam *et al.,* 2012). Embryonic RALDH transcripts do not express in the developing embryo until E7.5, while RARE-LacZ studies further demonstrate RA is detected at E7.5 in posterior tissues (Rossant *et al.,* 1991; Haselbeck, Hoffmann and Duester, 1999). Therefore RA levels in the developing embryo are fixed (after pre-implantation) throughout the pre-gastrulation and early gastrulation (E6.5-7.5) windows. When our *Gsc:Cyp26A1* transgenic mouse model activates during *Gsc* expression from E6.4-E6.9 (early gastrulation) (Blum *et al.,* 1992). *Gsc* mediated Cyp26A1 expression causes retinoic acid deficiency during a window in which there is no exogenous or endogenous sources of RA in the embryo due to the Cyp26A1/C1 and RALDH mechanisms in place to regulate RA during pre- and early gastrulation. Taken all together, the Gsc:Cyp26A1 model is capable of studying embryonic development and viability using the two lines with varying Cyp26A1expression while suggesting that RA deficiency at gastrulation is a cause of embryonic lethality (stillbirths).

The Gsc:Cyp26A1 model is also well positioned to further study the RA signaling pathways that are impaired during PAE. New experimental questions can now we addressed; like whether supplemental ethanol exposure causes increased teratogenicity, or whether Gsc:Cyp26A1 mice have brain and behavioral deficits, or more importantly, can Vitamin A supplementation be used as a preventative treatment for FASD.

i) Sensitized PAE study. Our hypothesis predicts, if this is truly modeling an alcohol-induced mechanism, our *Gsc:Cyp26A1* embryo model will be hypersensitive to PAE. If true, we should observe increased impairment of RA mediated signaling pathways at early gastrulation, and more severe expression of FASD-like phenotypic outcomes. These studies will underscore that

acute alcohol exposure during early gastrulation does mediate RA deficiency and is a major etiology of FASD.

ii) Vitamin A supplementation reduces or prevents FASD-like outcomes in Gsc:Cyp26A1 and PAE mice. Our hypothesis predicts that Vitamin A supplementation to the pregnant dam will reduce or prevent FASD-like outcomes following PAE. Our collaborator Dr. Abraham Fainsod has performed ethanol exposure paradigms in *Xenopus*, observing the most severe FASD-like craniofacial outcomes when ethanol exposure occurs at stage 11 (gastrulation) compared to other developmental time points (Yelin *et al.* 2005, 2007). Moreover, Vitamin A supplementation of ethanol exposed Stage 11 tadpoles rescues the FASD-like outcome, producing a normal adult tadpole (Yelin *et al.*2005, 2007). Furthermore, when Stage 11 tadpoles were subjected to a retinoic acid synthesis inhibitor (DEAB), the adult tadpoles produced FASD-like craniofacial outcomes (Yelin *et al.* 2007) – directly linking the PAE and RA deficiency outcomes by the same mechanism. Mouse models which impair RA synthesis (RDH10, RALDH1, 2, 3), RA response elements (RARs, RXRs), cause RA deficiency (VAD) and all produce FASD-like craniofacial outcomes to some degree. Unfortunately, due to the cellular importance of RA many of these mouse models produce severe outcomes and in most cases embryo lethality occurs. This is a phenotype seen in the Gsc:Cyp26A1 model, but it is also common in heavy or binge alcohol exposures during the first trimester in humans (Bailey and Sokol, 2011).

iii) Assessment of behavioral deficits. FASD with sentinel facial features is the most severe form of the disorder, including brain and behavioral deficits. Reduction in white matter volume of the anterior commissure of E180 *Gsc:Cyp26A1* mice suggests (fore)brain development is affected, indicating structural neuroectoderm-derived development may also be affected, in addition to the NCC-derived craniofacial abnormalities we have observed. Intriguingly, anterior commissure

volume has already been shown to be significantly reduced by 23% in an acute E7.0, I.p. PAE paradigm (Cao *et al.*, 2014). This same phenotype suggests that PAE mediated RA deficiency has a role in brain deficits seen much later in development. It will be very interesting to assess Gsc:Cyp26A1 mice for learning, memory, and cognition impairments. Coupled with the penetrance of FASD-like outcomes in our Gsc:Cyp26A1 mice (>90% affected) these results will be the first to describe FASD-like behavior deficits and would be the first full spectrum model of.FASD. Behavioral experiments to consider using adult mice starting at P60 include: Open Field Test to test for general locomotor activity and anxiety-like behavior; Elevated Plus Maze to test for anxiety –like behavior; Novel Object Test to test for learning and memory impairments; Olfactory Discrimination Test to test for olfactory impairments; and Morris Water Maze to test for spatial learning, memory, and cognition. In addition, live MicroCT and MRI imaging and IHC analysis can be undertaken to more fully assess underlying structural deficits, particularly in specific brain regions (hippocampus and hypothalamus) controlling this behavior.

In summary, FASD is the leading cause of neurodevelopmental abnormalities in Canadian children. FASD with sentinel facial features (FAS) produces the full spectrum of outcomes: craniofacial malformations, brain aberrations, and behavioral deficits. We have reviewed all PAE mouse model paradigms and identified those that best recapitulate these FASD-like outcomes in mice, taking into consideration alcohol dosage, duration, and gestational timing. We then engineered Gsc:Cyp26A1 mice taking into consideration Dr. Fainsod's Vitamin A Hypothesis and its experimental validation in *Xenopus* studies. Our studies here strongly support the hypothesis that retinoic acid deficiency at early gastrulation is an underlying mechanism of FASD-like outcomes in a mammalian model. Taken together, our data provide *in vivo* evidence that strongly supports retinoic acid deficiency as a major molecular etiology of craniofacial

malformations and brain aberrations associated with FASD. Vitamin A supplementation may significantly reduce or prevent FASD outcomes in children with PAE, reducing the burden of this disorder on children, their families, and society.

Literature Cited:

Abdelrahman, A. and Conn, R. (2009) 'Eye abnormalities in fetal alcohol syndrome', *Ulster Medical Journal*, 78(3), pp. 164–165.

Akers, K. G. *et al.* (2011) 'Fetal alcohol exposure leads to abnormal olfactory bulb development and impaired odor discrimination in adult mice', *Molecular Brain*, 4, p. 29. doi: 10.1186/1756-6606-4-29.

Alberry, B. and Singh, S. M. (2016) 'Developmental and behavioral consequences of early life maternal separation stress in a mouse model of fetal alcohol spectrum disorder', *Behavioural Brain Research*. Elsevier B.V., 308, pp. 94–103. doi: 10.1016/j.bbr.2016.04.031.

Alexandria J. Hill, MD, Nathan Dreve, MD, Huaizhi Yin, MS, Esther Tamayo, G. S. and MD, and Egle Bytautiene, MD, P. (2014) 'The role of NADPH oxidase in a mouse model of fetal alcohol syndrome', *Am J Obstet Gynecol*, 210(5), pp. 1–13. doi: 10.1016/j.ajog.2013.12.019.The.

Allan, A. M., Goggin, S. L. and Caldwell, K. K. (2014) 'Prenatal alcohol exposure modifies glucocorticoid receptor subcellular distribution in the medial prefrontal cortex and impairs frontal cortex-dependent learning', *PLoS ONE*, 9(4). doi: 10.1371/journal.pone.0096200.

Anderson, R. (1981) 'Endocrine balance as a factor in the etiology of the fetal alcohol syndrome', *Neurobehav Toxicol Teratol*, 3(2), pp. 89–104.

Angelucci, L. *et al.* (1985) 'A model for later-life effects of perinatal drug exposure: maternal hormone mediation', *Neurobehav Toxicol Teratol1*, 7(5), pp. 511–517.

Anthony, B. *et al.* (2010) 'Alcohol-induced facial dysmorphology in C57BL/6 mouse models of fetal alcohol spectrum disorder', *Alcohol*. doi: 10.1016/j.alcohol.2010.04.002.

Assadi, F. (2014) 'Renal dysfunction in fetal alcohol syndrome: a potential contributor on developmental disabilities of offspring.', *Journal of renal injury prevention*, 3(4), pp. 83–6. doi: 10.12861/jrip.2014.24.

Astley, S. and Clarren, S. (1996) 'A case definition and photographic screening tool for the facial phenotype of fetal alcohol syndrome', *The Journal of Pediatrics*, 129(1), pp. 33–41. doi: 10.1016/S0022-3476(96)70187-7.

Astley, S. J., Bledsoe, J. M. and Davies, J. K. (2016) 'The essential role of growth deficiency in the diagnosis of fetal alcohol spectrum disorder', *Advances in Pediatric Research*, pp. 1–20. doi: 10.12715/apr.2016.3.9.

Autry, A. E. and Monteggia, L. M. (2012) 'Brain-derived neurotrophic factor and neuropsychiatric disorders', *Pharmacol Rev*, 64(2), pp. 238–258. doi: 10.1124/pr.111.005108.

Bake S, Tingling JD, M. R. (2013) 'NIH Public Access', *Ethanol exposure during pregnancy persistently attenuates cranially-directed blood flow in the developing fetus: Evidence from ultrasound imaging in a murine second trimester equivalent model*, 36(5), pp. 748–758. doi: 10.1111/j.1530-0277.2011.01676.x.Ethanol.

Bakker, J., Bel, F. van and Heijnen, C. (2001) 'Neonatal glucocorticoids and the developing brain: short-term treatment with life-long consequences', *Trends Neurosci*, 24(11), pp. 649–653.

Balmer, J. E. and Blomhoff, R. (2002) 'Gene expression regulation by retinoic acid', 43. doi: 10.1194/jlr.R100015-JLR200.

Bearer, C. (2001a) 'L1 cell adhesion molecule signal cascades: targets for ethanol developmental neurotoxicity', *Neurotoxicology*, 22(5), pp. 625–633.

Bearer, C. (2001b) 'Mechanisms of brain injury: L1 cell adhesion molecule as a target for ethanol-induced prenatal brain injury', *Semin Pediatr Neurol*, 8(2), pp. 100–107.

Blum, M. *et al.* (1992) 'Gastrulation in the mouse: The role of the homeobox gene goosecoid', *Cell*. Elsevier, 69(7), pp. 1097–1106. doi: 10.1016/0092-8674(92)90632-M.

Bohnsack, B. L. and Kahana, A. (2013) 'Thyroid hormone and retinoic acid interact to regulate zebrafish craniofacial neural crest development', *Developmental Biology*. Elsevier, 373(2), pp. 300–309. doi: 10.1016/j.ydbio.2012.11.005.

Bonthius, D. J., Goodlett, C. R. and West, J. R. (1988) 'Blood alcohol concentration and severity of microencephaly in neonatal rats depend on the pattern of alcohol administration', *Alcohol*, 5(3), pp. 209–214. doi: 10.1016/0741-8329(88)90054-7.

Boyadjieva, Nadka I. ; Sarkar, D. K. (2013) 'Cyclic Adenosine Monophosphate and Brain-Derived Neurotrophic Factor Decreased Oxidative Stress and Apoptosis in Developing Hypothalamic Neuronal Cells: Role of Microglia', *Alcoholism: Clinical and Experimental Research*, 37(8), pp. 1370–1379.

Brady, M. L., Allan, A. M. and Caldwell, K. K. (2013) 'A Limited Access Mouse Model of Prenatal Alcohol Exposure that produces long-lasting deficts in hippocampal-dependent learning and memory ';, 36(3), pp. 457–466. doi: 10.1111/j.1530-0277.2011.01644.x.A.

Brown, N., Goulding, E. and Fabro, S. (1979) 'Ethanol embryotoxicity: direct effects on mammalian embryos in vitro', *Science*, 206(4418), pp. 573–575.

Bruce M. Carlson, MD, P. (2014) 'Chapter 14 - Head and Neck -', *Human Embryology and Developmental Biology*, (5th edition), pp. 294–334.

Burd, L., Blair, J. and Dropps, K. (2012) 'Prenatal alcohol exposure, blood alcohol concentrations and alcohol elimination rates for the mother, fetus and newborn', *Journal of Perinatology*. Nature Publishing Group, 32(9), pp. 652–659. doi: 10.1038/jp.2012.57.

Caldwell, K. K. *et al.* (2008) 'Fetal alcohol spectrum disorder-associated depression: evidence for reductions in the levels of brain-derived neurotrophic factor in a mouse model', *Pharmacol Biochem Behav*, 90(4), pp. 614–624. doi: S0091-3057(08)00155-X [pii]\r10.1016/j.pbb.2008.05.004.

Cao, W. *et al.* (2014) 'Prenatal alcohol exposure reduces magnetic susceptibility contrast and anisotropy in the white matter of mouse brains', *NeuroImage*. doi: 10.1016/j.neuroimage.2014.08.035.

Cartwright, M. and Smith, S. (1995) ‘Increased cell death and reduced neural crest cell numbers in ethanol-exposed embryos: partial basis for the fetal alcohol syndrome phenotype’, *Alcohol Clin Exp Res.*, 19(2), pp. 378–386.

Chudley, A. E. (2005) ‘Canadian guidelines for FASD’, *CMAJ*.

Chudley, A. E. *et al.* (2005) ‘Guidelines for Diagnosis’, *CMAJ : Canadian Medical Association journal = journal de l’Association medicale canadienne*, 172.

Clagett-Dame, M. and Deluca, H. F. (2002) ‘The Role of Vitamin A in Mammalian Reproduction and Embryonic Development’, *Annual review of nutrition*, 22, pp. 347–381.

Clagett-Dame, M. and Knutson, D. (2011) ‘Vitamin a in reproduction and development’, *Nutrients*. doi: 10.3390/nu3040385.

Clarke, Margaret and Gibbard, B. (2003) ‘Overview of FASD for mental health professionals’, *Can Child Adolesc Psychiatr Rev*, 12(3), pp. 57–63.

Clarren, S. (1986) ‘Neuropathology in fetal alcohol syndrome’, *Alcohol and brain Development*, pp. 158–166.

Coleman, L. G. *et al.* (2012) ‘Postnatal day 7 ethanol treatment causes persistent reductions in adult mouse brain volume and cortical neurons with sex specific effects on neurogenesis’, *Alcohol*. doi: 10.1016/j.alcohol.2012.01.003.

Cook, J. L. *et al.* (2016) ‘Fetal alcohol spectrum disorder: a guideline for diagnosis across the lifespan’, *CMAJ : Canadian Medical Association journal = journal de l’Association medicale canadienne*, pp. 1–7. doi: 10.1503/cmaj.141593/-/DC1.

Coulter, C. L. *et al.* (1993) ‘Midline Cerebral Dysgenesis, Dysfunction of the Hypothalamic-Pituitary Axis, and Fetal Alcohol Effects’, *Archives of Neurology*, 50(7), pp. 771–775. doi: 10.1001/archneur.1993.00540070083022.

Cui, Z.-J. *et al.* (2010) ‘Prenatal Alcohol Exposure Induces Long-Term Changes in Dendritic Spines and Synapses in the Mouse Visual Cortex’, *Alcohol and Alcoholism*, 45(4), pp. 312–319. doi: 10.1093/alcalc/agq036.

Cunningham, T. J. *et al.* (2015) ‘Retinoic acid activity in undifferentiated neural progenitors is sufficient to fulfill its role in restricting Fgf8 expression for somitogenesis’, *PLoS ONE*. doi: 10.1371/journal.pone.0137894.

Cunningham, T. J., Zhao, X. and Duester, G. (2011) ‘Uncoupling of retinoic acid signaling from tailbud development before termination of body axis extension’, *Genesis*, 49(10), pp. 776–783. doi: 10.1002/dvg.20763.

Davis, J., Li, Y. and Rankin, C. (2008) ‘Effects of Developmental Exposure to Ethanol on Caenorhabditis elegans’, *Alcoholism: Clinical and Experimental Research2008*, 32(5), pp. 853–867.

DeMyer W, Zeman W, P. C. (1964) ‘The face predicts the brain: diagnostic significance of

median facial anomalies for holoprosencephaly (arhinencephaly)', *Pediatrics*, 34, pp. 256–263.

Diorio, D., Viau, V. and Meaney, M. J. (1993) 'The role of the medial prefrontal cortex (cingulate gyrus) in the regulation of hypothalamic-pituitary-adrenal responses to stress.', *The Journal of Neuroscience*, 13(9), pp. 3839–3847. doi: 10.1371/journal.pone.0096200.

Drew, P. D. *et al.* (2015) 'Pioglitazone blocks ethanol induction of microglial activation and immune responses in the hippocampus, cerebellum, and cerebral cortex in a mouse model of fetal alcohol spectrum disorders', *Alcoholism: Clinical and Experimental Research*. doi: 10.1111/acer.12639.

Dunty Jr., W. C., Zucker, R. M. and Sulik, K. K. (2002) 'Hindbrain and Cranial Nerve Dysmorphogenesis Result from Acute Maternal Ethanol Administration', *Developmental Neuroscience*, 24(4), pp. 328–342. Available at: http://www.karger.com/DOI/10.1159/000066748.

Feltes, B. C. *et al.* (2014) 'Fetal Alcohol Syndrome, Chemo-Biology and OMICS: Ethanol Effects on Vitamin Metabolism During Neurodevelopment as Measured by Systems Biology Analysis', *OMICS: A Journal of Integrative Biology*, 18(6), pp. 344–363. doi: 10.1089/omi.2013.0144.

Förstermann, U. and Sessa, W. C. (2012) 'Nitric oxide synthases: Regulation and function', *European Heart Journal*, 33(7), pp. 829–837. doi: 10.1093/eurheartj/ehr304.

Fried, P. A. (1983) 'HAT MATERNAL HEAVY during pregnan', 44(2).

Gallo, P. and Weinberg, J. (1986) 'Organ growth and cellular development in ethanol-exposed rats', *Alcohol*, 3(4), pp. 261–267.

Gilberti, D; Mohan, SS; Brown, LAS; Gauthier, T. (2013) 'Perinatal exposure to alcohol: implications for lung development and disease', *Paediatr Respir Rev.*, 14(1), pp. 17–21. doi: 10.1146/annurev-cellbio-092910-154240.Sensory.

Godin, E. A. *et al.* (2010a) 'Magnetic resonance microscopy defines ethanol-induced brain abnormalities in prenatal mice: Effects of acute insult on gestational day 7', *Alcoholism: Clinical and Experimental Research*. doi: 10.1111/j.1530-0277.2009.01071.x.

Godin, E. A. *et al.* (2010b) 'Magnetic resonance microscopy defines ethanol-induced brain abnormalities in prenatal mice: Effects of acute insult on gestational day 7', *Alcoholism: Clinical and Experimental Research*, 34(1), pp. 98–111. doi: 10.1111/j.1530-0277.2009.01071.x.

Goez, H. R., Scott, O. and Hasal, S. (2011) 'Fetal Exposure to Alcohol, Developmental Brain Anomaly, and Vitamin A Deficiency: A Case Report', *Journal of Child Neurology*, 26(2), pp. 231–234. doi: 10.1177/0883073810380458.

Goodlett, C., Horn, K. and Zhou, F. (2005) 'Alcohol Teratogenesis: Mechanisms of Damage and Strategies for Intervention', *Exp Biol Med*, 230(6), pp. 394–406.

Gubitosi-Klug, R., Larimer, C. and Bearer, C. (2007) 'L1 cell adhesion molecule is neuroprotective of alcohol induced cell death', *Neurotoxicology*, 28(3), pp. 457–462.

Guerri, C. *et al.* (1993) 'Derangement of astrogliogenesis as a possible mechanism involved in alcohol-induced alterations of central nervous system development', *Alcohol*, 2, pp. 203–208.

Guerri, C. (1998) 'Neuroanatomical and neurophysiological mechanisms involved in central nervous system dysfunctions induced by prenatal alcohol exposure', *Alcohol Clin Exp Res.*, 22(2), pp. 304–312.

Hales, C. A. *et al.* (2014) 'Modelling cognitive affective biases in major depressive disorder using rodents', *British journal of pharmacology*, 171(20), pp. 4524–4538. doi: 10.1111/bph.12603.

Halilagic, A. *et al.* (2007) 'Retinoids control anterior and dorsal properties in the developing forebrain', *Developmental Biology*, 303(1), pp. 362–375. doi: 10.1016/j.ydbio.2006.11.021.

Henderson, G. *et al.* (1995) 'In utero ethanol exposure elicits oxidative stress in the rat fetus', *Alcohol Clin Exp Res.*, 19(3), pp. 714–720.

Higashiyama, D. *et al.* (2007) 'Sequential developmental changes in holoprosencephalic mouse embryos exposed to ethanol during the gastrulation period', *Birth Defects Research Part A - Clinical and Molecular Teratology*, 79(7), pp. 513–523. doi: 10.1002/bdra.20367.

Hofer, R. and Burd, L. (2009) 'Review of published studies of kidney, liver, and gastrointestinal birth defects in fetal alcohol spectrum disorders', *Birth Defects Research Part A - Clinical and Molecular Teratology*, 85(3), pp. 179–183. doi: 10.1002/bdra.20562.

Hong, M. and Krauss, R. S. (2012) 'Cdon Mutation and Fetal Ethanol Exposure Synergize to Produce Midline Signaling Defects and Holoprosencephaly Spectrum Disorders in Mice', *PLoS Genetics*. doi: 10.1371/journal.pgen.1002999.

Huerta, S. *et al.* (2002) 'Vitamin a deficiency in a newborn resulting from maternal hypovitaminosis A after biliopancreatic diversion for the treatment of morbid obesity', *American Journal of Clinical Nutrition*, 76(2), pp. 426–429.

Humphrey, J. H., West, K. P. and Sommer, A. (1992) 'Vitamin A deficiency and attributable mortality among under-5-year-olds.', *Bulletin of the World Health Organization*, 70(2), pp. 225–32. Available at: http://www.pubmedcentral.nih.gov/articlerender.fcgi?artid=2393289&tool=pmcentrez&rendertype=abstract.

Ikonomidou, C. *et al.* (2000) 'Ethanol-induced apoptotic neurodegeneration and fetal alcohol syndrome', *Science*, 287(5455), pp. 1056–1060.

Jarrar, W. *et al.* (2015) 'Nkx2.2 and Nkx2.9 are the key regulators to determine cell fate of branchial and visceral motor neurons in caudal hindbrain', *PLoS ONE*, 10(4), pp. 1–20. doi: 10.1371/journal.pone.0124408.

Jones, K. L. (no date) 'The Effects of Alcohol on Fetal Development'. doi: 10.1002/bdrc.20200.

Kalberg, W. O. *et al.* (2006) 'Comparison of motor delays in young children with fetal alcohol syndrome to those with prenatal alcohol exposure and with no prenatal alcohol exposure',

Alcoholism: Clinical and Experimental Research, 30(12), pp. 2037–2045. doi: 10.1111/j.1530-0277.2006.00250.x.

Kam, R. K. T. *et al.* (2012) 'Retinoic acid synthesis and functions in early embryonic development', *Cell & Bioscience*, 2(1), p. 11. doi: 10.1186/2045-3701-2-11.

Kaminen-Ahola, N., Ahola, A., Maga, M., *et al.* (2010) 'Maternal ethanol consumption alters the epigenotype and the phenotype of offspring in a mouse model', *PLoS Genetics*, 6(1). doi: 10.1371/journal.pgen.1000811.

Kaminen-Ahola, N., Ahola, A., Flatscher-Bader, T., *et al.* (2010) 'Postnatal growth restriction and gene expression changes in a mouse model of fetal alcohol syndrome', *Birth Defects Research Part A: Clinical and Molecular Teratology*, 88(10), pp. 818–826. doi: 10.1002/bdra.20729.

Kane, C. J. M. *et al.* (2011) 'Protection of neurons and microglia against ethanol in a mouse model of fetal alcohol spectrum disorders by peroxisome proliferator-activated receptor-?? agonists', *Brain, Behavior, and Immunity*, 25(SUPPL. 1), pp. 137–145. doi: 10.1016/j.bbi.2011.02.016.

Karacay, Mahoney, Plume, B. (2015) 'Genetic absence of nNOS worsens fetal alcohol effects in mice. II: Microencephaly and neuronal losses', *Alcohol Clin Exp Res.*, 39(2), pp. 221–231. doi: 10.1038/ng.840.Principles.

Keen, C. L. *et al.* (2010) 'The plausibility of maternal nutritional status being a contributing factor to the risk for fetal alcohol spectrum disorders: the potential influence of zinc status as an example', *Biofactors*, 36(2), pp. 125–135. doi: 10.1002/biof.89.The.

Kietzman, H. W. *et al.* (2014) 'The teratogenic effects of prenatal ethanol exposure are exacerbated by sonic Hedgehog or Gli2 haploinsufficiency in the mouse', *PLoS ONE*, 9(2), pp. 1–5. doi: 10.1371/journal.pone.0089448.

Kim, J. H. *et al.* (2011) 'High cleavage efficiency of a 2A peptide derived from porcine teschovirus-1 in human cell lines, zebrafish and mice', *PLoS ONE*, 6(4), pp. 1–8. doi: 10.1371/journal.pone.0018556.

Kleiber, M. L. *et al.* (2013) 'Neurodevelopmental alcohol exposure elicits long-term changes to gene expression that alter distinct molecular pathways dependent on timing of exposure', *Journal of Neurodevelopmental Disorders*, 5(1), p. 6. doi: 10.1186/1866-1955-5-6.

Kleiber, M. L., Wright, E. and Singh, S. M. (2011) 'Maternal voluntary drinking in C57BL/6J mice: Advancing a model for fetal alcohol spectrum disorders', *Behavioural Brain Research*. Elsevier B.V., 223(2), pp. 376–387. doi: 10.1016/j.bbr.2011.05.005.

Knable, M. B. *et al.* (2004) 'Molecular abnormalities of the hippocampus in severe psychiatric illness: postmortem findings from the Stanley Neuropathology Consortium', *Molecular Psychiatry*, 9(6), pp. 609–620. doi: 10.1038/sj.mp.4001471.

Kot-Leibovich, H. and Fainsod, A. (2009) 'Ethanol induces embryonic malformations by competing for retinaldehyde dehydrogenase activity during vertebrate gastrulation', *Disease*

models & mechanisms, 2(5–6), pp. 295–305. doi: 10.1242/dmm.001420.

Kotch, L., Chen, S. and Sulik, K. (1995) 'Ethanol-induced teratogenesis: free radical damage as a possible mechanism', *Teratology*, 52(3), pp. 128–136.

Landgraf, D. *et al.* (2015) 'Dissociation of learned helplessness and fear conditioning in mice: A mouse model of depression', *PLoS ONE*, 10(4), pp. 1–17. doi: 10.1371/journal.pone.0125892.

LeBel, C. and Bondy, S. (1991) 'Oxygen radicals: common mediators of neurotoxicity', *Neurotoxicology and Teratology*, 13(3), pp. 341–346.

Lee, B. H. and Kim, Y. K. (2010) 'The roles of BDNF in the pathophysiology of major depression and in antidepressant treatment', *Psychiatry Investigation*, 7(4), pp. 231–235. doi: 10.4306/pi.2010.7.4.231.

Lee, L. M. Y. *et al.* (2012) 'A paradoxical teratogenic mechanism for retinoic acid', *Proceedings of the National Academy of Sciences*, 109(34), pp. 13668–13673. doi: 10.1073/pnas.1200872109.

Lipinski, R. J. *et al.* (2012) 'Ethanol-induced face-brain dysmorphology patterns are correlative and exposure-stage dependent', *PLoS ONE*. doi: 10.1371/journal.pone.0043067.

Lohnes, D. *et al.* (1994) 'Function of the retinoic acid receptors (RARs) during development (I). Craniofacial and skeletal abnormalities in RAR double mutants.', *Development (Cambridge, England)*, 120(10), pp. 2723–2748.

Lovely, C. B. (2016) 'Fishing for Fetal Alcohol Spectrum Disorders: Zebrafish as a Model for Ethanol Teratogenesis', *Zebrafish*, 13(5), pp. 391–398.

LUO, J. M. *et al.* (1995) 'Mice Lacking All Iso-Forms of Retinoic Acid Receptor-Beta Develop Normally and Are Susceptible To the Teratogenic Effects of Retinoic Acid', *Mechanisms of Development*, 53(1), pp. 61–71. doi: 10.1016/0925-4773(95)00424-6.

M Pilorge, C Fassier, H le Corronc, A. P. (2016) 'Genetic and functional analyses demonstrate a role for abnormal glycinergic signaling in autism', *Molecular Psychiatry*, 21, pp. 936–945.

Martinowich, K., Manji, H. and Lu, B. (2007) 'New insights into BDNF function in depression and anxiety', *Nature Neuroscience*, 10(9), pp. 1089–1093. doi: 10.1038/nn1971.

Matsubara, T. *et al.* (2006) 'Reduced glucocorticoid receptor ?? expression in mood disorder patients and first-degree relatives', *Biological Psychiatry*, 59(8), pp. 689–695. doi: 10.1016/j.biopsych.2005.09.026.

Matthews, S. (2002) 'Early programming of the hypothalamo-pituitary-adrenal axis', *Trends Endocrinol Metab*, 13(9), pp. 373–380.

McNeill, E. M. *et al.* (2010) 'Nav2 is necessary for cranial nerve development and blood pressure regulation.', *Neural development*, 5, p. 6. doi: 10.1186/1749-8104-5-6.

Michaelis, E. (1990) 'Fetal Alcohol Exposure: Cellular Toxicity and Molecular Events Involved in Toxicity', *Alcohol Clin Exp Res.*, 14(6), pp. 819–826.

Miller, M. (1992) ‘The effects of prenatal exposure to ethanol on cell proliferation and neuronal migration’, *Development of the Central Nervous System: Effects of Alcohol and Opiates*, pp. 47–69.

Moore, E. S. *et al.* (2002) ‘New perspectives on the face in fetal alcohol syndrome: What anthropometry tells us’, *American journal of medical genetics*, 109(4), pp. 249–260.

Muley, P. D. *et al.* (2008) ‘The atRA-responsive gene neuron navigator 2 functions in neurite outgrowth and axonal elongation’, *Developmental Neurobiology*, 68(13), pp. 1441–1453. doi: 10.1002/dneu.20670.

Naidoo, S. *et al.* (2006) ‘Foetal alcohol syndrome: A cephalometric analysis of patients and controls’, *European Journal of Orthodontics*, 28(3), pp. 254–261. doi: 10.1093/ejo/cji110.

Niederreither, K. *et al.* (2000) ‘Retinoic acid synthesis and hindbrain patterning in the mouse embryo.’, *Development (Cambridge, England)*, 127(1), pp. 75–85.

Niederreither, K. *et al.* (2002) ‘Embryonic retinoic acid synthesis is required for forelimb growth and anteroposterior patterning in the mouse.’, *Development (Cambridge, England)*, 129, pp. 3563–3574.

Niederreither, K. *et al.* (2003) ‘The regional pattern of retinoic acid synthesis by RALDH2 is essential for the development of posterior pharyngeal arches and the enteric nervous system.’, *Development (Cambridge, England)*, 130(11), pp. 2525–2534. doi: 10.1242/dev.00463.

Niederreither, K. *et al.* (no date) ‘Embryonic retinoic acid synthesis is essential for early mouse post-implantation development’.

Noel, M., Norris, E. H. and Strickland, S. (2011) ‘Tissue plasminogen activator is required for the development of fetal alcohol syndrome in mice’, *Proc Natl Acad Sci U S A*, 108(12), pp. 5069–5074. doi: 1017608108 [pii]\r10.1073/pnas.1017608108.

Norman, A. *et al.* (2009) ‘Neuroimaging and fetal alcohol spectrum disorders’, *Developmental disabilities research reviews*, 15(3), pp. 209–217. doi: 10.1002/ddrr.72.Neuroimaging.

O’Leary-Moore SK, Parnell SE, Godin EA, Dehart DB, Ament JJ, Khan AA, Johnson GA, S. and MA, S. K. (2010) ‘Magnetic resonance microscopy-based analyses of the brains of normal and ethanol-exposed fetal mice’, *Birth defects research Part A. Clinical and molecular teratology*, 88, pp. 953–964.

Pabst, O. *et al.* (2003) ‘Targeted disruption of the homeobox gene Nkx2.9 reveals a role in development of the spinal accessory nerve’, *Development*, 130(6), pp. 1193–1202. doi: 10.1242/dev.00346.

Paolicelli, R. C. *et al.* (2011) ‘Synaptic pruning by microglia is necessary for normal brain development.’, *Science (New York, N.Y.)*, 333(6048), pp. 1456–8. doi: 10.1126/science.1202529.

Parnell, S. E. *et al.* (2013) ‘Magnetic resonance microscopy-based analyses of the neuroanatomical effects of gestational day 9 ethanol exposure in mice’, *Neurotoxicology and Teratology*. Elsevier Inc., 39, pp. 77–83. doi: 10.1016/j.ntt.2013.07.009.

Paschaki, M. *et al.* (2013) 'Transcriptomic Analysis of Murine Embryos Lacking Endogenous Retinoic Acid Signaling', *PLoS ONE*, 8(4). doi: 10.1371/journal.pone.0062274.

Patten, A. R., Fontaine, C. J. and Christie, B. R. (2014) 'A Comparison of the Different Animal Models of Fetal Alcohol Spectrum Disorders and Their Use in Studying Complex Behaviors', *Frontiers in Pediatrics*, 2(September), pp. 1–19. doi: 10.3389/fped.2014.00093.

Pennimpede, T. *et al.* (2010) 'The role of CYP26 enzymes in defining appropriate retinoic acid exposure during embryogenesis', *Birth Defects Research Part A: Clinical and Molecular Teratology*. Wiley Subscription Services, Inc., A Wiley Company, 88(10), pp. 883–894. doi: 10.1002/bdra.20709.

Pennington, S. *et al.* (1983) 'The molecular mechanism of fetal alcohol syndrome (FAS). I. Ethanol-induced growth suppression', *Neurobehav Toxicol Teratol*, 5(2), pp. 259–262.

Pierce, D. R. and West, J. R. (1986) 'Alcohol-induced microencephaly during the third trimester equivalent: Relationship to dose and blood alcohol concentration', *Alcohol*, 3(3), pp. 185–191. doi: 10.1016/0741-8329(86)90043-1.

Popova, S. *et al.* (2016) 'Comorbidity of fetal alcohol spectrum disorder : a systematic review and meta-analysis', 387. doi: 10.1016/S0140-6736(15)01345-8.

Popova, S. *et al.* (2017) 'Estimation of national, regional, and global prevalence of alcohol use during pregnancy and fetal alcohol syndrome: a systematic review and meta-analysis', *The Lancet Global Health*, 5(3), pp. e290–e299. doi: 10.1016/S2214-109X(17)30021-9.

Ramanathan, R. *et al.* (1996) 'Alcohol inhibits cell-cell adhesion mediated by human L1', *J Cell Biol*, 133(2), pp. 381–390.

Randall, C. *et al.* (1989) 'Role of prostaglandins in alcohol teratogenesis', *Ann NY Acad Sci*, 562, pp. 178–182.

Randall, C., Anton, R. and Becker, H. (1987) 'Alcohol, pregnancy, and prostaglandins', *Alcohol Clin Exp Res.*, 11(1), pp. 32–36.

Randall, C., Ekblad, U. and Anton, R. (1990) 'Perspectives on the pathophysiology of fetal alcohol syndrome', *Alcohol Clin Exp Res.*, 14(6), pp. 807–812.

Rasmussen, C. *et al.* (2008) 'Neurobehavioural outcomes of children with fetal alcohol spectrum disorders: A Canadian perspective.', *Paediatrics & child health*, 13(3), pp. 185–191.

Rawat, A. (1975) 'Ribosomal proteins synthesis in the fetal and neonatal rat brain as influenced by maternal ethanol consumption', *Res Commun Chem Pathol Pharmacol*, 12(4), pp. 723–732.

Rema, V. and Ebner, F. F. (1999) 'Effect of enriched environment rearing on impairments in cortical excitability and plasticity after prenatal alcohol exposure.', *The Journal of neuroscience : the official journal of the Society for Neuroscience*, 19(24), pp. 10993–1006. Available at: http://www.ncbi.nlm.nih.gov/pubmed/10594080.

Rhinn, M. *et al.* (2011) 'Involvement of retinol dehydrogenase 10 in embryonic patterning and

rescue of its loss of function by maternal retinaldehyde treatment', *Proceedings of the National Academy of Sciences*, 108(40), pp. 16687–16692. doi: 10.1073/pnas.1103877108.

Rhinn, M. and Dolle, P. (2012) 'Retinoic acid signalling during development', *Development*, 139(5), pp. 843–858. doi: 10.1242/dev.065938.

Ribes, V. *et al.* (2006) 'Retinaldehyde dehydrogenase 2 (RALDH2)-mediated retinoic acid synthesis regulates early mouse embryonic forebrain development by controlling FGF and sonic hedgehog signaling.', *Development (Cambridge, England)*, 133(2), pp. 351–61. doi: 10.1242/dev.02204.

Rivera-pérez, J. A. *et al.* (1995) 'is required for craniofacial and rib development', 3012, pp. 3005–3012.

Roessler E, M. M. (2010) 'The molecular genetics of holoprosencephaly', *Am J Med Genet C Semin Med Genet*, 154C(7), pp. 52–61.

Ross, A. and Zolfaghari, R. (2011) 'Cytochrome P450s in the regulation of cellular retinoic acid metabolism', *Annual review of nutrition*, 450(Figure 1), pp. 65–87. doi: 10.1146/annurev-nutr-072610-145127.Cytochrome.

Rudeen, P. and Taylor, J. (1992) 'Fetal alcohol neuroendocrinopathies', *Alcohol and Neurobiology: Brain Development and Hormone Regulation*, pp. 109–138.

S, F.-L. and , Montesinos J, G. C. (2013) 'Ethanol induces TLR4/TLR2 association, triggering an inflammatory response in microglial cells', *J Neurochem*, 126(2), pp. 261–273.

Sari, Y. (2009) 'Activity-dependent neuroprotective protein-derived peptide, NAP, preventing alcohol-induced apoptosis in fetal brain of C57BL/6 mouse', *Neuroscience*, 158(4), pp. 1426–1435.

Scott E. Parnell, Shonagh K. O'Leary-Moore, Elizabeth A. Godin, Deborah B. Dehart, B. and W. Johnson, G. Allan Johnson, Martin A. Styner, and K. K. S. (2009) 'Magnetic Resonance Microscopy Defines Ethanol-Induced Brain Abnormalities in Prenatal Mice: Effects of Acute Insult on Gestational Day 8', *Alcohol Clin Exp Res.*, 33(6), pp. 1001–1011.

Shabtai, Y. *et al.* (2016) 'Kinetic characterization and regulation of the human retinaldehyde dehydrogenase 2 enzyme during production of retinoic acid', *Biochem. J*, 473, pp. 1423–1431. doi: 10.1042/BCJ20160101.

Sharon, N. *et al.* (2011) 'Molecular and functional characterizations of gastrula organizer cells derived from human embryonic stem cells', *Stem Cells*. doi: 10.1002/stem.621.

El Shawa, H., Abbott, C. W. and Huffman, K. J. (2013) 'Prenatal Ethanol Exposure Disrupts Intraneocortical Circuitry, Cortical Gene Expression, and Behavior in a Mouse Model of FASD', *Journal of Neuroscience*, 33(48), pp. 18893–18905. doi: 10.1523/JNEUROSCI.3721-13.2013.

Shen, L. *et al.* (2013) 'Effect of Prenatal Alcohol Exposure on Bony Craniofacial Development: A Mouse MicroCT Study', *Alcohol*, 47(5), pp. 405–415. doi: 10.1016/j.alcohol.2013.04.005.

Shibley, I., McIntyre, T. and Pennington, S. (1999) ‘Review. Experimental models used to measure direct and indirect ethanol teratogenicity’, *Alcohol and Alcoholism*, 34(2), pp. 125–140.

Smiley, J. F. *et al.* (2015) ‘Selective reduction of cerebral cortex GABA neurons in a late gestation model of fetal alcohol spectrum disorder’, *Alcohol*. Elsevier Inc, 49(6), pp. 571–580. doi: 10.1016/j.alcohol.2015.04.008.

Soto-Gutiérrez, A. *et al.* (2007) ‘Differentiation of mouse embryonic stem cells to hepatocyte-like cells by co-culture with human liver nonparenchymal cell lines’, *Nature Protocols*, 2(2), pp. 347–356. doi: 10.1038/nprot.2007.18.

Sowell, E. R. *et al.* (2008) ‘Abnormal cortical thickness and brain-behavior correlation patterns in individuals with heavy prenatal alcohol exposure’, *Cerebral Cortex*, 18(1), pp. 136–144. doi: 10.1093/cercor/bhm039.

Spadoni, A. D. *et al.* (2007) ‘Neuroimaging and fetal alcohol spectrum disorders’, *Neurosci Biobehav Rev*, 31(2), pp. 239–245. doi: S0149-7634(06)00109-6 [pii]\r10.1016/j.neubiorev.2006.09.006.

Spong, C. *et al.* (2001) ‘Prevention of fetal demise and growth restriction in a mouse model of fetal alcohol syndrome’, *J Pharmacol Exp Ther*, 297(2), pp. 774–779.

Streissguth, A. P., Clarren, S. K. and Jones, K. L. (1985) ‘NATURAL HISTORY OF THE FETAL ALCOHOL SYNDROME: A 10-YEAR FOLLOW-UP OF ELEVEN PATIENTS’, *Lancet*, 326(8446), pp. 85–91.

Sulik, K. and Johnston, M. (1983) ‘Sequence of Developmental Alterations Following Acute Ethanol Exposure in Mice: Craniofacial Features of the Fetal Alcohol Syndrome’, *The American Journal of Anatomy*, pp. 257–269.

Sulik KK, Cook CS, W. W. (1988) ‘Teratogens and craniofacial malformations: relationships to cell death’, *Development*, 103, pp. 213–231.

Suttie, M. *et al.* (2013) ‘Facial Dysmorphism Across the Fetal Alcohol Spectrum’, *Pediatrics*, 131(3), pp. e779–e788. doi: 10.1542/peds.2012-1371.

Szanto, A. *et al.* (2004) ‘Retinoid X receptors: X-ploring their (patho)physiological functions’, *Cell Death and Differentiation*, 11, pp. S126–S143. doi: 10.1038/sj.cdd.4401533.

Tay, S. *et al.* (2010) ‘A Comparison of the Roles of Peroxisome Proliferator- Activated Receptor and Retinoic Acid Receptor on CYP26 Regulation’, *Molecular Pharmacology*, 77(2), pp. 218–227. doi: 10.1124/mol.109.059071.

Twigg, S. R. F. *et al.* (2009) ‘Skeletal analysis of the Fgfr3P244R mouse, a genetic model for the muenke craniosynostosis syndrome’, *Developmental Dynamics*, 238(2), pp. 331–342. doi: 10.1002/dvdy.21790.

Volgin, D. V. (2008) ‘Perinatal alcohol exposure leads to prolonged upregulation of hypothalamic GABAA receptors and increases behavioral sensitivity to gaboxadol’, *Neuroscience Letters*. doi: 10.1016/j.neulet.2008.05.011.

Wahlsten, D. *et al.* (2007) 'Stability of inbred mouse strain differences in behavior and brain size between laboratories and across decades', *Pnas*, 103(44), pp. 16364–16369. doi: 10.1073/pnas.0605342103.

Wang, X. *et al.* (2007) 'Effects of acute alcohol intoxication in the second trimester of pregnancy on development of the murine fetal lung', *American Journal of Obstetrics and Gynecology*, 197(3), pp. 1–4. doi: 10.1016/j.ajog.2007.06.031.

Watari, N. *et al.* (2001) 'Hoxa3 regulates integration of glossopharyngeal nerve precursor cells', *Developmental Biology*, 240(1), pp. 15–31. doi: 10.1006/dbio.2001.0447.

Webster, M. J. *et al.* (2002) 'Regional specificity of brain glucocorticoid receptor mRNA alterations in subjects with schizophrenia and mood disorders', *Molecular Psychiatry*, 7(9), pp. 985–994. doi: 10.1038/sj.mp.4001139.

Weinberg, J. (1989) 'Prenatal Ethanol Exposure Alters Adrenocortical Development of Offspring', *Alcoholism: Clinical and Experimental Research*, 13(1), pp. 73–83. doi: 10.1111/j.1530-0277.1989.tb00287.x.

Weinberg, J. (1993) 'Prenatal alcohol exposure: Endocrine function of offspring', *Alcohol and the Endocrine System*, pp. 363–382.

Weinberg, J. (1994) 'Recent studies on the effects of fetal alcohol exposure on the endocrine and immune systems', *Alcohol*, 2, pp. 401–409.

Weinberg, J., Nelson, L. and Taylor, A. (1986) 'Hormonal effects of fetal alcohol exposure', *Alcohol and Brain Development*, pp. 310–342.

Weinberg J (1993) 'Neuroendocrine effects of prenatal alcohol exposure', *Ann NY Acad Sci*, 697, pp. 86–96.

Welberg, L. and Seckl, J. (2001) 'Prenatal stress, glucocorticoids and the programming of the brain', *J Neuroendocrinol*, 13(2), pp. 113–128.

Wellen, K. E. and Thompson, C. B. (2010) 'Cellular metabolic stress: Considering how cells respond to nutrient excess', *Mol Cell.*, 40(2), pp. 323–332. doi: 10.1016/j.molcel.2010.10.004.Cellular.

West, J., Chen, W. and Pantazis, N. (1994) 'Fetal alcohol syndrome: the vulnerability of the developing brain and possible mechanisms of damage', *Metab Brain Dis*, 9(4), pp. 291–322.

White, J. C. *et al.* (1998) 'Defects in embryonic hindbrain development and fetal resorption resulting from vitamin A deficiency in the rat are prevented by feeding pharmacological levels of all-trans-retinoic acid', *Biochemistry*, 95, pp. 13459–13464.

Wieczorek, L., , Eric W. Fish, Shonagh K. O'Leary-Moore, Scott E. Parnell, A. and Sulik, K. K. (2015) 'Hypothalamic-pituitary-adrenal axis and behavioral dysfunction following early binge-like prenatal alcohol exposure in mice', *Alcohol*, 49(3), pp. 207–217. doi: 10.1002/nbm.3369.Three.

Wilkemeyer, M. *et al.* (2002) 'Peptide Antagonists of Ethanol Inhibition of L1-Mediated Cell-Cell Adhesion', *Journal of Pharmacology and Experamental Therapeutics*, 303(1), pp. 110–116.

Williams, J. F. and Smith, V. C. (2015) 'CLINICAL REPORT Guidance for the Clinician in Rendering Pediatric Care Fetal Alcohol Spectrum Disorders', *American Academy of Pediatrics*, 136(5), pp. 1395–1406. doi: 10.1542/peds.2015-3113.

Yelin, R. *et al.* (2005) 'Ethanol exposure affects gene expression in the embryonic organizer and reduces retinoic acid levels', *Developmental Biology*, 279(1), pp. 193–204. doi: 10.1016/j.ydbio.2004.12.014.

Yelin, R. *et al.* (2007) 'Early molecular effects of ethanol during vertebrate embryogenesis', *Differentiation*, 75(5), pp. 393–403.

Young, C. *et al.* (2003) 'Ethanol-induced neuronal apoptosis in vivo requires BAX in the developing mouse brain.', *Cell death and differentiation*, 10(10), pp. 1148–55. doi: 10.1038/sj.cdd.4401277.

Zakhari, S. and Hoek, J. B. (2015) 'Alcohol and breast cancer: Reconciling epidemiological and molecular data', *Advances in Experimental Medicine and Biology*. doi: 10.1007/978-3-319-09614-8_2.

Appendix 1: PAE Rodent Models: Dosage, Duration, and Gestational Timing causing Developmental Malformations

Exposure Paradigm				Model			Developmental Malformations			References
Level	**Treatment**		**Time**	**Species**	**Age at Assessment**	**Sex**	**Craniofacial**	**Brain**	**Behavioral**	
C	10% v/v EtOH	LD	GD 0-19	Mouse C57Bl6	PN60	M/F	-	Reduced OB Volume	Impaired Odor Discrimination	(Akers et al. 2011)
C	4.8% v/v EtOH	LD	GD 0-19	Mouse C57Bl6	GD17	M/F	Facial Malformations, Small bigonial line	-	-	(Anthony et al. 2010)
A	2.9g/kg (2X/day)	Ip	GD 7	Mouse C57Bl6	PN45	M/F	-	Smaller CC, AC, HC	-	(Cao et al. 2014)
A	2.5g/kg (1X/day)	I-B	PN 7	Mouse C57Bl6	PN82	M/F	-	Reduced Brain Volume (<4%)	-	(Coleman et al. 2012)
C	4g/kg (1X/day)	G	PN 4-9	Mouse C57Bl6	PN10	M/F	-	Increased Level Cytokines in H, C, & CC* & Microglial Activation	-	(Drew et al. 2015)
A	2.8g/kg (2X/day)	Ip	GD 8	Mouse C57Bl6	GD17	M/F	Microphthalmia and Irideo-Retinal Coloboma	Reduced Brain Regions: OB, H, C and Whole Body Volumes,	-	(Parnell et al. 2009)
A	2.9g/kg (2X/day)	Ip	GD 7	Mouse C57Bl6	GD17	M/F	Medial Facial Cleft, Cleft Palate, Micrognathia	P Agenesis, TV Dilation, Forebrain Malformations	-	(Godin et al. 2010)

A	2.9g/kg (2X/day)	Ip	GD 7	Mouse 129S6	GD10-19	M/F	Reduced Nasal Pit Distance, Severe HPE, Abnormal Ventral Midline, Deficient Philtrum, Underdeveloped Maxillary Shelves, Fused Pre-maxillary Bones	Partitioned Forebrain, Loss of Telencephalic Structure	-	(Hong and Krauss 2012)
A	2.9g/kg (2X/day)	Ip	GD 7	Mouse C57Bl6	GD17	M/F	Severe Midfacial Hypoplasia, Micrognathia, Reduced Snout Width, Longer Upper Lip Length	Microcephaly,Reduced OB, SR, and P Volumes, Increased OB, SR, and P Volumes	-	(Lipinski et al. 2012)
			GD 8				Midfacial Hypoplasia, Reduced Snout Width, Shorter Upper Lip Length		-	
C	4.2% v/v EtOH	LD	GD7-16	Mouse C57Bl6	PN7	M/F	-	Reduced Parietal Region, Head Size and Head Circumference	-	(Shen et al. 2013)
					PN21		Reduced Mandible size	Reduced Skull: Parietal, Occipital, Frontal Regions, Head Size, & Head Circumference	-	

A	2.5g/kg (2X/day)	G	PN 7	Mouse C57Bl6	PN 72-89	M/F	-	Decrease brain volume, body weight, and cortical neuron numbers (sex dependent)	-	(Smiley et al., 2015)
C	10% v/v EtOH	LD	GD0-PN6	Mouse C57Bl6	PN 90-150	M	-	-	Decrease in delay fear freezing and trace fear freezing Fewer correct arm entries.	(Brady et al. 2012)
C	10% v/v EtOH	LD	GD0-PN6	Mouse C57Bl6	PN 40-50	M	-	Reduced GR nuclear localization levels and Increase MR cytosolic localization levels in mPFC	Decrease in ability to learn reversal phase of Y-maze.	(Allan et al. 2014)
A	3.0g/kg (1X Day)	Ip	GD 8	Mouse C57Bl6	GD 18	M/F	-	Increased DUOX2, NOXA1, and NOXO1 mRNA expression in whole fetal brain	-	(Hill et al. 2014)
A	2.9g/kg (2X/day)	Ip	GD 7	Mouse C57Bl6	PN 45	M/F	-	Reduction of Anterior Commissure Volume	-	(Cao et al. 2014)
C	5% v/v EtOH	LD	GD0-PN6	Mouse C57Bl6	PN 60-90	M	-	Reduced proBDNF and BDNF mRNA and protein levels in mPFC and reduced proBDNF and BDNF mRNA levels in H	Demonstrate learned helplessness, increased immobility,	(Caldwell et al. 2008)
A	2.9g/kg (2X/day)	Ip	GD 9	Mouse C57Bl6	GD 17	M/F	-	Reduced C and CC* volume, lateral, third, and fourth ventricles were enlarged,	-	(Parnell et al. 2013)

A	2.9g/kg (2X/day)	Ip	GD 7	Mouse C57Bl6 (Shh +/-)	GD 17	M/F	Upper midfacial deficiency, exencephaly, agnathia, anophthalmia, proboscis,	True HPE, Reduction in brain size (Specifically Forebrain), Hypoplasia and or Loss of OB, Hypoplasia of the CC*	-	(Kietzman et al. 2014)
C	10% v/v EtOH	LD	GD 0 – PN 10	Mouse C57Bl6	PN 2-21	M/F	-	-	Increase in days taken to complete negative geotaxis, auditory startle, and air righting tests	(Kleiber et al. 2011)
					PN 25-70		-	Decreased Glra1 and Grin2c mRNA expression in whole adult brain	Increased anxiety (openfield test)	
C	25% v/v EtOH	LD	GD 0 - 19	Mouse CD1	P0-P20	M/F	-	Aberrant somatosensory and visual cortex neuron development, specifically cortical neuron lengths	Increased anxiety and impaired gross and fine motor coordination	(El Shawa et al. 2013)

C	10% v/v EtOH	AbL	GD 0 - 8.5	Mouse C57Bl6	GD 16.5	M/F	-	Reduced body weight in weaned (P21) and 3rd to 16th week old mice Downregulated genes mRNA expression: Hamp1, Hamp2, Vldlr, Socs2, Cables1	-	(Kaminen-Ahola et al. 2010)
A	2.9g/kg (2X/day)	Ip	GD 7	Mouse C57Bl6	GD 14	M/F	Frontonasal prominence malformations, deficient medial nasal process, abnormal longer maxillary processes	Incidence of reabsorptions, eye malformations (microphthalmia and anophthalmia)	-	(Sulik et al. 1981)
C	2.2g/kg	Ip	PD 4-9	Mouse F2 129SVJ x C57Bl6	PD 85-90	M/F	-	-	-	(Karacay et al. 2016)
	4.4g/kg						-	Smaller body weight PN 9-10	Impaired learning/memory (morris water maze)	
	2.2 & 4.4 g/kg			Mouse F2 129SVJ x C57Bl6 (nNos -/-)			-	Smaller body weight PN9-10 and into adulthood	Increased anxiety, Impaired learning/memory (morris water maze), Impaired startle response	

C	2.0g/kg	G	GD 5 - 19	Mouse C57Bl6	PD 0-30	M/F	-	Increase in dendritic spine length and decrease in dendritic spine density	-	(Cui et al. 2010)
	4.0 g/kg						-	Increase in dendritic spine length and decrease in dendritic spine density, reduction in width of synaptic cleft and number of synaptic vesicles	-	
C	10% v/v EtOH	AbL	GD 0 - 8.5	Mouse C57Bl6	PD 21-30	M/F	Smaller cranium size, Midfacial dysmorphisms, Increase in cranial and orbital width	Increase epigenetic modulation (pseudoagouti epigenetics), Smaller body weight at weaning Downregulated genes mRNA expression: Hamp1, Lima1, Socs2, Cables1, Vldlr	-	(Kaminen-Ahola et al. 2010)
A	2.9g/kg (2X/day)	Ip	GD 10	Mouse C57Bl6	GD 17	M/F	-	Reduced CC volume, increase third ventricle volume, and altered morphology in lateral and fourth ventricles	-	(O'Leary et al. 2010)

Abbreviations: C - Chronic A – Acute Ip – Intraperitoneal G – Oral Gavage AbL – *ab libitum* I-B – Inject-Back

LD – Liquid Diet M – Male F – Female GD – Gestational Day PD – Post-natal Day